

Precast Concrete Elements for Accelerated Bridge Construction

Volume 2. Laboratory Testing, Field Testing, and Evaluation of a Precast Concrete Bridge: Madison County Bridge



Final Report
January 2009

Sponsored by

the Iowa Highway Research Board (IHRB Project TR-561),
the Iowa Department of Transportation (CTRE Project 06-262),
and
Madison County, Iowa, through the Federal Highway Administration's
Innovative Bridge Research and Construction Program



IOWA STATE
UNIVERSITY

About the Bridge Engineering Center

The mission of the Bridge Engineering Center is to conduct research on bridge technologies to help bridge designers/owners design, build, and maintain long-lasting bridges.

Disclaimer Notice

The contents of this report reflect the views of the authors, who are responsible for the facts and the accuracy of the information presented herein. The opinions, findings and conclusions expressed in this publication are those of the authors and not necessarily those of the sponsors.

The sponsors assume no liability for the contents or use of the information contained in this document. This report does not constitute a standard, specification, or regulation.

The sponsors do not endorse products or manufacturers. Trademarks or manufacturers' names appear in this report only because they are considered essential to the objective of the document.

Nondiscrimination Statement

Iowa State University does not discriminate on the basis of race, color, age, religion, national origin, sexual orientation, gender identity, sex, marital status, disability, or status as a U.S. veteran. Inquiries can be directed to the Director of Equal Opportunity and Diversity, (515) 294-7612.

GENERAL ABSTRACT

Precast Concrete Elements for Accelerated Bridge Construction

Precast concrete elements and accelerated bridge construction techniques have the potential to improve the health of the U.S. highway system. In precast bridge construction, the individual components are manufactured off-site and assembled on-site. This method usually increases the components' durability, reduces on-site work and construction time, minimizes traffic disruption, and lowers life-cycle costs. Before widespread implementation, however, the benefits of precast elements and accelerated bridge construction must be verified in the laboratory and field.

For this project, precast bridge elements and accelerated bridge construction techniques were investigated in the laboratory and at three bridge projects in Iowa: in Boone County, Madison County, and Black Hawk County. The objectives were to evaluate the precast bridge elements, monitor the long-term performance of the completed bridges, and evaluate accelerated bridge construction techniques.

The results of these investigations are presented in three volumes, as described below; this volume is Volume 2.

Vol. 1-1. Laboratory Testing of Precast Substructure Components: Boone County Bridge

1-2. Laboratory Testing of Full-Depth Precast, Prestressed Concrete Deck Panels: Boone County Bridge

1-3. Field Testing of a Precast Concrete Bridge: Boone County Bridge

In 2006, a continuous four-girder, three-span bridge was constructed that included precast abutments, pier cap elements, prestressed beams, and precast full-depth deck panels. All of the precast elements performed well during strength testing and were set quickly and smoothly during construction, and the completed bridge experienced very small displacements and strains when subjected to live loads.

Vol. 2. Laboratory Testing, Field Testing, and Evaluation of a Precast Concrete Bridge: Madison County Bridge

In 2007, a two-lane single-span bridge was constructed that had precast box girders with precast abutments. The elements performed well during laboratory load transfer and strength testing, and the completed bridge performed well in terms of maximum deflections and differential displacements between longitudinal girder joints.

Vol. 3. Laboratory Testing, Field Testing, and Evaluation of a Precast Concrete Bridge: Black Hawk County

In 2007, two precast modified beam-in-slab bridge (PMBISB) systems were constructed, each of which included precast abutment caps, backwalls, and deck panels. Various deck panel configurations transferred load effectively during laboratory testing, and all precast elements met expectations. The completed bridges experienced very low induced stresses and met AASHTO deflection criteria, while the PMBSIB system effectively transferred load transversely.

Technical Report Documentation Page

1. Report No. IHRB Project TR-561	2. Government Accession No.	3. Recipient's Catalog No.	
4. Title and Subtitle Precast Concrete Elements for Accelerated Bridge Construction: Laboratory Testing, Field Testing, Evaluation of a Precast Concrete Bridge, Madison County Bridge		5. Report Date January 2009	
		6. Performing Organization Code	
7. Author(s) Brent Phares, Terry Wipf, Jake Bigelow, Ryan Bowers, and F. Wayne Klaiber		8. Performing Organization Report No. CTRE Project 06-262	
9. Performing Organization Name and Address Bridge Engineering Center Iowa State University 2711 South Loop Drive, Suite 4700 Ames, IA 50010-8664		10. Work Unit No. (TRAIS)	
		11. Contract or Grant No.	
12. Sponsoring Organization Name and Address Iowa Highway Research Board Iowa Department of Transportation 800 Lincoln Way Ames, IA 50010		13. Type of Report and Period Covered Final Report	
		14. Sponsoring Agency Code	
15. Supplementary Notes Visit www.ctre.iastate.edu for color PDF files of this and other research reports.			
16. Abstract The importance of rapid construction technologies has been recognized by the Federal Highway Administration (FHWA) and the Iowa DOT Office of Bridges and Structures. Recognizing this a two-lane single-span precast box girder bridge was constructed in 2007 over a stream. The bridge's precast elements included precast cap beams and precast box girders. Precast element fabrication and bridge construction were observed, two precast box girders were tested in the laboratory, and the completed bridge was field tested in 2007 and 2008.			
17. Key Words accelerated bridge construction—Boone County, Iowa—field testing—laboratory strength testing—precast concrete box girders and abutments		18. Distribution Statement No restrictions.	
19. Security Classification (of this report) Unclassified.	20. Security Classification (of this page) Unclassified.	21. No. of Pages 96	22. Price NA

PRECAST CONCRETE ELEMENTS FOR ACCELERATED BRIDGE CONSTRUCTION: LABORATORY TESTING, FIELD TESTING, EVALUATION OF A PRECAST CONCRETE BRIDGE, MADISON COUNTY BRIDGE

**Final Report
January 2009**

Co-Principal Investigators

Terry J. Wipf, Director, Bridge Engineering Center
Center for Transportation Research and Education, Iowa State University

Brent M. Phares, Associate Director, Bridge Engineering Center
Center for Transportation Research and Education, Iowa State University

F. Wayne Klaiber, Professor, Department of Civil, Construction, and Environmental Engineering
Iowa State University

Research Assistant

Ryan P. Bowers

Authors

Brent Phares, Terry Wipf, Jake Bigelow, Ryan P. Bowers, and F. Wayne Klaiber

Sponsored by
the Iowa Highway Research Board (IHRB Project TR-561)
and Madison County, Iowa,
through the Federal Highway Administration's
Innovative Bridge Research and Construction Program

Preparation of this report was financed in part
through funds provided by the Iowa Department of Transportation
through its research management agreement with the
Center for Transportation Research and Education (CTRE Project 06-262).

Center for Transportation Research and Education

Iowa State University

2711 South Loop Drive, Suite 4700

Ames, IA 50010-8664

Phone: 515-294-8103

Fax: 515-294-0467

www.ctre.iastate.edu

TABLE OF CONTENTS

ACKNOWLEDGMENTS	XI
EXECUTIVE SUMMARY	XIII
1 . GENERAL INFORMATION	1
1.1 Introduction.....	1
1.2 Background.....	1
1.3 Objectives and Scope.....	2
2 . BRIDGE DESCRIPTION.....	3
2.1 Box Girder Properties	5
2.2 Fabrication Observations	9
2.3 Field Construction Observations	12
3 . LABORATORY TESTING.....	15
3.1 Concrete Strength Test.....	15
3.2 Variable Post-Tensioning Force Test	16
3.3 Flexural Strength Test.....	18
3.4 Shear Strength Test.....	19
3.5 Guardrail Connection Test.....	22
4 . LABORATORY TEST RESULTS	24
4.1 Concrete Strength Test Results.....	24
4.2 Variable Post-Tensioning Force Test Results.....	24
4.3 Flexural Strength Test Results	28
4.4 Shear Strength Test Results	33
4.5 Guardrail Connection Test Results	36
5 . FIELD TESTING.....	43
5.1 Evaluation methodology and instrumentation	43
6 . FIELD TEST RESULTS	47
6.1 Static Loading	47
6.2 Dynamic Loading.....	60
6.3 Corrosion Monitoring	64
7 . CONCLUSIONS AND RECOMMENDATIONS	66
REFERENCES	68
APPENDIX A. MADISON COUNTY BOX GIRDER BRIDGE PLANS.....	A-1

LIST OF FIGURES

Figure 2.1. Location of Madison Co. precast bridge	3
Figure 2.2. Photographs of Madison Co. precast bridge	3
Figure 2.3. Plan and section of bridge	4
Figure 2.4. Photograph of bridge guardrail system	5
Figure 2.5. Box girder dimensions.....	6
Figure 2.5. Box girder reinforcement layout	7
Figure 2.6. Box girder guardrail properties	9
Figure 2.7. Photograph of box girder form with bottom pretension strands	10
Figure 2.8. Photograph of top of beam reinforcing and foam core.....	10
Figure 2.9. Photograph of end reinforcing and lift points	11
Figure 2.10. Photograph of midspan transverse tie duct.....	11
Figure 2.11. Photograph of crew lifting girder out of forms	12
Figure 2.12. Photographs of precast pile cap beam installation	12
Figure 2.13. Photographs of box girder placement sequence	14
Figure 3.1. Photograph of a precast box girder used for laboratory testing	15
Figure 3.2. Box girder concrete core locations.....	15
Figure 3.3. Photographs of laboratory setup for variable post-tensioning force tests	16
Figure 3.4. Variable post-tensioning loading locations	17
Figure 3.5. Photograph of tandem wheel footprint used during the variable post-tensioning force tests	18
Figure 3.6. Instrumentation grid for variable post-tensioning force tests.....	18
Figure 3.7. Laboratory setup to test flexural strength of a box girder	19
Figure 3.8. Instrumentation locations	19
Figure 3.9. Shear strength test setup	20
Figure 3.10. Transducer and concrete strain gage grid for shear strength test	21
Figure 3.11. Rosette layout for shear strength test	21
Figure 3.12. Guardrail connection test load locations	22
Figure 3.13. Guardrail connection test setup	22
Figure 3.14. Guardrail post instrumentation.....	23
Figure 4.1. Total strain at midspan with load at D1 and a post-tensioning force of 17 kips	24
Figure 4.2. Deflection results at point D1 with a 17 kip post-tensioning force.....	25
Figure 4.3. Load fractions at midspan for various post-tensioning forces and load at D1	26
Figure 4.4. Load fractions at quarterspan for various post-tensioning forces and load at D1	27
Figure 4.5. Load fractions at midspan for various post-tensioning forces and load at B1	27
Figure 4.6. Load fractions at quarterspan for various post-tensioning forces and load at B1	28
Figure 4.7. Photograph of flexural cracking after flexure test.....	29
Figure 4.8. Moment at midspan of the box girder	30
Figure 4.9. Tensile stress at midspan of the box girder	30
Figure 4.10. Total compressive stress at midspan of the box girder	31
Figure 4.11. Compressive stress due to applied load and one-half the dead load and prestressing force at midspan of the box girder	32
Figure 4.12. Deflection versus load plot for box girder flexural strength test.....	32
Figure 4.13. Photographs of box girder after shear failure	33
Figure 4.14. Shear force in the box girder	34
Figure 4.15. Principle strains due to applied load at rosette 2N during shear strength testing	34

Figure 4.16. Principal stresses due to the total load at rosette 2N	35
Figure 4.17. Theoretical and experimental deflections at quarterspan during shear test	36
Figure 4.18. Photographs of failed guardrail connection elements	36
Figure 4.19. Post deflections during test 1.....	38
Figure 4.20. Deflected shape of the top of the guardrail at failure	39
Figure 4.21. Post strains during test 1.....	39
Figure 4.22. Post displacements for test 2	40
Figure 4.23. Deflected shape of the guardrail during test 2.....	41
Figure 4.24. Photograph of deflected guardrail during test 4	41
Figure 4.25. Post strains during test 2.....	42
Figure 5.1. Instrumentation layout.....	43
Figure 5.2. Transverse load positions: Vehicle traveled west into page	45
Figure 5.3. Madison County load truck	46
Figure 5.4. Vehicle configuration and axle loads	46
Figure 6.1. Representative time history deflections	48
Figure 6.2. 2007 and 2008 transverse deflected shape at midspan and quarterspan	49
Figure 6.3. 2007 and 2008 differential deflections	52
Figure 6.4. 2007 Experimental strains; LC 7.....	55
Figure 6.5. 2008 Experimental strains; LC 7.....	55
Figure 6.6. 2007 Experimental and analytical strain comparison; LC 3	56
Figure 6.7. 2008 Experimental and analytical strain comparison; LC 3	57
Figure 6.8. Experimentally obtain load fraction.....	58
Figure 6.9. Experimental and codified load distributions.....	59
Figure 6.10. Experimental neutral axis location.....	60
Figure 6.11. Transducer B6 dynamic response LC2	61
Figure 6.12. 2007 and 2008 DAF LC 2	62
Figure 6.13. Transducer B11 dynamic response LC7	62
Figure 6.14. 2007 and 2008 DAF LC7	63
Figure 6.15. Acceleration and frequency plots for 2007 testing.....	63
Figure 6.16. Acceleration and frequency plots for 2008 testing.....	64
Figure 6.17. Corrosion electrode wrapped around strand.....	64

LIST OF TABLES

Table 3.1. Post-tensioning forces applied during testing.....	17
Table 4.1. Box girder concrete core strengths	24
Table 4.2. Differential deflection for load point D1 and various post-tensioning forces	26
Table 4.3. Load fractions for a load at D1 for a hand-tight post-tensioning force	28
Table 4.4. Box girder cracking moment	29
Table 4.5. Box girder flexural strength.....	29
Table 4.6. Box girder shear strength.....	33
Table 4.7. Guardrail connection test summary	37
Table 6.1. 2007 Maximum midspan girder deflection.....	47
Table 6.2. 2008 Maximum midspan girder deflection.....	48
Table 6.3. 2007 Maximum midspan girder strains	54
Table 6.4. 2008 Maximum midspan girder strains	54
Table 6.5. Vetek V2000 electrode readings.....	65
Table 6.6. V2000 millivolt electrode readings	65

ACKNOWLEDGMENTS

The authors would like to thank the Iowa Highway Research Board, the Iowa Department of Transportation, Madison County and the Federal Highway Administration for providing funding, design expertise, and research collaboration for this project. Special recognition is give to the following individuals for their significant contributions to the research: Ahmad Abu-Hawash, Jim Nelson, Stuart Nielsen, and many other staff from the Office of Bridges and Structures at the Iowa Department of Transportation; Curtis Monk, Iowa Division, Federal Highway Administration; Todd Hagen and other staff from Madison County; and Doug Wood, Iowa State University along with numerous graduate and undergraduate students.

EXECUTIVE SUMMARY

The importance of rapid construction technologies has been recognized by the Federal Highway Administration (FHWA) and the Iowa DOT Office of Bridges and Structures. Recognizing this fact a two-lane single-span precast box girder bridge was constructed in 2007 over a stream. The bridge's precast elements included precast cap beams and precast box girders. Precast element fabrication and bridge construction were observed, two precast box girders were tested in the laboratory, and the completed bridge was field tested in 2007 and 2008. The superstructure and substructure bridge elements performed well during laboratory and field testing.

1. GENERAL INFORMATION

1.1 Introduction

Recently, there has been increased interest in constructing bridges that last longer, are less expensive, and take less time to construct. The idea is to generally increase the cost-effectiveness of bridges by increasing their durability (i.e., useful life) and by minimizing disruptions to the traveling public. There may be many ways to achieve more durable, less expensive and rapidly constructed structures, however, the most commonly discussed ideas currently include using some form of precast, segmental construction. This type of construction has the advantage that the individual components are manufactured off-site where increased quality is usually achieved. Further, because much of the work is completed away from the bridge site, user disruptions are minimized since the amount of labor intensive on-site work is reduced, leading to reduced on-site construction time.

Using accelerated construction methods, a precast bridge was constructed by Madison County with the assistance of the Iowa Department of Transportation (DOT) and the Iowa State University Bridge Engineering Center (BEC). The design concept involved the use of precast components for both the bridge substructure and superstructure. The successful implementation of this approach has far reaching implications in Iowa as well as nationwide, as there are many instances where proven rapid construction techniques could result in significant reductions in costs. This project directly demonstrates the effectiveness of innovative materials and construction techniques for the construction of new bridge structures.

This report documents the Madison Co. Precast Bridge including fabrication, construction, laboratory testing, and field testing of the bridge. The Madison Co. Precast Bridge is a longitudinal pretensioned, two-lane, single span, box girder bridge spanning 46 ft-8 in. center to center of supports.

1.2 Background

The box girder design used for the Madison Co. bridge is based on designs used by the Illinois DOT. Illinois DOT box girders are either 36 in. or 48 in. wide and vary in depth. Shallower beams contain circular voids and welded wire fabric for the shear reinforcement. Deeper beams contain rectangular voids and the shear reinforcement consists of deformed bars. The deeper beams are limited to the 36 in. width to restrict the weight and size of the girders. This allows for easy transportation to the project site and placement with a mobile crane (Hawkins and Fuentes, 2002).

Precast prestressed concrete box girder bridges were widely used for Illinois State Highways during the 1960s and 1970s. Use of these bridges was discontinued for state highways due to corrosion problems. Approximately 10 percent of prestressed box girder bridges inventoried on Illinois State Highways had experienced significant corrosion, leading to a decreased bridge rating and the installment of load restrictions. Because these bridges are economical to build, they are still widely used on county roads throughout Illinois (Hawkins and Fuentes, 2002).

According to published literature differential deflections between adjacent girders allowed the development of reflective cracks along the longitudinal joint between girders. Corrosion of the prestressing strands resulted from salt laded water seeping through the cracked joint and into the girder. County engineers believe a lack of transverse load distribution between adjacent girders is the cause for the longitudinal cracking (Hawkins and Fuentes, 2003).

Two solutions used by the Illinois DOT to resolve this problem include transversely post-tensioning the girders together and providing a composite cast-in-place concrete deck. Both solutions have worked satisfactorily, but add considerably to the cost of construction, do not ensure that corrosion will be prevented, and make replacing damaged girders more difficult. These also are not reasonable solutions for retrofitting bridges currently in service (Hawkins and Fuentes, 2003).

1.3 Objectives and Scope

The overall objective of this project was to perform laboratory and field tests to evaluate the Madison Co. precast bridge components and asses the overall design, construction, and performance.

To satisfy the objectives, the project scope included the following tasks:

- Design of the substructure and superstructure (Note: completed by the Iowa DOT Office of Bridges and Structures).
- Inspection and documentation of the fabrication and construction of the bridge.
- Laboratory evaluation of the influence of transverse post-tensioning force on differential deflection between adjacent box girders.
- Verification of design assumptions for the box girders through ultimate flexural and shear strength testing.
- Laboratory testing to confirm the adequacy of the box girder-to-guardrail connection.
- Monitoring of prestress strand corrosion through the use of instrumentation installed during fabrication.
- Evaluation of in-situ structural performance under live loads.

2. BRIDGE DESCRIPTION

The subject bridge is located on a low volume road in the southern part of Madison Co., Iowa, as shown in Figure 2.1. Elevation and end view photographs of the completed bridge are shown in Figure 2.2. The bridge is a single span precast box girder bridge with a span length of 46 ft-8 in. from center-to-center of support, as illustrated in Figure 2.3. The bridge has an out-to-out deck width of 24 ft-1 in. and an out-to-out length of 47 ft-10 in. A crushed rock wearing surface is present on the bridge.

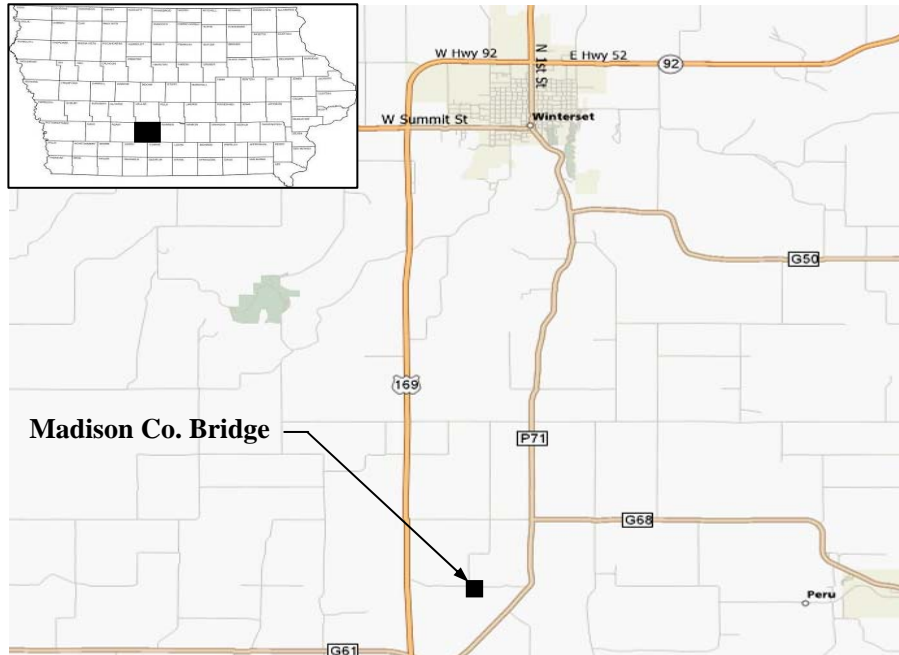


Figure 2.1. Location of Madison Co. precast bridge

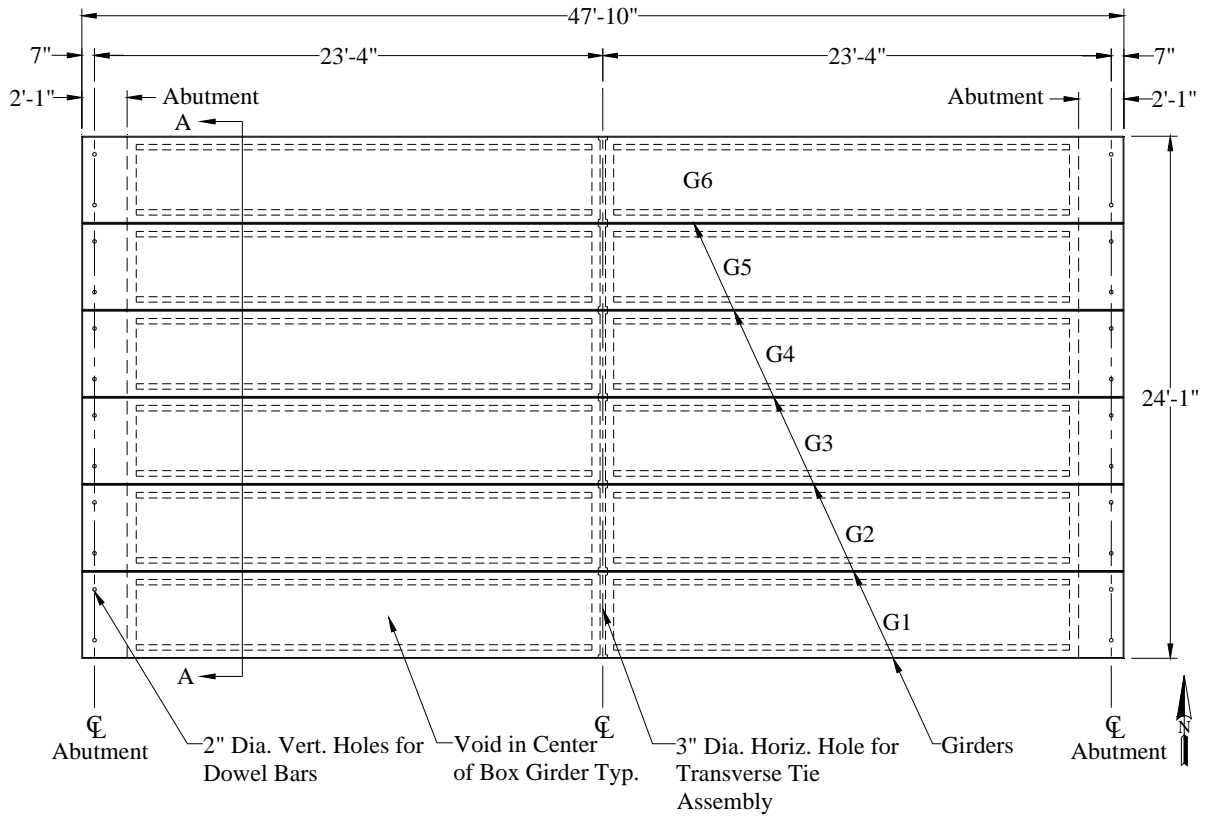


a. elevation

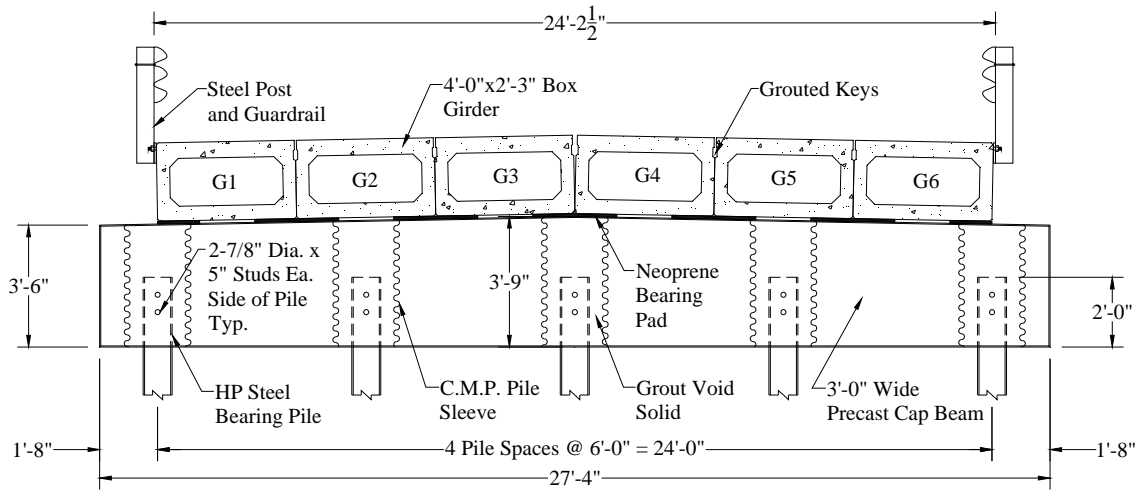


b. end view

Figure 2.2. Photographs of Madison Co. precast bridge



a. plan view



b. section A-A

Figure 2.3. Plan and section of bridge

The supporting substructure consists of five HP10x42 piles at each abutment and a precast cap beam. The precast cap beam is 27 ft-4 in. long, 3 ft wide, and varies in depth from 3 ft-6 in. at the ends to 3 ft-9 in. in the middle, as illustrated in Figure 2.3b. The cap beams were precast with five corrugated metal pipes (CMP) placed vertically at the pile locations illustrated in Figure

2.3b. Detailed plans of the cap beam can be found in Appendix A. During construction, the precast cap beam was lowered over the piles. In this way the CMP served as sleeves for the piles. After placement, the void in the CMP where the pile had been inserted was grouted solid. Wing walls and backwalls were constructed utilizing traditional cast-in-place concrete construction techniques.

The bridge guardrail consists of the galvanized steel post and three beam extending the full length of the bridge shown in Figure 2.4. The guardrail posts are bolted to the exposed face of each exterior girder with two 1 in. diameter embedded bolts. No curbs are present on the bridge.



Figure 2.4. Photograph of bridge guardrail system

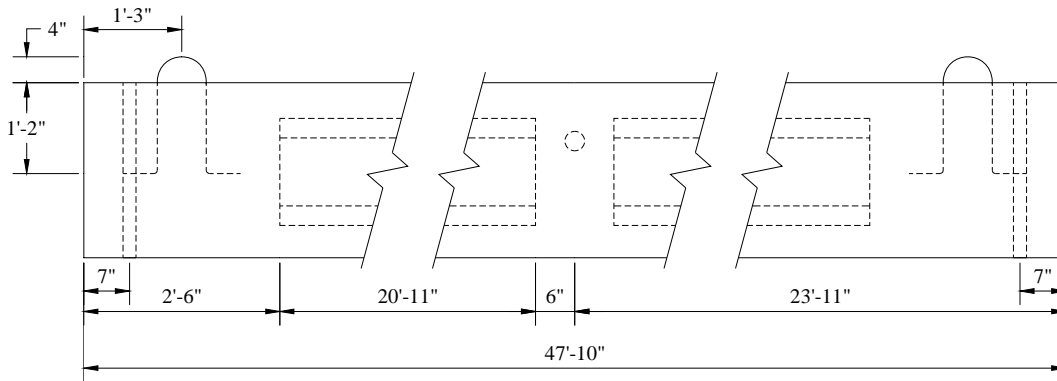
2.1 Box Girder Properties

Concrete for the box girders was specified to be in accordance with Section 9 of the AASHTO Standard Specifications for Highway Bridges (2002). The concrete compressive strength was specified to be 5000 psi.

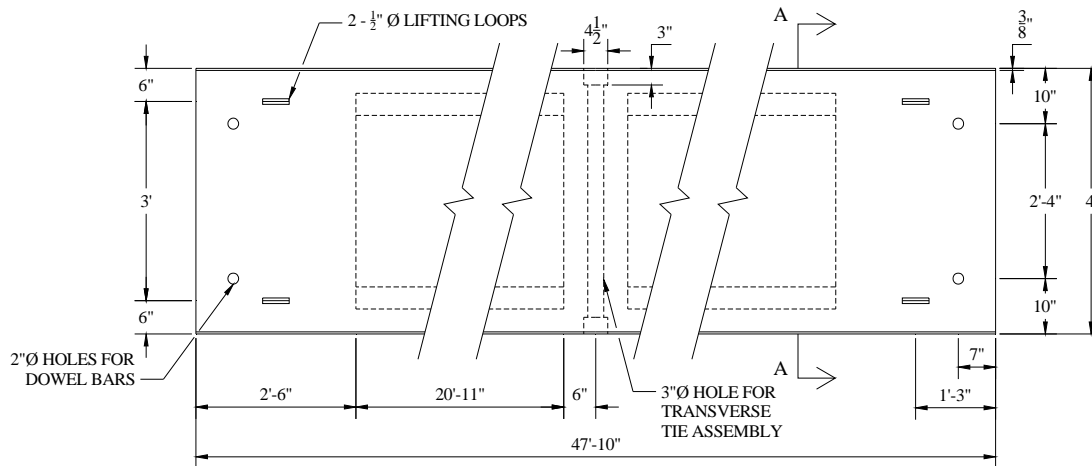
Dimensions for the box girders are given in Figure 2.5. The box girders had an overall length of 47 ft-10 in. Each girder was 4 ft wide.

As illustrated in Figure 2.6, the hollow section within the box girder began 2 ft-6 in. from the end of the girder, continued for 20 ft-11 in., and ended 6 in. from midspan. The girder, at midspan and at the ends, were solid concrete. The hollow portion of the girder had dimensions of approximately 1 ft-4 1/2 in. by 3 ft-3 in. This resulted in two 4 1/2 in. thick webs, a top slab with a 5 1/2 in. thickness, and a bottom slab with a 5 in. thickness.

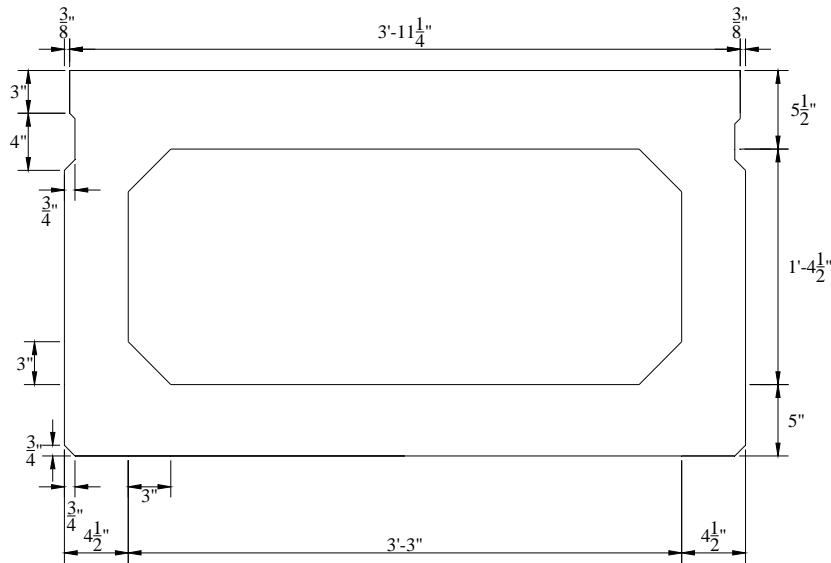
The 4 in. by 3/4 in. shear key can be seen in Figure 2.5c in the vertical face of the box girder. The purpose of the shear key is to assist in transferring load between adjacent box girders. Only girders with webs adjacent to other girders contained a shear key; the exterior face of the exterior girders did not possess a shear key.



a. profile view

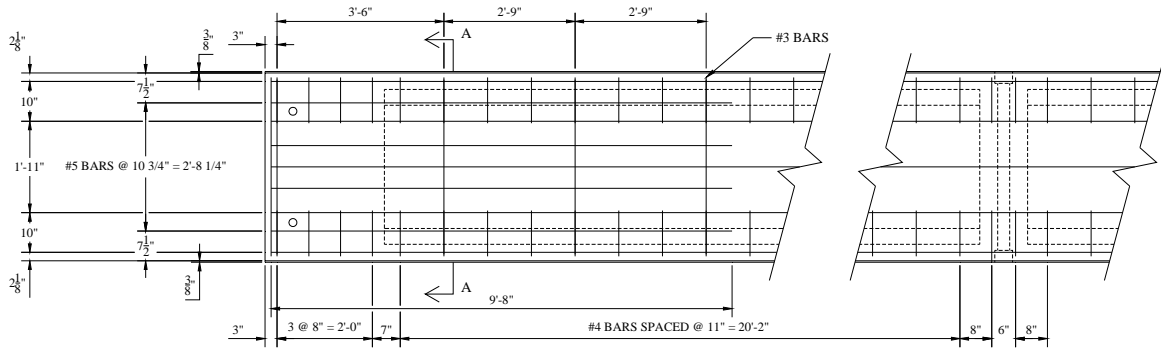


b. plan view

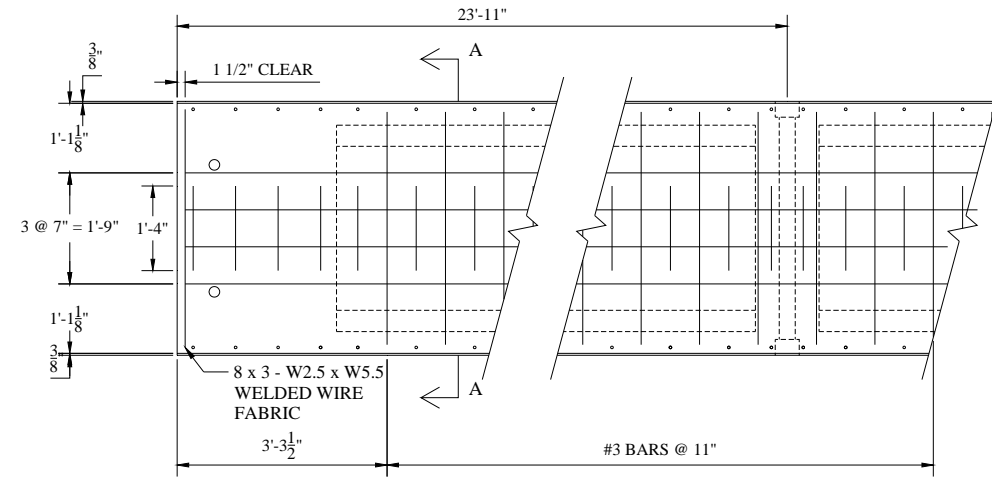


c. section A-A

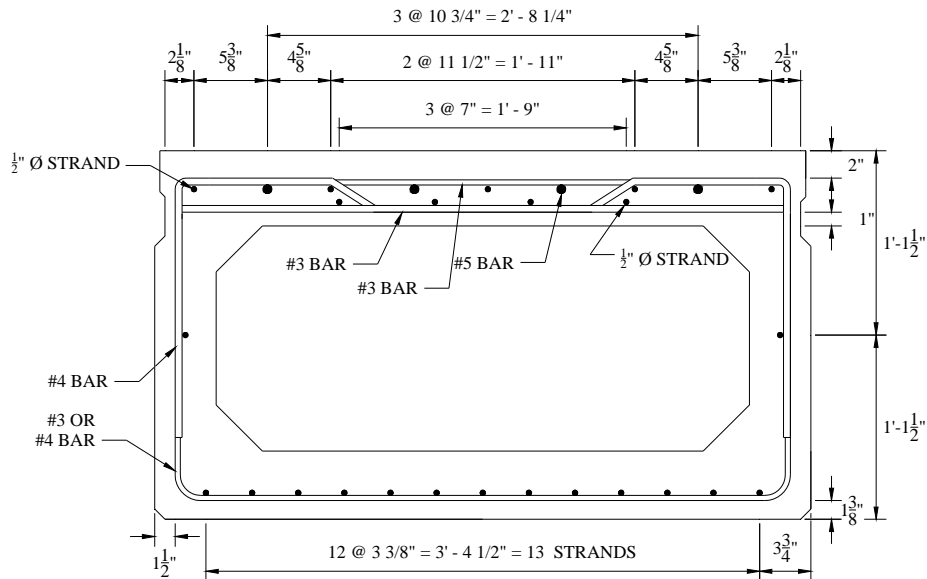
Figure 2.5. Box girder dimensions



a. top of top slab reinforcement

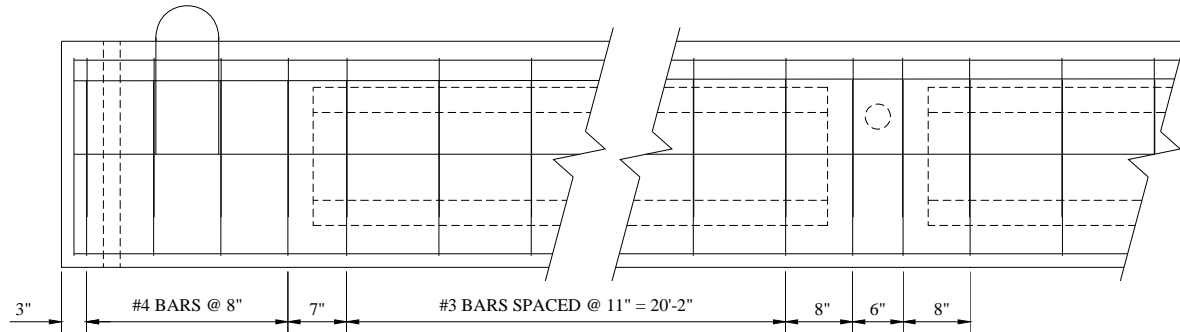


b. bottom of top slab reinforcement



c. section A-A

Figure 2.5. Box girder reinforcement layout



d. profile view of reinforcing layout

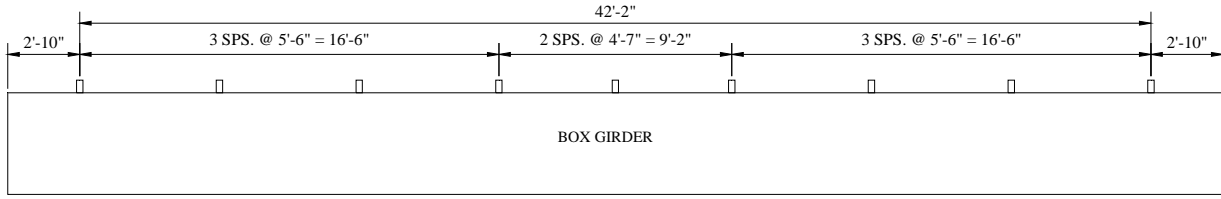
Figure 2.5. Box girder reinforcement layout

Reinforcement details for the box girders are shown in Figure 2.5. One-half inch diameter, seven-wire, uncoated, low-relaxation prestressing strand plus mild #5 reinforcing bars provided the flexural reinforcement. Thirteen strands were placed in the bottom slab and tensioned to a total force of 390 kips. Strands located in the web and in the top slab were not prestressed. These strands, at the request of the fabricator, replaced the #4 and #5 mild reinforcing bars which ran the full girder length in the original plans.

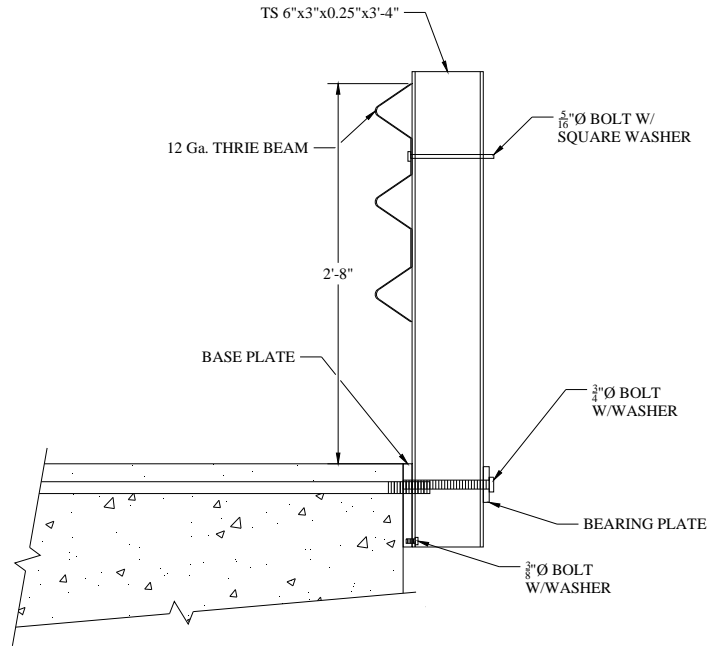
Shear reinforcement consisted of overlapping U-shaped bars. These bars were spaced at 8 in. for the first 2 ft of the girder, then at 7 in., and finally at 11 in. At midspan the stirrups were spaced at 8 in., 6 in., and 8 in., as shown in Figure 2.5a and d. Number 4 bars were used for all of the top U-bars. The first four bottom stirrups from either end of the box girder were #4 bars, while the rest of the bottom U-bars were #3 bars.

The box girders specified to be exterior girders contained 1 in. diameter anchor bolts for connecting the guardrail posts. The spacing for the posts is shown in Figure 2.6 and varied from 4 ft-7 in. to 5 ft-6 in. The guardrail posts consisted of 3 ft-4 in. HSS6x3x1/4 sections. Nine posts connected the guardrail to the box girder. A 12 gauge thrie beam was used for the guardrail.

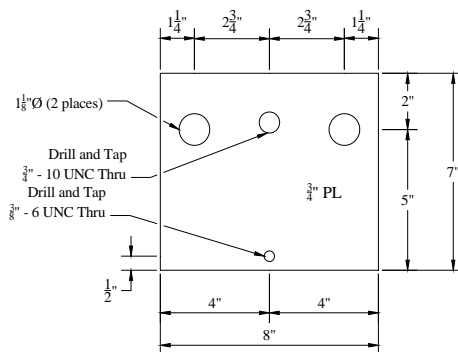
Each post is connected to a steel base plate with a 3/4 in. diameter ASTM A325 bolt and a 3/8 in. bolt. Base plates were 7 in. by 8 in. and had a thickness of 3/4 in. The base plates were bolted to two 1 in. diameter anchor bolts embedded in the box girder. A steel bearing plate, shown in Figure 2.6d, fit between the head of the 3/4 in. diameter bolt and the post.



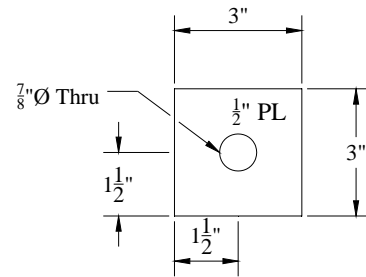
a. plan view of guardrail post spacing



b. profile view of guardrail and connection



c. base plate



d. bearing plate

Figure 2.6. Box girder guardrail properties

2.2 Fabrication Observations

The research team was present during various stages of the girder fabrication. Initial casting began on November 16, 2006. Because of cracking that developed in two girders during curing,

the final girders were not cast until December 21, 2006. A total of eight box girders were cast, with six used for the field bridge and two for laboratory testing.

For convenience, two box girders were cast at a time and occurred in one prestressing bed, with bulkheads separating the two girders. Thirteen prestressing strands can be seen in the bottom of the form in Figure 2.7. Strands were run the entire length of the form for both girders and stressed to a total initial force of 390 kips.



Figure 2.7. Photograph of box girder form with bottom pretension strands

Figure 2.8 shows the top reinforcing steel and the foam block used to form the girder core. The foam core formed the hollow box shape within the girder without having a significant impact on the box girder properties. Also seen in the figure are steel plates placed across the foam core. These plates provided ballast to keep the foam from rising during concrete placement.



Figure 2.8. Photograph of top of beam reinforcing and foam core

Two lifting loops were cast into the ends of each girder and are shown in Figure 2.9. The lifting loops consisted of two 1/2 in. 270 ksi strands placed 1 ft-3 in. from the girder ends. The lifting loops were to be cut off at or slightly below the girder surface once the girders were set in place at the bridge site. Also seen in Figure 2.9 is the end reinforcing steel and the termination of the foam core at approximately 2 ft-6 in. from the girder end.

The midspan transverse tie duct is shown in Figure 2.10. A duct with an inside diameter equal to 3 in. was used. The duct provided a space for the 1 in. diameter threaded rods used for lateral post-tensioning of all box girders.



Figure 2.9. Photograph of end reinforcing and lift points



Figure 2.10. Photograph of midspan transverse tie duct

The box girders were cured for 18 hours prior to releasing the prestressing force. The concrete was to have a compressive strength equal to at least 3,587 psi at release. Heat was provided at the ends of the formwork and blown along the length of the girders during curing. The relative humidity during curing was specified to be 75%. A girder being removed from the forms after curing is shown in Figure 2.11.



Figure 2.11. Photograph of crew lifting girder out of forms

2.3 Field Construction Observations

The research team was not present during the construction of the precast abutment cap beam. However, the contractor stated the placement of cap beam went relatively quickly and no major problems were encountered. The contractor did state when driving the piles that close attention must be paid to the location and tolerances of the pile head. Pile heads could not deviate from the specified plan locations more than 3” in any direction in order to allow easy installation of the precast beam. **Figure 2.13** displays some of the steps required to install the precast pile cap beam.



a. finished installation of steel piles



b. lifting of precast abutment cap

Figure 2.12. Photographs of precast pile cap beam installation



c. finished precast abutment

Figure 2.13. Photographs of precast pile cap beam installation

Figure 2.15 shows some of the processes involved in erecting the box girders. The girders were delivered individually to the site on a flatbed trailer. Fifteen to twenty minutes were spent unloading and placing each girder. The longest process during erection was eliminating any difference in elevation at the joints of adjacent girders by adding neoprene pad shims between the girder and cap beam. After each successive girder was placed, the transverse tie rod was thread through the girder. When the placement of all the girders was complete the tie rod was hand tightened to apply a transverse post-tensioning force to the girders. The girders were secured to the abutments by two vertical dowel bars that were drilled and placed in the abutment cap beam. Erection completed with the grouting of the longitudinal keyways, dowel bars connections, and transverse tie rod duct.



a. delivery of box girder to site



b. moving box girder into place

Figure 2.14. Photographs of box girder placement sequence



c. placing girder into final position



d. box girders in final position

Figure 2.15. Photographs of box girder placement sequence

3. LABORATORY TESTING

Laboratory testing conducted during this work included concrete material testing, testing to determine the influence of transverse post-tensioning, flexural capacity testing, shear capacity testing, and guardrail connection strength testing. One of the two precast box girders used for this testing sequence is shown in Figure 3.1.



Figure 3.1. Photograph of a precast box girder used for laboratory testing

3.1 Concrete Strength Test

Three concrete cores were obtained to determine the concrete compressive strength of the box girders. Cores were taken once all subsequently described tests were completed. Locations of the cores are shown in Figure 3.2 (labeled as “A”, “B”, and “C”). All cores were taken from the midspan of the girder at locations above the post-tensioning duct. This location allowed a specimen of the appropriate length to be obtained and easily removed after coring.

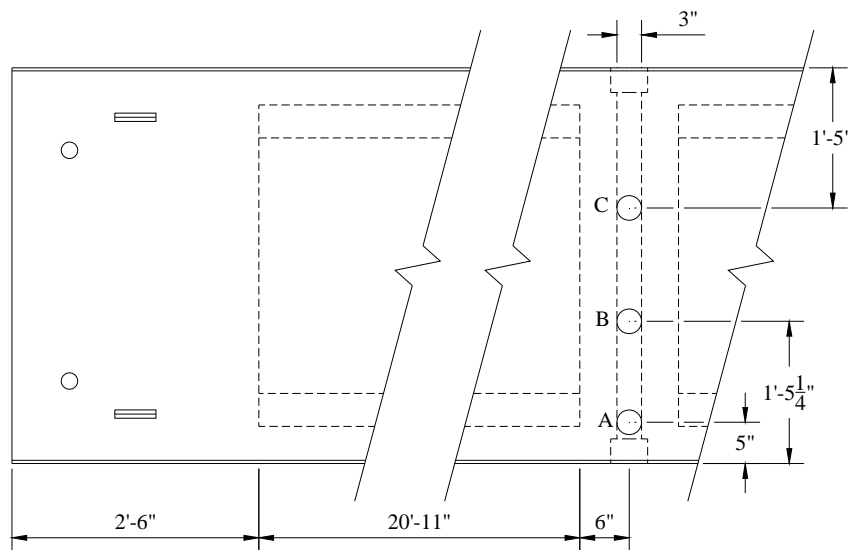


Figure 3.2. Box girder concrete core locations

The provisions of ASTM C 42 were strictly followed when obtaining the three previously mentioned concrete cores. Cores had a diameter of 3 in. and a length of 7.25 in. at the time taken. Once removed from the girder, both ends of the core were cut to leave a 6 in. specimen. The cores were then tested in accordance with ASTM C 39 to determine the compressive strength of the concrete.

3.2 Variable Post-Tensioning Force Test

The objective of the variable post-tensioning force test was to determine the amount of post-tensioning force required to reduce or eliminate differential displacement between adjacent box girders and to improve the lateral load transfer between adjacent girders. Figure 3.3 illustrates the setup for this testing. First, abutments allowing sufficient space for deflection transducers below the girders were positioned to provide the desired span length. Once the abutments were set, pin and roller connections were placed. Two box girders were then positioned as shown in Figure 3.3b. Next, a shear key was cast. In this case Five Star Grout was used for the shear key. After allowing the shear key adequate time to cure and obtain a constant compressive strength equal to 7900 psi, the post-tensioning force was applied at midspan.



a. abutment and roller placement



b. placement of girders on supports



c. girders with the shear key cast.



d. post-tensioning bar and jack

Figure 3.3. Photographs of laboratory setup for variable post-tensioning force tests

Presented in Table 3.1 are the post-tensioning forces applied during testing. A 1 in. diameter Dywidag bar was used to apply the force to the girders. Testing began with application of the

largest post-tensioning force and ended with no force. This sequence was utilized to postpone damaging the shear key. After these tests concluded, a set of tests were conducted with the combination of no shear key (removed by splitting apart the girders with a crane and chipping away the shear key grout with a chipping hammer) and a hand-tight post-tensioning force.

Table 3.1. Post-tensioning forces applied during testing

Condition	Force (kips)
No bar	0
Hand-tight	4.3
20% of F_y	11.8
30% of F_y	17.7
40% of F_y	23.6
50% of F_y	29.5
70% of F_y	41.3

Point loads were applied at 1/8, 1/4, 3/8, and 1/2 the length of the span longitudinally (sections A, B, C, and D in Figure 3.4). Transversely, the loads were applied at the center of each girder and at a distance of 1 ft- 4 in. from the exterior edge of the girder (positions 1, 2, 3, and 4 in Figure 3.4). With this arrangement 16 load positions were evaluated. The designation of each of these load locations is given in Figure 3.4. The 1 ft- 4 in. distance was chosen to place the load as close as possible to the girder edge without being directly on a concrete strain gage.

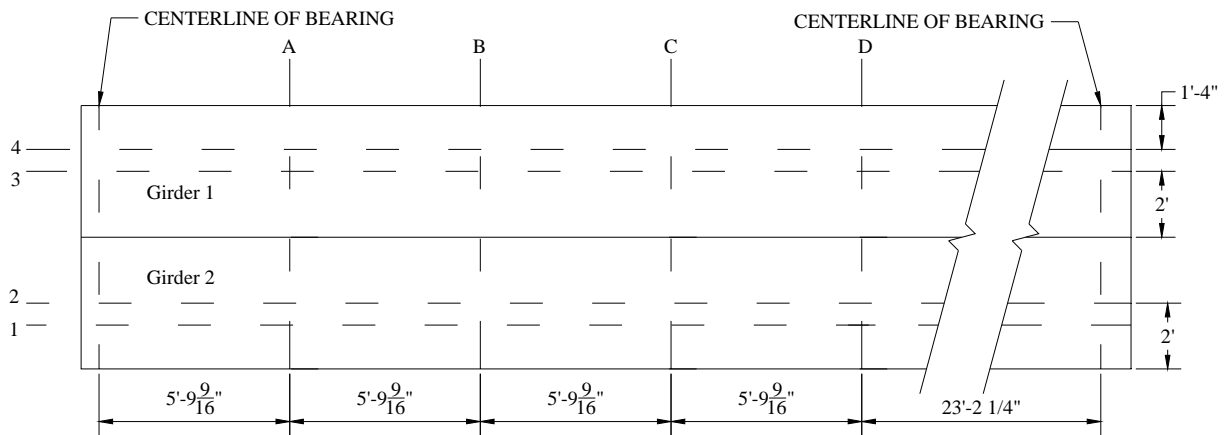


Figure 3.4. Variable post-tensioning loading locations

A 10 in. by 20 in. steel plate was used to transfer the load to the box girders for this series of tests. This footprint was selected to simulate that of the tandem truck wheel. Neoprene pads were placed between the steel plate and the girder in an attempt to more equally apply the load to the girder surface. The tandem wheel footprint along with the load cell and hydraulic load cylinder are shown in Figure 3.5.



Figure 3.5. Photograph of tandem wheel footprint used during the variable post-tensioning force tests

The total vertical load applied at each load point was 32 kips. Data were recorded in 4 kip increments. Instrumentation on each girder included 10 deflection transducers and 12 concrete strain gages (a total of 20 deflection transducers and 24 strain gages). Deflection transducers were located at locations 1/8, 1/4, 3/8, 1/2, and 3/4 of the span length and were placed 1 in. from each girder edge. Concrete strain gages were installed at the quarterspan and midspan, 4 in. from the girder edge. Strain gages were placed on the top and bottom girder surfaces. Figure 3.6 shows the instrumentation grid for this series of tests.

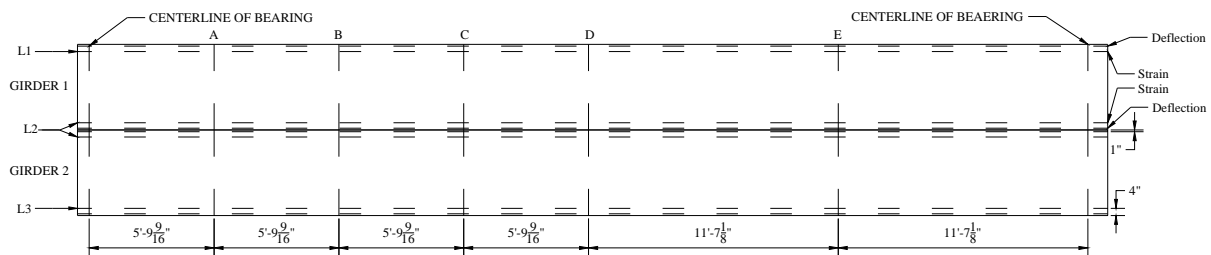


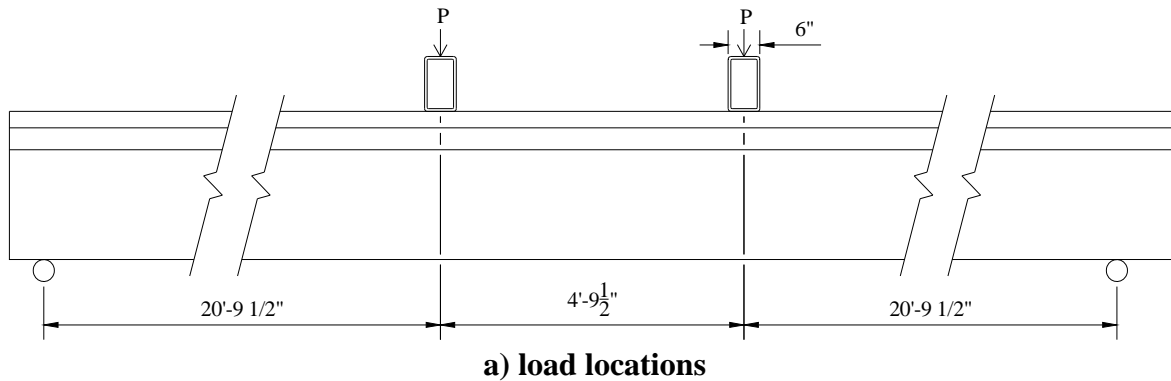
Figure 3.6. Instrumentation grid for variable post-tensioning force tests

Examples for gage names for this test are G1L2C.CB and G2L3D.T. The name consists of four parts: first is a G1 or G2, representing if the gage is connected to girder 1 or girder 2; second is L#, explaining which longitudinal line the gage is on, L1, L2, or L3; third is a letter A, B, C, D, or E to represent the transverse line located at 1/8, 1/4, 3/8, 1/2, and 3/4 the span length, respectively; and finally a .CT, .CB, or T standing for the type of gage and surface, a concrete strain gage on the top surface, concrete strain gage on the bottom surface, or a deflection transducer, respectively.

3.3 Flexural Strength Test

The goal of this testing was to experimentally determine the flexural strength of a single box girder. In order to test the box girder in a moment only condition, two line loads were applied equidistant from the supports. By doing this, a region of constant moment and zero shear was developed between the applied loads. Loads were positioned 20 ft-9.5 in. from the supports and

4 ft-9.5 in. apart. An HSS10x6x1/4 served as the footprint for the line load. The setup and spacing of loads for the flexural strength test is shown in Figure 3.7.



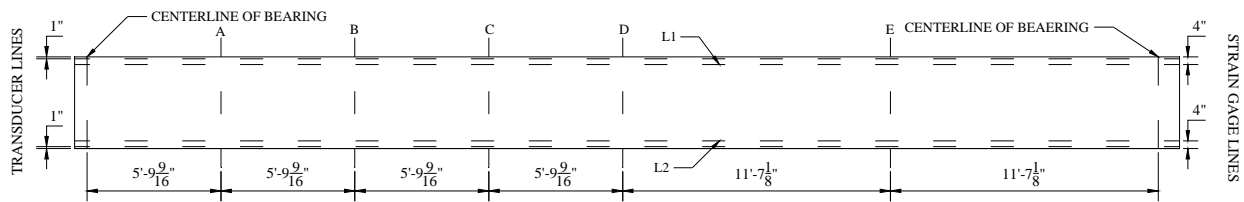
b. photograph of test setup



c. photograph of load points

Figure 3.7. Laboratory setup to test flexural strength of a box girder

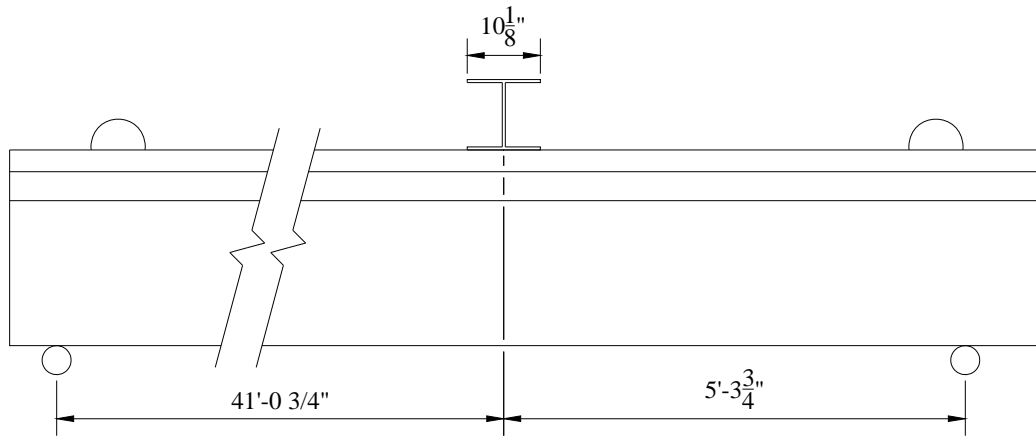
Instrumentation used for this test included ten deflection transducers and twelve strain gages. Locations for the gages are shown in Figure 3.8. Deflection transducers were located at points 1/8, 1/4, 3/8, 1/2, and 3/4 of the girder span and 1 in. from the longitudinal girder edges. Strain gages were attached at quarterspan and midspan, at a distance of 4 in. from the longitudinal girder edge.



3.4 Shear Strength Test

The goal of this test was to experimentally determine the shear strength of a single box girder. The same girder that was tested in flexure was used for the shear test. For this testing an

HP10x42 beam was used to apply a line load to the girder a distance of 5 ft-3.75 in. from the support. Figure 3.9 shows the load location and general setup for the test.



a. location of load



b. photograph of test setup

Figure 3.9. Shear strength test setup

Instrumentation used for this test includes twelve concrete strain gages, ten deflection transducers, and eight strain rosettes. Locations for the twelve concrete strain gages and ten deflection transducers are shown in Figure 3.10. Deflection transducers were placed at the 1/8, 1/4, 3/8, 1/2, and 3/4 points longitudinally, and strain gages were at the 1/4, 1/2, and 3/4 points.

Four rosettes were installed on each web of the tested girder, resulting in eight rosettes total and a total of 24 strain measurements. Locations for the rosettes shown in Figure 3.11 were selected with the goal of developing a shear crack between the rosettes. An example of a rosette number is R1N, with R1 located at the position shown in Figure 3.11a and N indicating the rosette is on the north web of the girder.

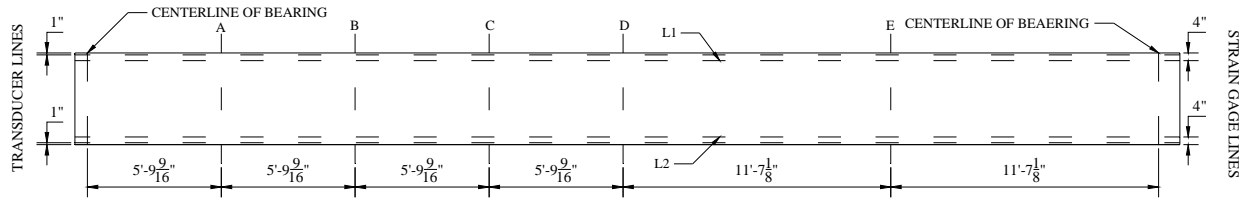
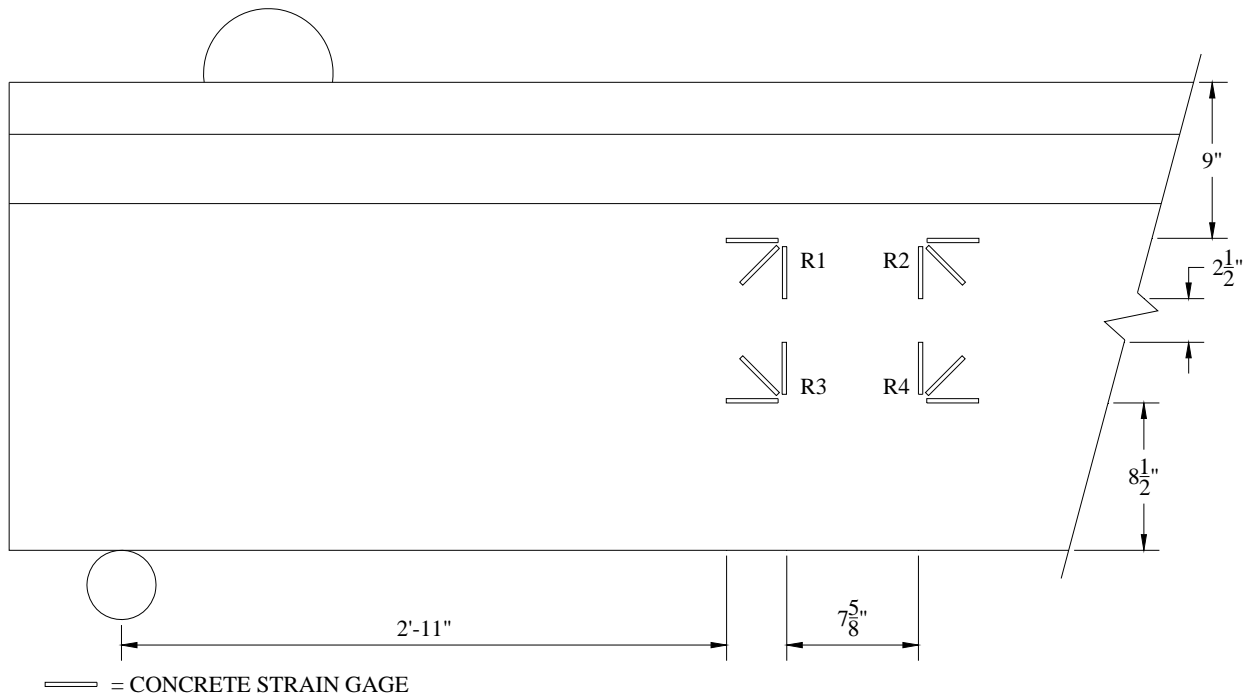
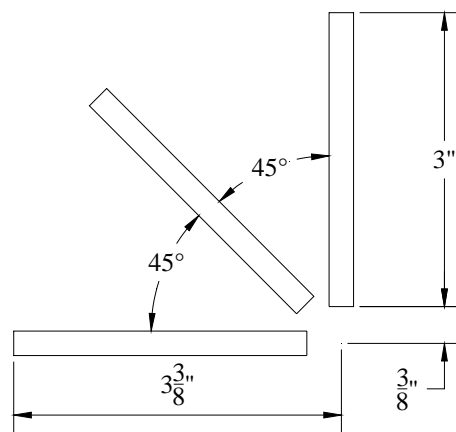


Figure 3.10. Transducer and concrete strain gage grid for shear strength test



a. rosette positions



b. rosette configuration

Figure 3.11. Rosette layout for shear strength test

3.5 Guardrail Connection Test

To test the guardrail system, six posts and two guardrail sections were connected to a box girder for testing. This allowed for four test locations, shown in Figure 3.12, to be examined. Test 1 and 3 involved loading the guardrail between two posts, posts 1 and 2 and posts 5 and 6, respectively. The load was applied directly to post 4 for test 2 and to post 3 for test 4.

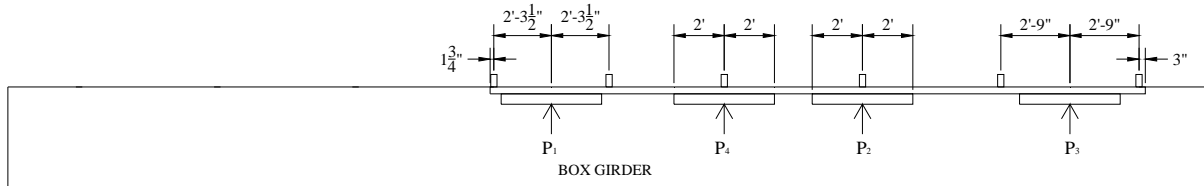
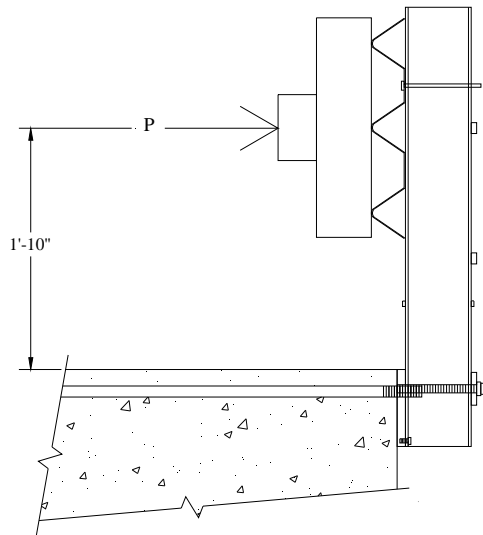


Figure 3.12. Guardrail connection test load locations

Load was applied at a height of 20 in. above the box girder surface, as shown in Figure 3.13. A timber box with a 48 in. length, 20 in. width, and 5 in. depth was used to apply the load to the guardrail. The box was 48 in. long to meet AASHTO requirements for transverse design forces for guardrails. Figure 3.13 shows the test setup.



a. profile view of test setup

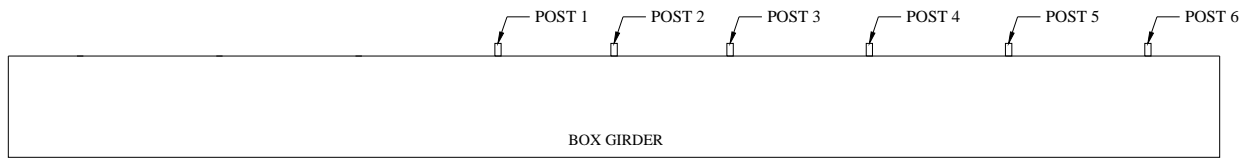


b. photograph of laboratory setup

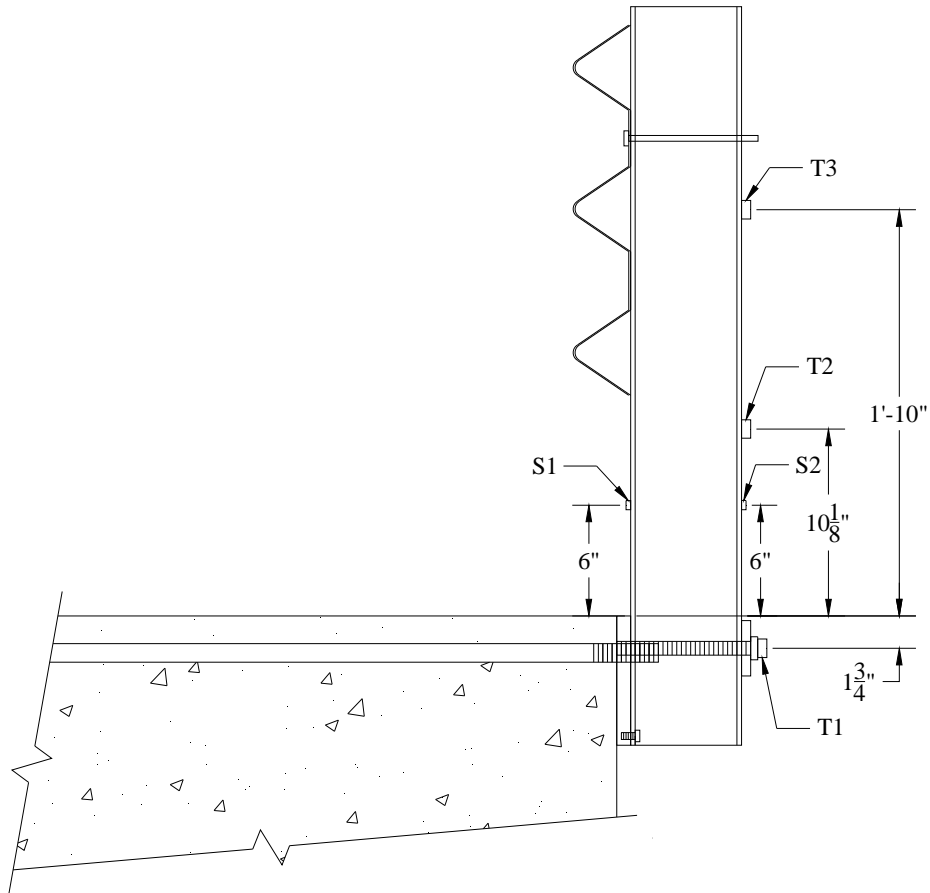
Figure 3.13. Guardrail connection test setup

All six guardrail posts and connections were instrumented for the guardrail strength tests. Figure 3.14a shows the order the posts were numbered and how they will be referred to herein. Figure 3.14b shows where the instrumentation was installed. Two steel strain gages and three deflection transducers were installed on each post. Strain gages were attached 6 in. above the surface of the box girder on opposite faces of the post. Deflection transducers were connected at 22 in. above the box girder surface, on the 3/4 in. connection bolt, and at 10 1/8 in. above the box girder

surface. An example of a gage number for a post gage is 3S2, which represents post 3, a steel strain gage, and gage 2.



a. guardrail post numbering system



b. guardrail post instrumentation locations

Figure 3.14. Guardrail post instrumentation

4. LABORATORY TEST RESULTS

The following chapter presents an analysis and summary of the results obtained from the previously described laboratory testing. Presented here are concrete strength results, variable post-tensioning force results, girder flexural and shear strength results, and guardrail connection capacity results.

4.1 Concrete Strength Test Results

Compressive strength results for the concrete cores taken from the box girder are presented in Table 4.1. The compressive strengths ranged from 10,150 psi to 11,550 psi. In this work 11,000 psi (the average of the three tests) was used for calculations requiring a concrete compressive strength.

Table 4.1. Box girder concrete core strengths

Core	Compressive Strength (psi)
A	10,150
B	11,260
C	11,550
Average	11,000

4.2 Variable Post-Tensioning Force Test Results

Figure 4.1 presents the strains at midspan for the case of a load applied at location D1 (see Figure 3.4) and a post-tensioning force of 17 kips. The 17 kip results are representative of the results for any post-tensioning force, as the strain did not vary significantly with the post-tensioning force. Loading along line “D” resulted in the highest magnitude strains.

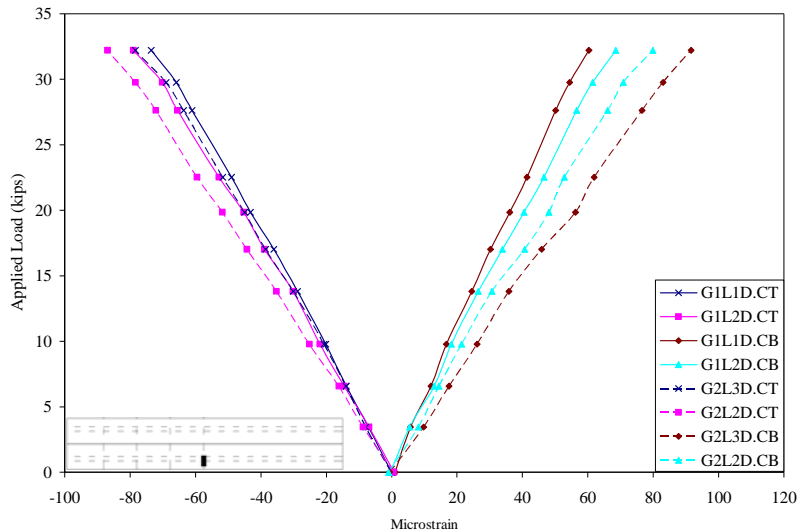
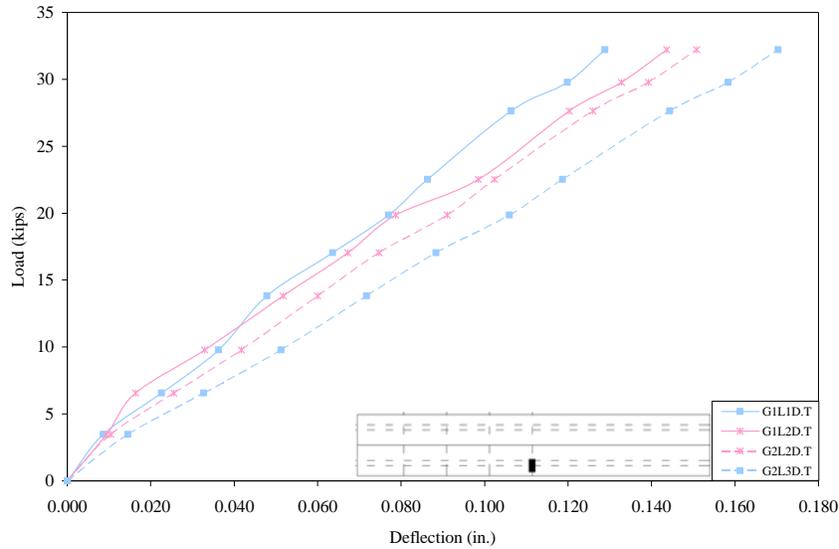


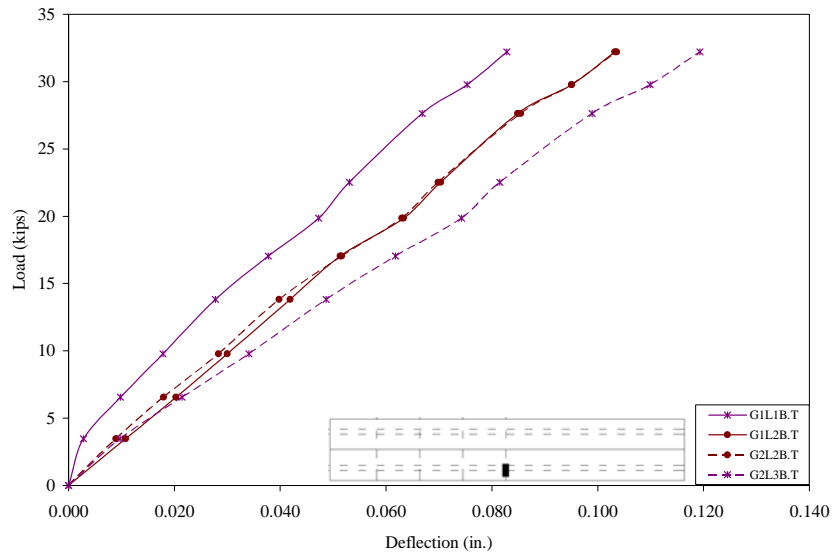
Figure 4.1. Total strain at midspan with load at D1 and a post-tensioning force of 17 kips

From Figure 4.1, one can see the induced strains were small in magnitude. Cracking did not occur during this test (or any of the variable post-tensioning tests). Strains along line 2 were similar in magnitude from girder 1 to girder 2, which shows the load is being transferred between the girders.

Measured deflections for a load at D1 and post-tensioning force of 17 kips are shown in Figure 4.2. As with the strain results, results for this location are typical of all combinations of load along line “D”.



a. deflections at midspan



b. deflections at quarterspan

Figure 4.2. Deflection results at point D1 with a 17 kip post-tensioning force

Figure 4.2 shows deflections were largest directly below and in the vicinity of the load. Deflections also generally increase linearly with increasing load. Transducers along line 2, which were located on either side of the shear key, recorded similar deflections for each box girder. This would indicate that there is minimal differential movement between the girders at the shear key.

Table 4.2 presents a summary of the differential deflections calculated from the transducers located along line 2 for the different post-tensioning force levels. All the results are for a load at location D1. The data do not support the theory of a decreased post-tensioning force resulting in an increased differential deflection. Instead, the differential deflections are consistent, with those at midspan (L2D) being the only exception. Midspan differential deflections do not show a trend; rather, the differential deflection increased significantly when decreasing the post-tensioning force from 29.5 kips to 23.6 kips, but then tended to decrease as the force decreased.

Table 4.2. Differential deflection for load point D1 and various post-tensioning forces

PT Force (kips)	L2A (in.)	L2B (in.)	L2C (in.)	L2D (in.)	L2E (in.)
41.3	0.005	0.001	0.003	0.001	0.001
29.5	0.001	0.000	0.002	0.003	0.000
23.6	0.000	0.002	0.002	0.011	0.000
17.7	0.000	0.001	0.004	0.007	0.002
11.8	0.002	0.005	0.002	0.006	0.002
4.3	0.002	0.000	0.004	0.004	0.003
0	0.004	0.001	0.003	0.010	0.001

Presented in Figure 4.3 and Figure 4.4 are the load fractions for a load at D1 for the various post-tensioning levels. Figure 4.3 shows the load fractions calculated from the midspan deflections, and Figure 4.4 shows the load fractions for the deflections at quarterspan. In both cases the figures show the load fraction plotted against the post-tensioning force.

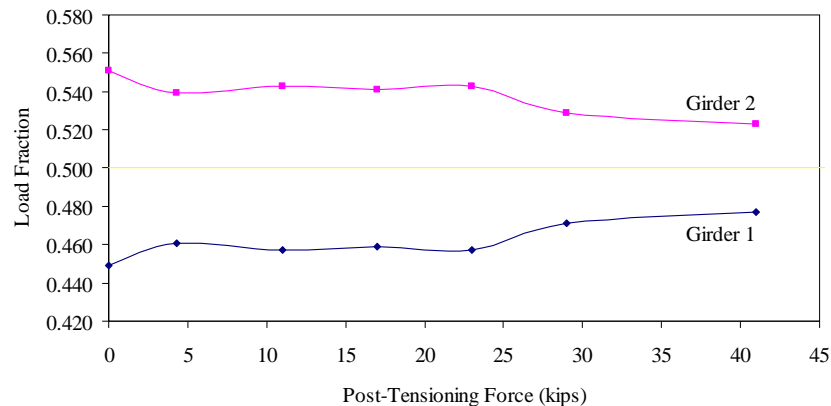


Figure 4.3. Load fractions at midspan for various post-tensioning forces and load at D1

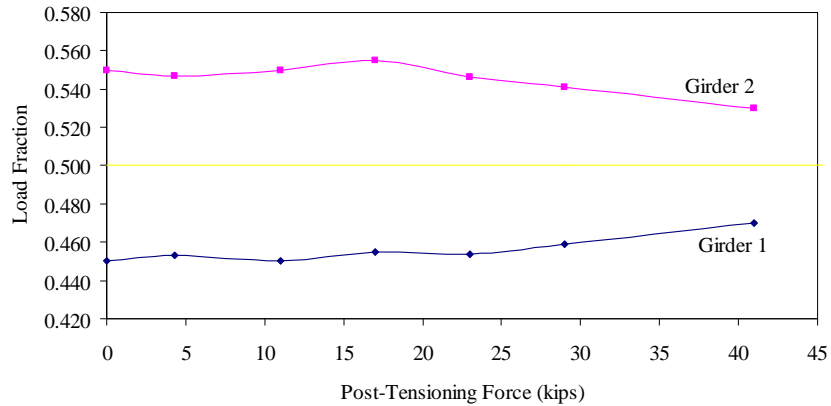


Figure 4.4. Load fractions at quarterspan for various post-tensioning forces and load at D1

Comparing Figure 4.3 and Figure 4.4 one can see that the load is being transferred equally along the entire length of the box girders. Also shown is that a low post-tensioning force did not negatively impact the load fraction. Once the post-tensioning force reached 25 kips, the load transferred between girders increased. However, testing showed the difference in the load fractions for each girder with zero post-tensioning force and with a 41.3 kip post-tensioning force was approximately 2%, which is likely insignificant.

For comparison with Figure 4.3 and Figure 4.4, Figure 4.5 and Figure 4.6 show plots of the load fraction for a load at B1 (as opposed to at D1 in Figure 4.3 and Figure 4.4) for the deflection at midspan and quarterspan, respectively. A comparison of the figures shows load is transferred better at midspan than at quarterspan, because the midspan load fractions are closer to 0.50. This is as one would expect because the post-tensioning force was located at midspan.

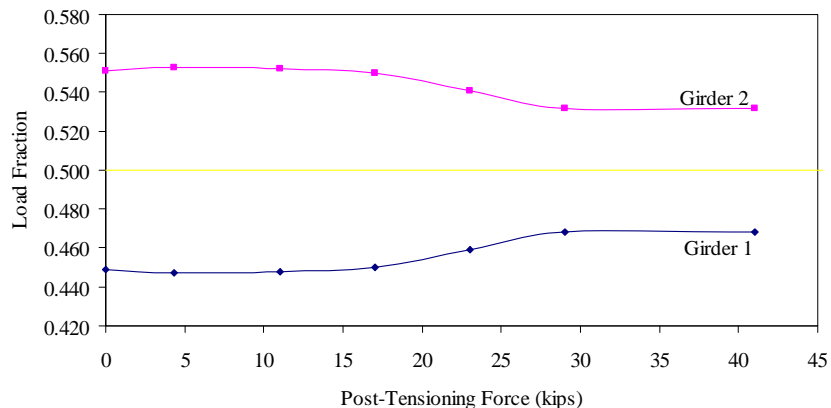


Figure 4.5. Load fractions at midspan for various post-tensioning forces and load at B1

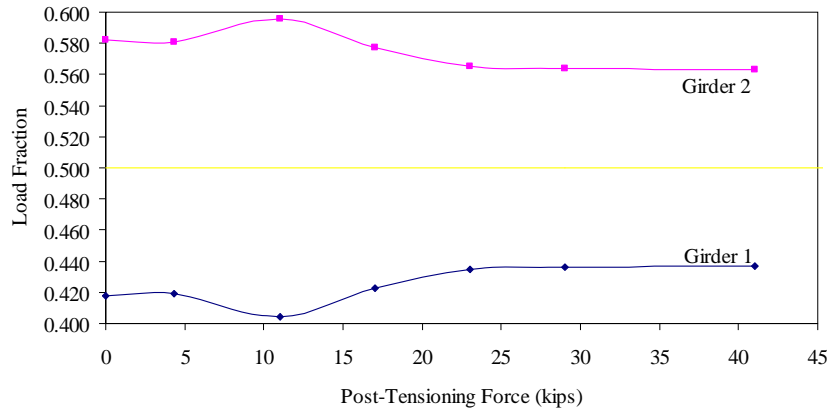


Figure 4.6. Load fractions at quarterspan for various post-tensioning forces and load at B1

Table 4.3 presents a comparison of the load fractions with and without the shear key intact for a load at D1 and a hand-tight post-tensioning force (i.e., that was used in the constructed bridge). The values illustrate the majority of the load is transferred through the shear key. Without the presence of the shear key, only 5 percent of the load was transferred to Girder 1, whereas Girder 1 carried 45 percent of the load with the shear key in place.

Table 4.3. Load fractions for a load at D1 for a hand-tight post-tensioning force

Condition	Girder 1	Girder 2
With Shear Key	0.453	0.547
No Shear Key	0.049	0.951

4.3 Flexural Strength Test Results

A photograph of the cracked box girder after testing is shown in Figure 4.7. The first cracks were observed at a load of 56.5 kips, which is equivalent to a moment of 781 kip*ft. Cracks tended to progress horizontally after reaching the shear key. Coincidentally, this is approximately the location where the chamfer began and the thickness of the web increased.

Table 4.4 presents the theoretical and experimental cracking moment values. The Iowa DOT calculated the theoretical cracking moment to be 721 kip*ft. Two different experimental cracking moments were calculated. One was calculated using the strains measured during loading and Hooke’s Law, while the other value was based on the moment due to the measured applied load. Using the measured strain value, cracking occurred at a moment of 856 kip*ft. Similarly, a cracking moment of 781 kip*ft was calculated from the applied loads. Both of the experimental values exceed the theoretical crack moment. Note that the theoretical cracking moment was calculated assuming a concrete strength of 5,000 psi.



Figure 4.7. Photograph of flexural cracking after flexure test

Table 4.4. Box girder cracking moment

Cracking Moment	Moment (kip*ft)
Theoretical	721
Experimental - From Strains	856
Experimental – From Loading	781

The theoretical and experimental capacities of the box girder are presented in Table 4.5. The theoretical flexural strength was determined by the Iowa DOT (with the same compressive strength assumption as stated previously). It should be noted that the experimental capacity is not the point at which failure occurred; the box girder was not failed in flexure. Loading was stopped at this point because of the desire to keep the box girder intact for the shear strength test.

Table 4.5. Box girder flexural strength

Strength	Moment (kip*ft)
Theoretical	955
Experimental*	962

* testing was concluded prior to failure

The moment at midspan due to the applied loading is plotted in Figure 4.8. Also plotted is the moment induced by the design HS20-44 loading. HS20-44 loading with half the load acting on the box girder and a 14 ft wheel spacing will develop a maximum moment equal to 278 kip*ft. The midspan moment exceeded the HS20-44 moment at a load equal to 26.7 kips.

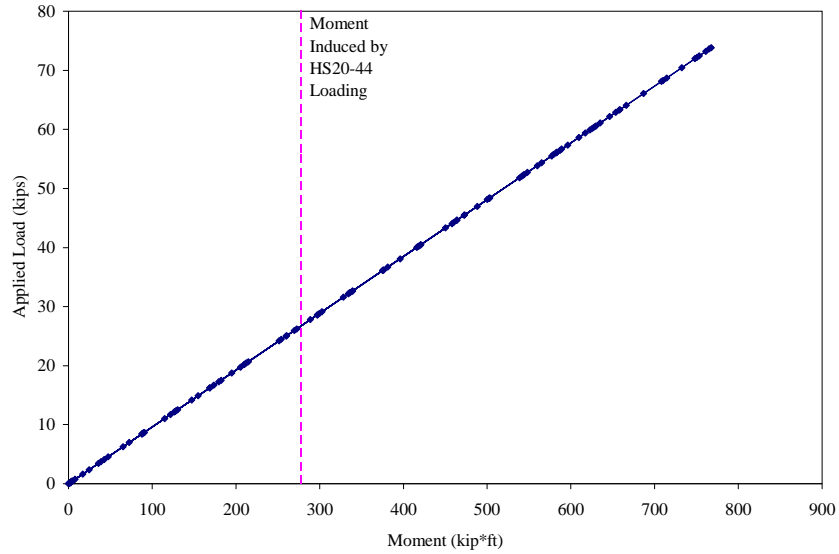


Figure 4.8. Moment at midspan of the box girder

A plot of the total stress at midspan versus the applied load is shown in Figure 4.9. These stresses are the total stress in the bottom fiber of the box girder due to the applied load, prestressing force, and self weight. When loading began, the fibers were estimated to be under an 800 psi compressive stress. This was an approximate value calculated using a concrete compressive strength of 11 ksi and a modulus of elasticity determined from an empirical relationship (Nawy, 2003). Assumptions regarding prestress losses had to be made to determine the stresses due to prestressing. Losses due to elastic shortening, creep, concrete shrinkage, and relaxation were assumed to equal 29.6 ksi.

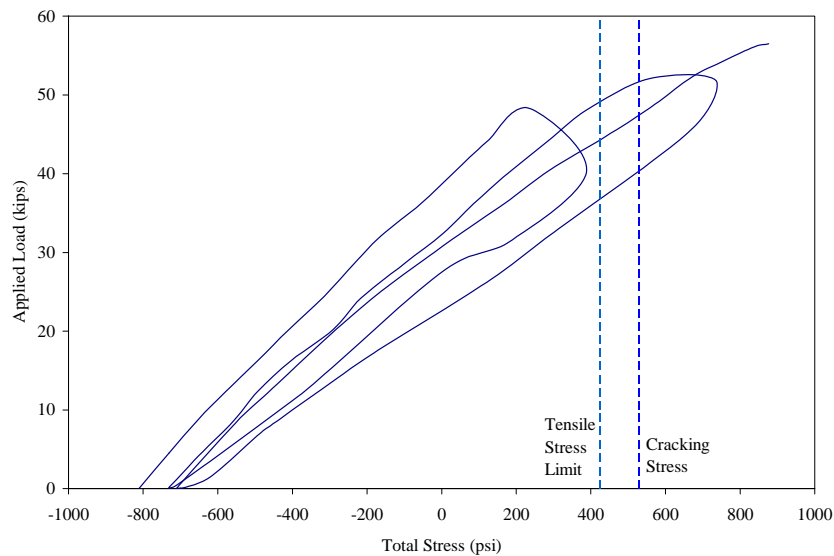


Figure 4.9. Tensile stress at midspan of the box girder

Stresses first became tensile at a load of approximately 38 kips, which exceeds the 26.7 kip applied load that develops a moment equivalent to that of the design truck. During the subsequent load cycles, the bottom fibers experienced tension at lower loads. This resulted from residual stresses in the girder due to nonlinear behavior.

AASHTO specifies a maximum service limit state tensile stress equal to 424 psi for a concrete compressive strength of 5000 psi. This stress was first exceeded with an applied load of 49 kips. The stress was exceeded at a lower applied load during following cycles, most likely due to nonlinear behavior. Tensile stresses at quarterspan never exceeded the service limit state stress.

The Iowa DOT calculated the cracking stress for the box girder was equal to 530 psi. This stress was reached at a load of 52 kips. Cracking was observed at a load of 56.5 kips.

Figure 4.10 shows the total compressive stress at midspan versus the applied load. The total compressive stress is due to the applied load, self weight, and prestressing force. Stresses were calculated by assuming prestress losses related to elastic shortening, creep, concrete shrinkage, and relaxation equal to 29.6 ksi and the using an empirical relationship to calculate the modulus of elasticity. Compressive stresses were a maximum in the top fibers at midspan. AASHTO specifies a maximum compressive stress equal to 3,000 psi for the service limit state and a concrete compressive strength of 5,000 psi. The service level compressive stress was first exceeded at an applied load of 62 kips and at lower loads during subsequent load cycles due to nonlinear behavior.

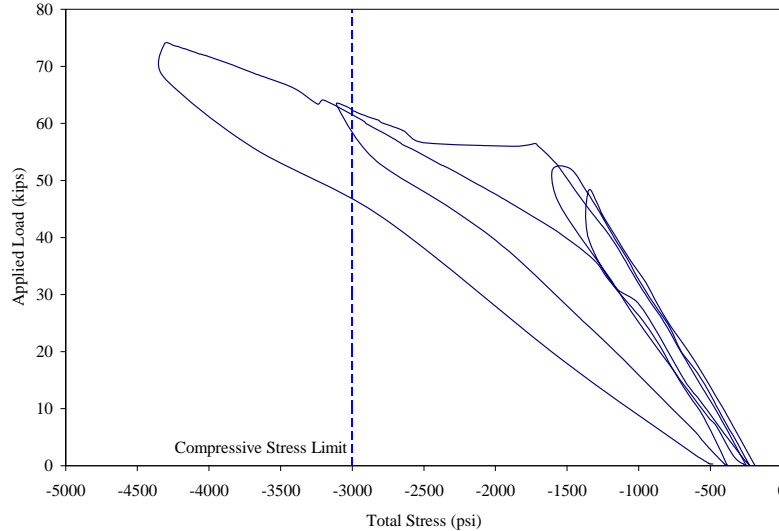


Figure 4.10. Total compressive stress at midspan of the box girder

AASHTO also specifies a maximum compressive stress for the service limit state based on the summation of the live load and one-half the sum of the effective prestress and dead load. The allowable stress is 2,000 psi for this limit state for a concrete compressive strength equal to 5,000 psi. Figure 4.11 presents the stresses for this limit state plotted against the applied load. The

service limit state compressive stress is first exceeded at a load equal to 56.5 kips and at lower loads during subsequent load cycles due to nonlinear behavior.

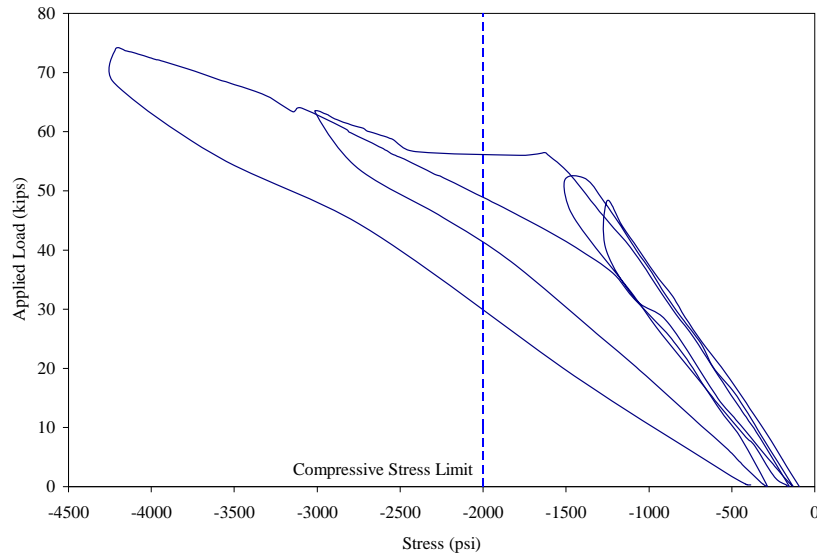


Figure 4.11. Compressive stress due to applied load and one-half the dead load and prestressing force at midspan of the box girder

In Figure 4.12 the theoretical deflection at midspan calculated by the research team is compared to the experimental deflection. The experimental results show the box girder had a lower flexural stiffness than the theoretical results predicted for higher loads. When loading ended, the deflection was 3.00 in. Theoretically, the deflection should have been 2.50 in. for the same load.

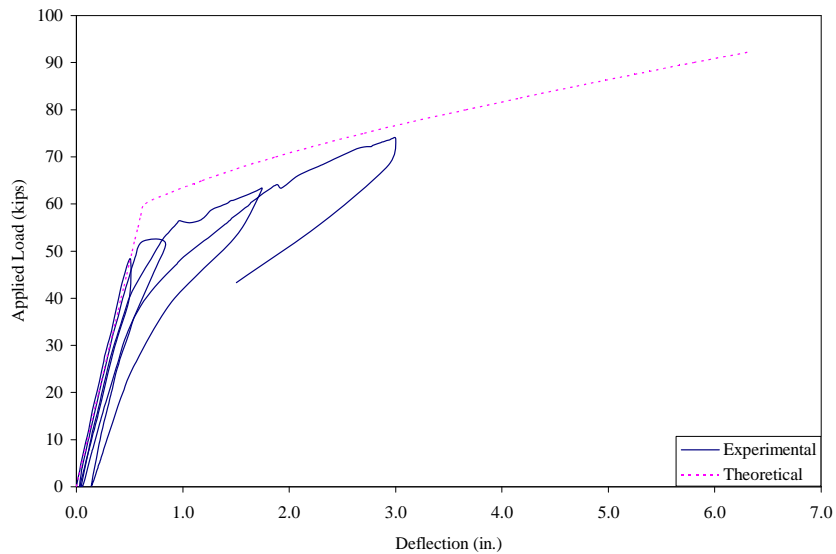


Figure 4.12. Deflection versus load plot for box girder flexural strength test

4.4 Shear Strength Test Results

Figure 4.13a shows the shear crack after testing concluded. The angle of the shear crack was measured to be approximately 45 degrees. Inspection of the failure afterwards revealed a #3 stirrup fractured at the time of failure. This can be seen in Figure 4.13b.



a. shear crack after failure



b. fractured stirrup

Figure 4.13. Photographs of box girder after shear failure

Both the theoretical and experimental box girder shear strengths are presented in Table 4.6. The theoretical shear strength calculated by the Iowa DOT was 79 kips, and the experimental shear strength was 197 kips. The discrepancy between these values is likely because the theoretical strength was calculated using a concrete compressive strength equal to 5,000 psi, not the 11,000 psi strength the concrete had.

Table 4.6. Box girder shear strength

Strength	Shear Force (kips)
Theoretical	79
Experimental	197

A plot of shear force versus the applied load is shown in Figure 4.14. Included in the figure is the maximum shear force induced by an HS20-44 loading. This shear force is equal to 27.0 kips and is reached during testing at a load equal to 30.5 kips.

The principle strains at rosette 2N due to the applied load are plotted in Figure 4.15. Strains for rosettes at the same height and on opposite webs were the same. As shown in the figure, the tensile and compressive strains were similar for equal loading until just prior to cracking. Prior to cracking the tensile strain increased suddenly, whereas the compressive strain still exhibited linear behavior. The maximum compressive strain was 138 microstrain, and the maximum tensile strain was 150 microstrain.

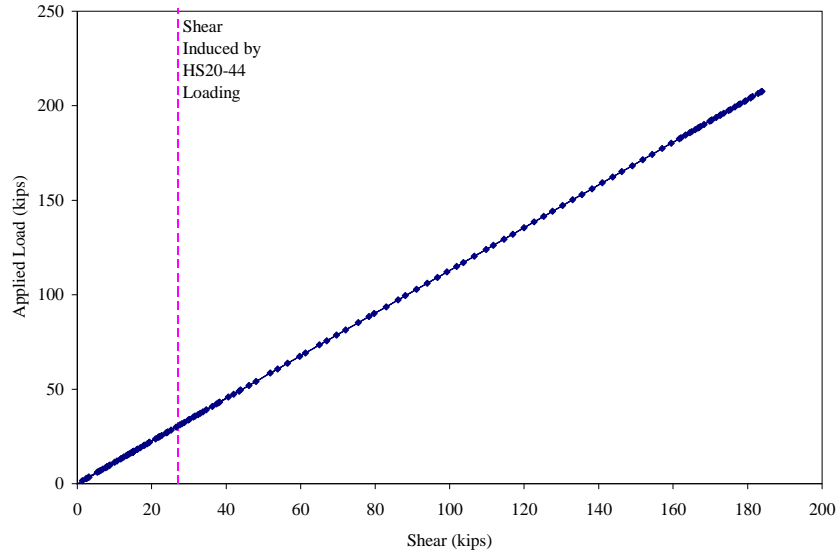


Figure 4.14. Shear force in the box girder

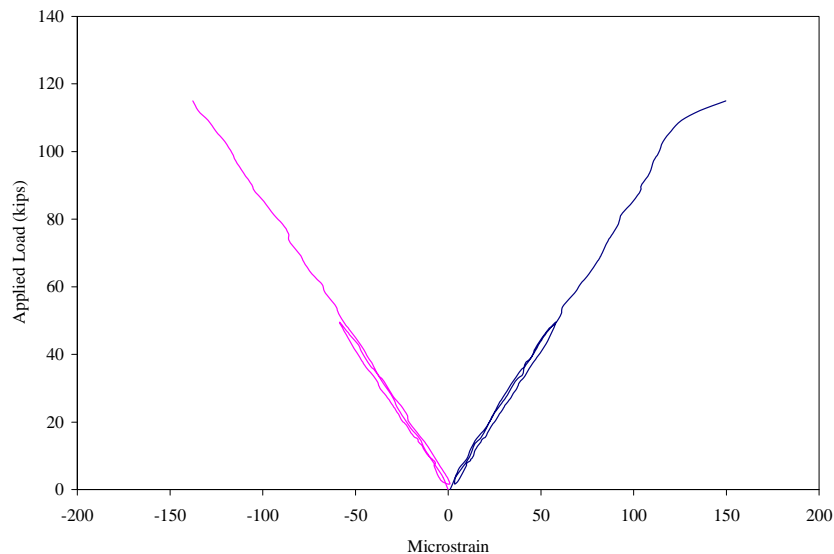


Figure 4.15. Principle strains due to applied load at rosette 2N during shear strength testing

Figure 4.16 displays the total principal stress plotted against the applied load for rosette 2N. Stress calculations required assumptions regarding prestress losses related to elastic shortening, creep, concrete shrinkage, and relaxation (the same assumptions used previously were made here). An empirical relationship was used to calculate the modulus of elasticity. At a load of 63.5 kips, the total tensile principal stress exceeded the AASHTO maximum allowable tensile stress for the service limit state, 424 psi. The theoretical cracking stress calculated by the Iowa DOT was 530 psi and was reached at a load of 85 kips. Cracking actually occurred at 115 kips. The difference between when cracking was predicted to occur and when cracking occurred is a

function of the theoretical value using a concrete compressive strength equal to 5,000 psi. Maximum compressive stresses specified by AASHTO for the service limit state were not approached during the shear test.

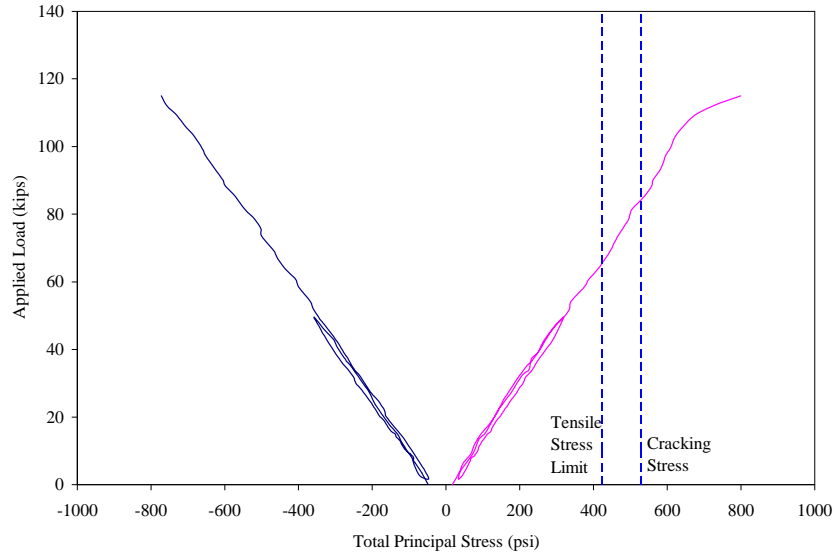


Figure 4.16. Principal stresses due to the total load at rosette 2N

Deflections measured at quarterspan during the shear test are plotted in Figure 4.17. These deflections are plotted along with two plots of theoretical deflections. The theoretical deflections were calculated by the research team. One theoretical deflection uses the gross moment of inertia for the box girder, and the second uses the final effective moment of inertia from the flexural strength test. As can be seen in the figure, the majority of the experimental deflections plot between the two theoretical curves, meaning the moment of inertia lies between the uncracked value and effective value from the flexural test. The deflection prior to failure was 2.48 in., whereas the maximum theoretical deflection was 1.98 in.

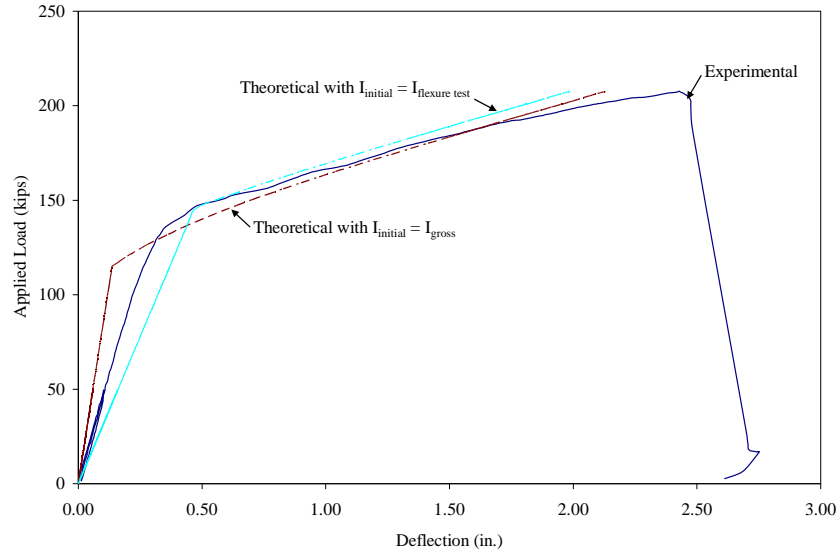


Figure 4.17. Theoretical and experimental deflections at quarterspan during shear test

4.5 Guardrail Connection Test Results

Figure 4.19 shows the components of the guardrail connection after different post failures. The base plate for each post yielded during testing. **Figure 4.19a** shows the yielded base plate for post 1, along with a longitudinal concrete crack that developed. Post 1 was the only location where longitudinal concrete cracking occurred. During loading, the portion of the post base bearing against the base plate buckled, which is shown in **Figure 4.19b**. The width of the posts was measured to have increased as much as 1/2 in. to 3.5 in. A ruptured 3/4 in. bolt from test 2 is shown in **Figure 4.19c**, and sheared base plate threads can be seen in between the threads of a 3/4 in. bolt in **Figure 4.19d**. A summary of the results for the guardrail connection tests are presented in Table 4.7. Values presented in the table include the magnitude of the maximum applied load, at which post the failure occurred, the force carried by the post, the force applied to the 3/4 in. bolt at failure, the capacity of the connection, and the failure type.



a. yielded base plate and concrete cracking



b. buckled post

Figure 4.18. Photographs of failed guardrail connection elements



c. ruptured bolt



d. bolt with sheared base plate threads

Figure 4.19. Photographs of failed guardrail connection elements

Table 4.7. Guardrail connection test summary

Test Number	Applied Load (kips)	Failed Post	Post Force (kips)	Applied Bolt Force (kips)	Connection Capacity (kips)	Failure Type
1	15.4	1	7.29	41.0	39.7	Bolt Rupture
2	16.9	4	7.45	41.9	39.7	Bolt Rupture
3	13.4	6	6.52	36.7	32.2	Sheared Threads
4	11.1	3	5.68	32.0	32.2	Sheared Threads

Loading during test 1 reached 15.4 kips. At this load, the 3/4 in. bolt connecting post 1 to the base plate ruptured. Using the strain data collected during testing, a 7.29 kip force was resisted by the post at failure. Using simple statics, this is equivalent to a tensile force of 41.0 kips in the bolt. The published strength of a 3/4 in. bolt is 39.7 kips.

The applied load during test 2 reached 16.9 kips. The 3/4 in. bolt connecting post 4 to the base plate ruptured during the test. The bolt force equaled 41.9 kips.

Failure during Test 3 occurred when the threads of the post 6 base plate sheared. The theoretical force required to shear the base plate threads was 32.2 kips, and the applied bolt force was calculated to be 36.7 kips. One explanation for this discrepancy would be the shear area of the threads exceeding the area used in the calculations.

Test 4 ended when the threads sheared from the base plate for post 3. The maximum applied load equaled 11.1 kips, which resulted in a force of 5.68 kips acting on post 3. This resulted in a force of 32.0 kips acting on the bolt.

One observation of the test results is that tests 1 and 2 exceeded the 13.5 kip AASHTO design transverse force for a level 1 bridge rail. The maximum load for test 3 was 13.4 kips, slightly less than the AASHTO design force. Loading during test 4 reached 11.1 kips, 82% of the design load. However, all tests conducted after test 1 were to a damaged specimen. Yielded base plates and ruptured bolts were not replaced between the tests. Therefore, the load in test 1 was applied to a guardrail supported by six posts, whereas during test 4 the load was distributed to three posts. This may explain the decreased capacity of the connection in tests 3 and 4. Test 2 had the largest applied load because there were posts on either side to distribute load to.

A second observation of Table 4.7 is the post where the connection failure occurred carried between 44% and 52% of the applied load. This would be expected because the location where failure occurred had the load either applied directly to the post or to the span adjacent to the post.

Figure 4.20 shows the post deflections during test 1. Post 1 underwent the largest deflection, reaching 6.34 in. prior to failure. Posts 1, 2, and 3 deflected outward from the box girder, whereas posts 4 and 5 deflected inward 0.28 in. Deflections for posts 4, 5, and 6 were excluded from the plot because they were approximately zero. Deflection 5T3 was plotted because this was the largest inward deflection, equaling 0.285 in. Minimal load reached post 6, with the post deflected outward 0.003 in. at failure. The deflected shape of the top of the guardrail immediately prior to failure is plotted in Figure 4.21.

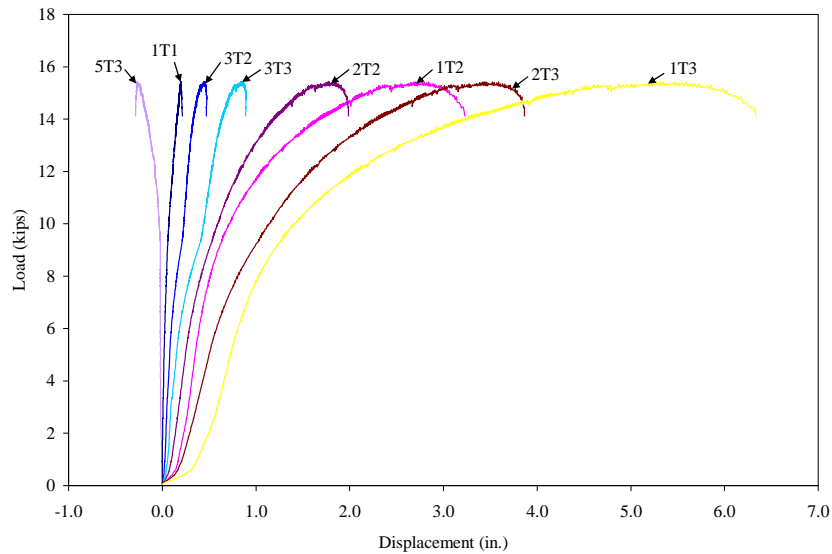


Figure 4.20. Post deflections during test 1

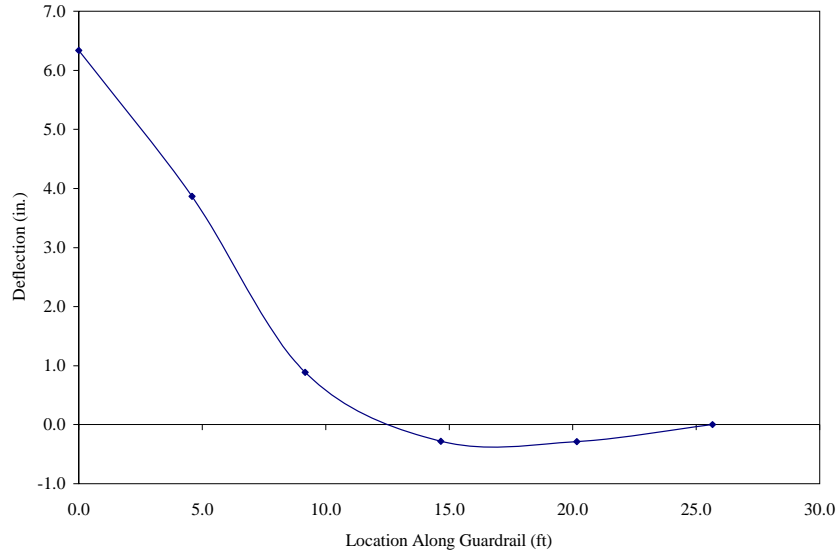


Figure 4.21. Deflected shape of the top of the guardrail at failure

Post strains recorded during test 1 are plotted in Figure 4.22. All strains exhibited a linear response under loading. Posts 1 and 2 carried the majority of the load. Post 3 did not carry any load until the applied load reached 8 kips. The maximum strain equals a stress of 20.7 ksi in post 1, which is less than the 46 ksi yielding stress. Strains for posts 4, 5, and 6 were insignificant when compared to the strains of posts 1, 2, and 3.

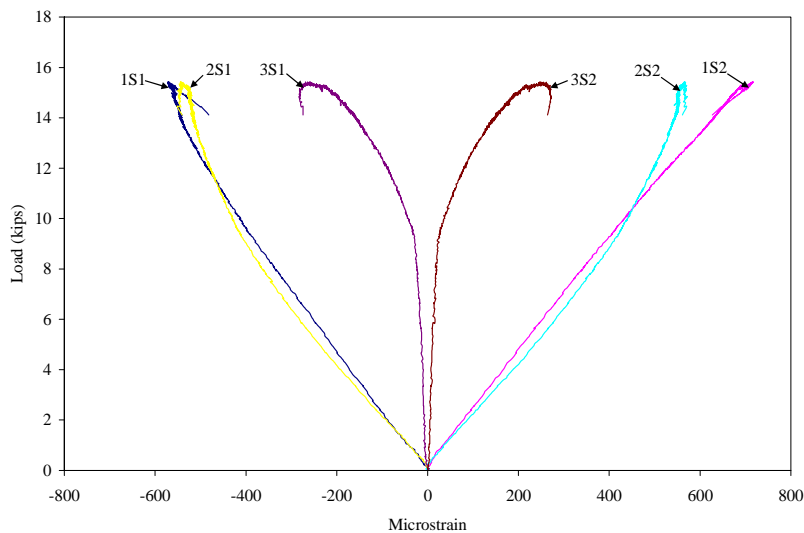


Figure 4.22. Post strains during test 1

Results for test 2 are presented to supplement those for test 1. Test 2 results better represent the field conditions because the guardrail is continuous over the entire bridge span. The load was applied next to an end post during test 1, which would not occur in the field. An interior post was

loaded for test 2, resulting in better load distribution and eliminating a free end subject to large deflections. However, the results of test 1 would represent a worse-case scenario.

Displacements for each post during test 2 are plotted in Figure 4.23. All deflections approximately equal to zero were removed from the plot for clarity. Post 4 exhibited the greatest deflections, reaching 3.99 in. Equal deflections were measured for posts 3 and 5. This was expected because the posts are located on either side of and equidistant from post 4.

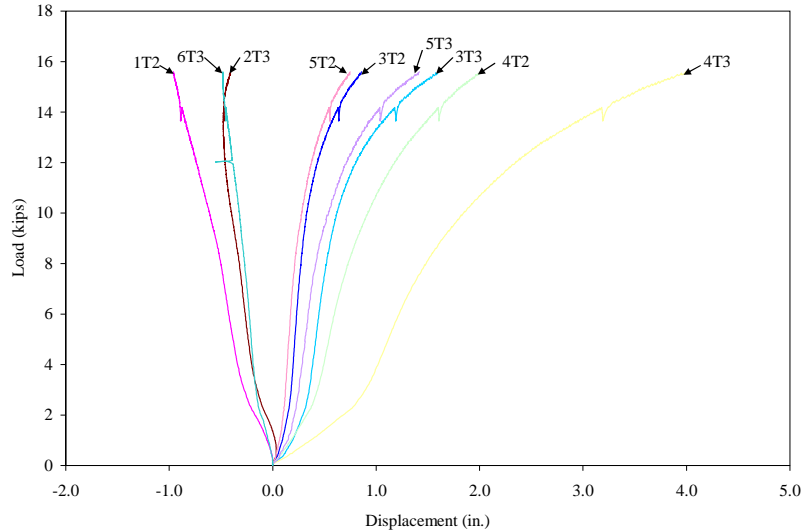


Figure 4.23. Post displacements for test 2

Deflections in the field may actually be greater than those recorded because testing had to be done in two cycles. During the first cycle, once a 15.6 kip load was applied the box girder moved horizontally. Testing was halted when this occurred and the girder was further secured to the ground. When testing resumed, the guardrail was loaded to failure. Yielding of the 3/4 in. bolt was observed following the first test cycle; therefore some of the plastic deformation capacity was used.

The deflected shape of the guardrail at a load of 15.6 kips is shown in Figure 4.24. The plotted deflections are the deflections measured at the top of each post. Post 1 is not included in the plot because the transducer measuring displacement at the top of the post had been removed after test 1. The deflected shape of the rail is symmetric. Posts 3, 4, and 5 deflected outward and away from the girder, with post 4 deflecting the farthest. Posts 2 and 6 deflected inward to a position over the girder. Figure 4.25 is a photograph showing the deflected shape of the guardrail during testing.

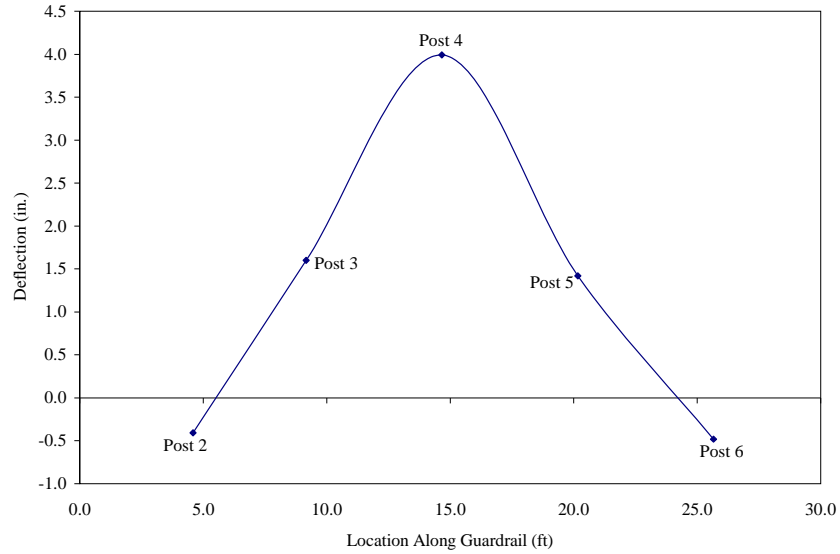


Figure 4.24. Deflected shape of the guardrail during test 2



Figure 4.25. Photograph of deflected guardrail during test 4

Strains measured in the posts are plotted in Figure 4.26. Posts 1 and 2 are not plotted for clarity because the strains were less than 20 microstrain. As expected, post 4 experienced the largest strains. The strains in posts 3 and 5 were similar during loading, with post 5 strains approaching that of post 4 near the end of the test. Posts 1, 2, and 6 were lightly strained. The maximum strain is equivalent to a stress of 18.2 ksi, which is less than the yield stress of 46 ksi.

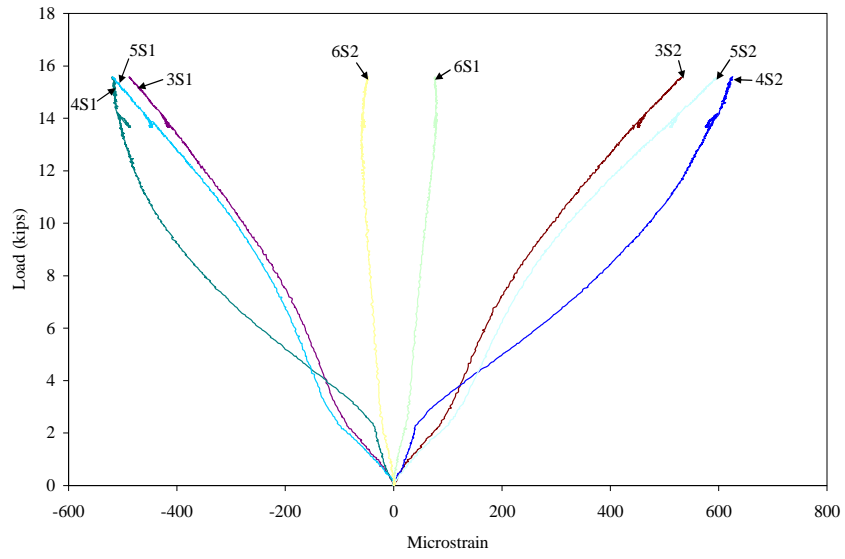


Figure 4.26. Post strains during test 2

5. FIELD TESTING

Field testing of the Madison Co. Precast Bridge took place in both 2007 and 2008 to allow for quantification of behavior changes of the bridge. The following sections describe the test procedures/protocols used for testing the bridge, and test results for the bridge.

5.1 Evaluation methodology and instrumentation

The Iowa State University Bridge Engineering Center in conjunction with Madison County and the Iowa Department of Transportation developed the monitoring and evaluation plan for the bridge. The plan entailed investigating the long term performance of individual members and joints and the long term performance and overall behavior of the completed bridge.

Instrumentation was placed at important locations to collect deflection, strain, acceleration, and corrosion data. Figure 5.1 illustrates the instrumentation layout of the bridge. Corrosion electrodes were permanently installed on two strands in each girder prior to casting. The strands that were instrumented with corrosion electrodes are located in the top corners or the bottom corners of the girder. Figure 5.1 show the electrode number and top or bottom designations of the strand location.

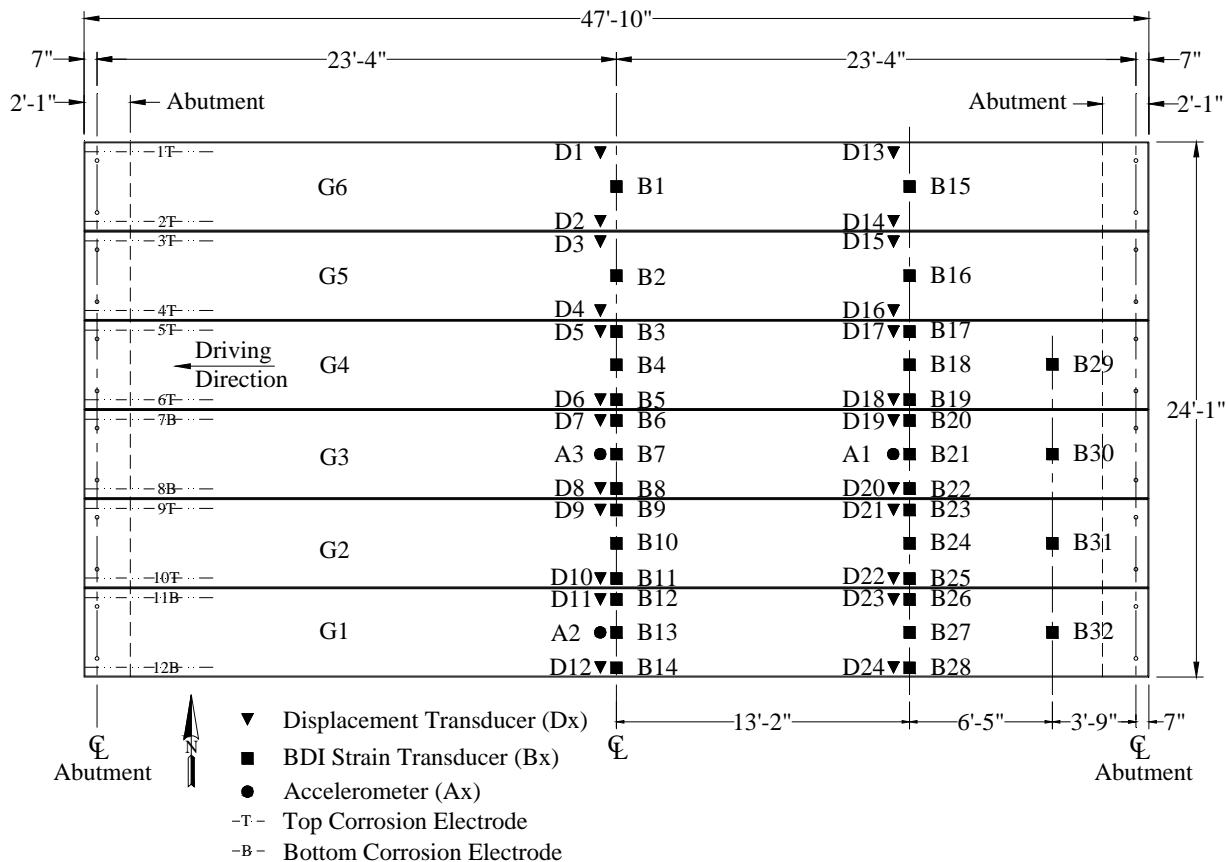
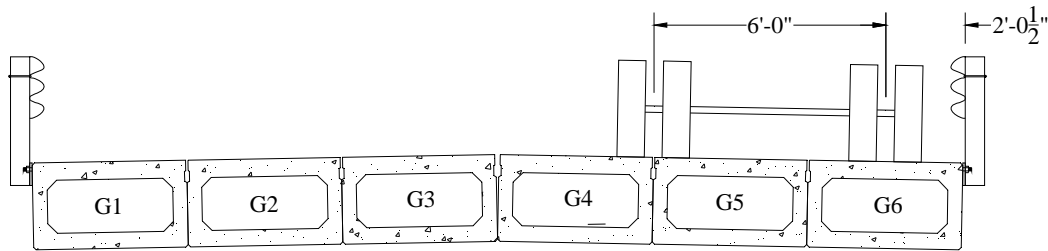
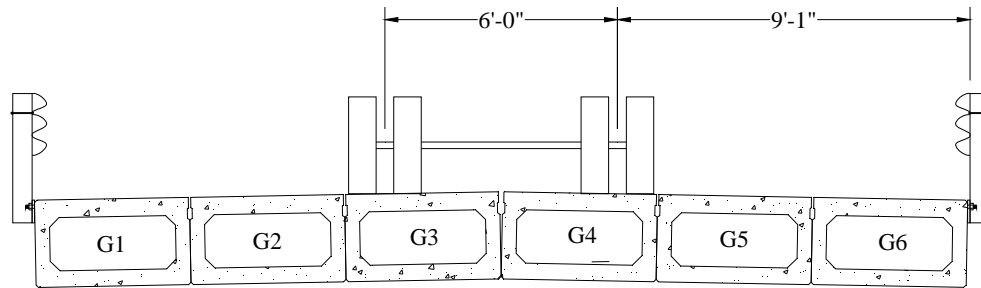


Figure 5.1. Instrumentation layout

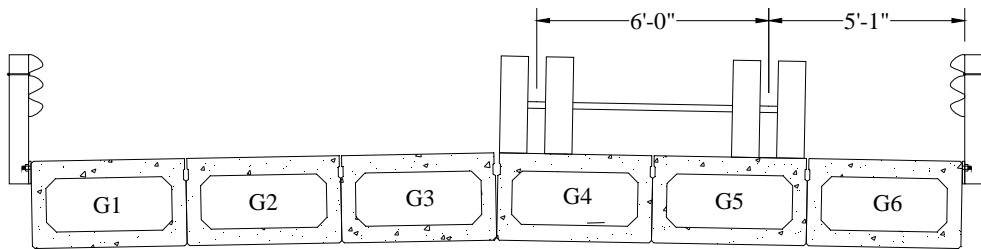
Field testing took place in 2007 and then again approximately one year later in 2008 to allow for quantification of behavior changes. In both instances the testing consisted of point in time live load testing with at fully loaded three axle dump truck that was driven over the bridge. The transverse position of the truck was varied with seven load cases(load case (LC) 1 through LC 7 in 2007), as shown in Figure 5.2. The same load cases were used in 2008 with the exception of LC 6, which is nearly identical in location and 2007 results to LC 5. The same loaded dump truck was used for both the 2007 and 2008 testing and can be seen in Figure 5.3. The axle configurations and weights can be seen in Figure 5.4. The front and rear axles were weighed in 2007 giving the axle loads shown in Figure 5.4. In 2008, however, only the total truck weight was obtained, therefore, load distribution of the 2007 truck was used to determine the 2008 axle loads.



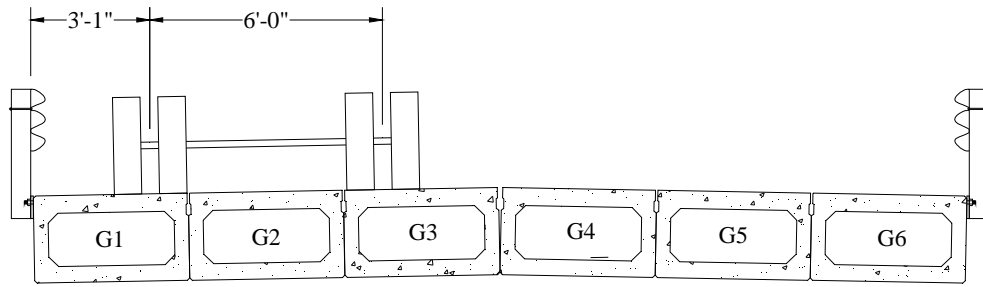
a. LC 1



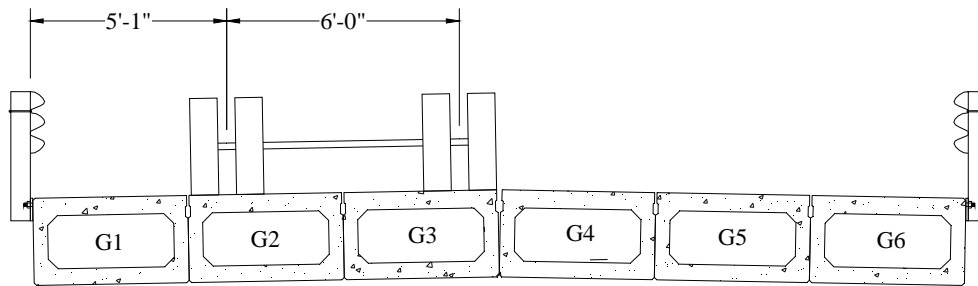
b. LC 2



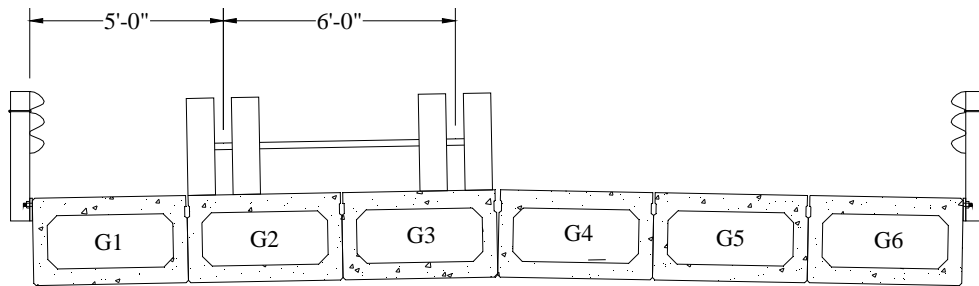
c. LC 3



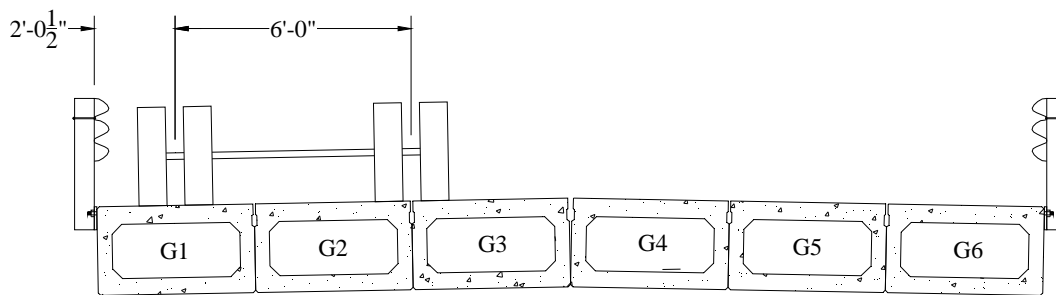
d. LC 4



e. LC 5



f. LC 6



g. LC 7

Figure 5.2. Transverse load positions: Vehicle traveled west into page

6. FIELD TEST RESULTS

Field testing of the Madison Co. Precast Bridge took place in both 2007 and 2008 to allow for behavior changes of the bridge to be studied. The following sections describe the test results for the static and dynamic testing of the bridge.

6.1 Static Loading

The seven transverse load position shown in Figure 5.2 were used for the static load testing conducted 2007. The same load cases were used for 2008 testing with the exception of LC 6. The load cases were selected to meet the goals of this project and general bridge engineering concepts. The truck traversed the bridge from east to west at crawl speeds in each load position in order to obtain displacement and strain information. The bridge response obtained from the load testing was used to determine bridge deflection, girder differential deflection, girder load fraction, girder distribution factor, fixity and neutral axis information.

6.1.1 Bridge Deflection

The maximum measured girder deflection for the load case investigated in 2007 and 2008 are show in Tables 6.1. and 6.2 respectively. In general for all load cases, the maximum deflection occurred when the trucks front axle position was approximately 40ft from the east abutment of the bridge. In 2007 the maximum girder deflection occurred at girder G1 during LC 7 with a deflection of 0.109 in. The maximum deflection during the 2008 testing also occurred during LC 7 at girder G1 with a magnitude of 0.088 in.

The code serviceability limit state for defection is $L/800$ for a bridge loaded with two HS20 trucks and an applied dynamic amplification factor (AASHTO 1998, 1996). The limit state corresponds to a maximum deflection of approximately 0.70 in. For reference the estimated deflection from design calculations was 0.33 in, with two trucks. In order to compare the field tests results with the code and design values, two load cases (LC 3 plus LC7 and LC 1 plus LC5) were added together. The maximum deflection obtained from test was then 0.15 in. and 0.13 in. for 2007 and 2008 respectively. When the load truck is normalized by weight to the standard HS20 truck and a dynamic amplification factor of 1.29 is used, the maximum deflection is 0.25 in., which corresponds to a span to deflection ratio of $L/2236$.

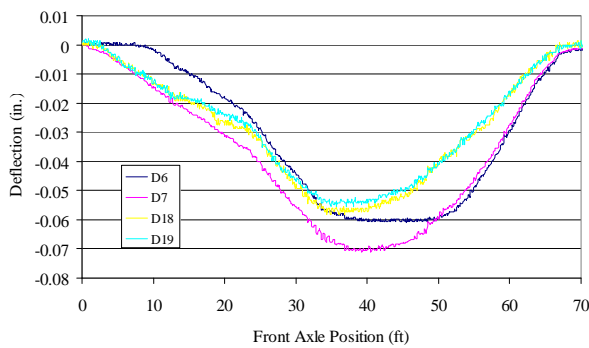
Table 6.1. 2007 Maximum midspan girder deflection

	Load Case						
	LC 1	LC 2	LC 3	LC 4	LC 5	LC 6	LC 7
Deflection (in.)	0.097	0.074	0.078	0.097	0.083	0.084	0.109
Deflection Location	G6 (D1)	G3 (D7)	G5 (D3)	G1 (D12)	G1 D(12)	G1 (D12)	G1 (D12)

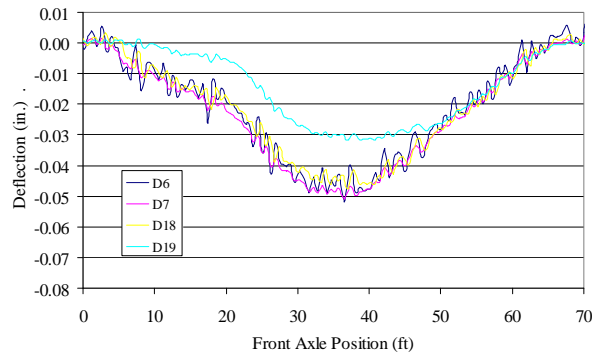
Table 6.2. 2008 Maximum midspan girder deflection

	Load Case						
	LC 1	LC 2	LC 3	LC 4	LC 5	LC 6	LC 7
Deflection (in.)	0.083	0.068	0.066	0.082	0.073	-	0.088
Deflection Location	G6 (D1)	G3 (D8)	G5 (D3)	G2 (D10)	G2 (D10)	-	G1 (D12)

Representative time-history deflections for LC 3 tests in 2007 and 2008 are shown in Figure 6.1. The time history deflection plots shows deflection at midspan and quarterspan at the joint between girder G4 and G3. Figure 6.2 shows the transverse deflection of the bridge when the longitudinal position of the truck produced the maximum deflection at the midspan for 2007 and 2008 testing. For comparison purposes all 2008 deflections shown in Figure 6.2 were normalized to the 2007 load truck weight. In general the girders that had the largest deflection were located closest to the load. Transverse load distribution is evident in Figure 6.2 as the girders adjacent to the directly loaded girders also deflecting creating a continuous deflected shape. The 2007 and 2008 testing produced nearly the same transverse deflected shape.

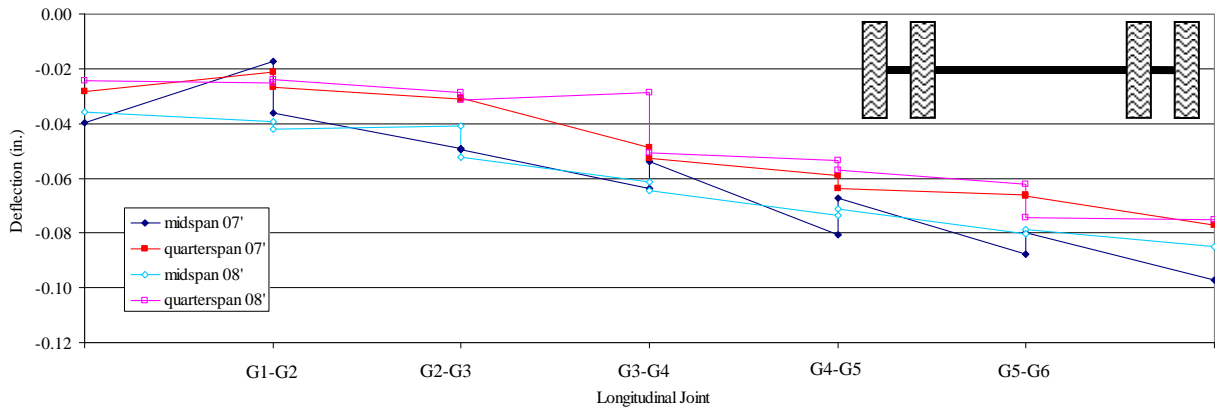


a. 2007; LC 3

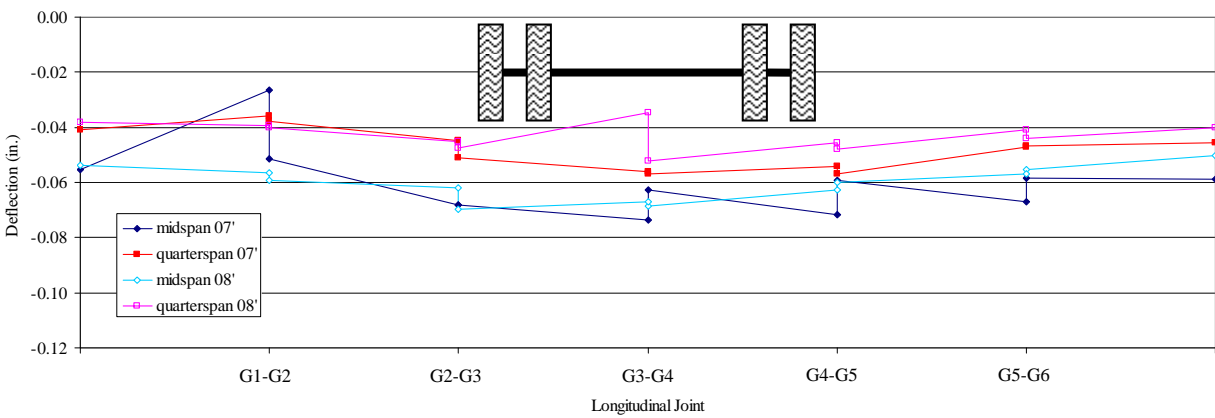


b. 2008; LC 3

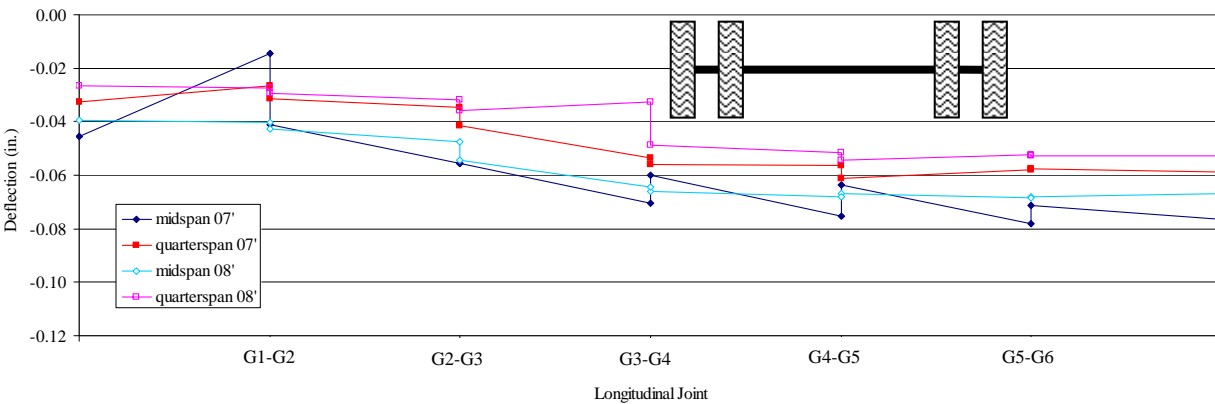
Figure 6.1. Representative time history deflections



a. LC 1

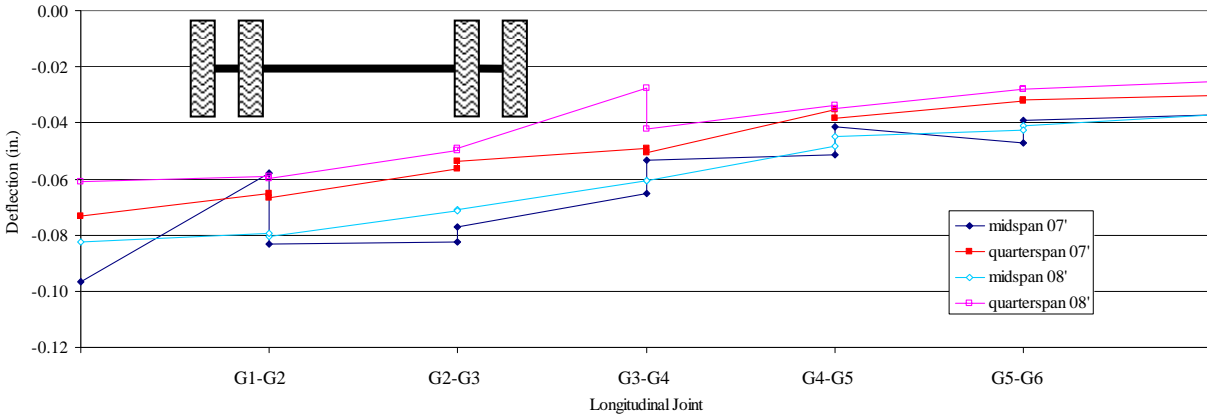


b. LC 2

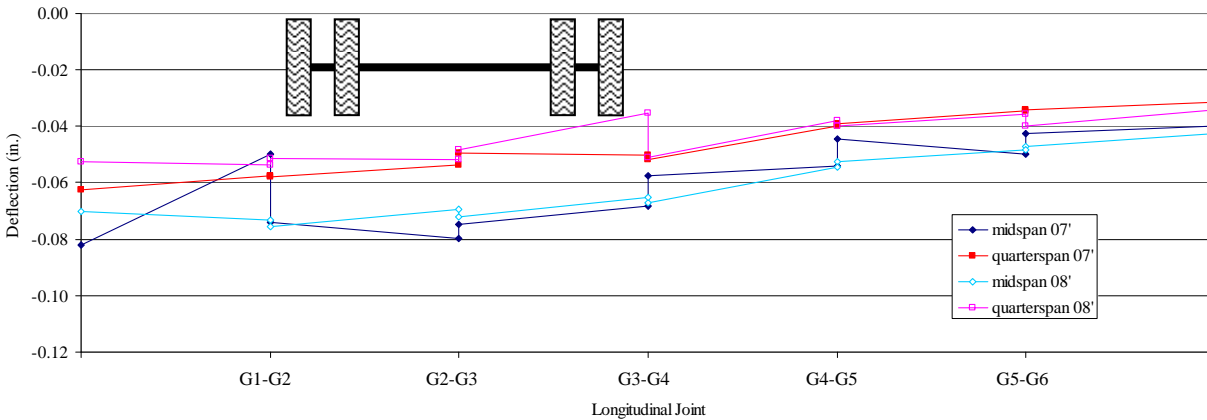


c. LC 3

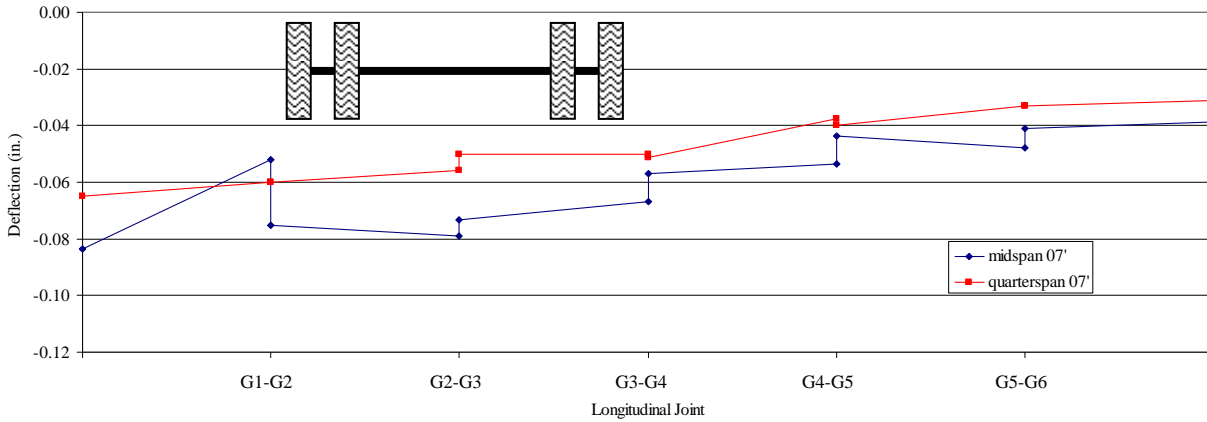
Figure 6.2. 2007 and 2008 transverse deflected shape at midspan and quarterspan



d. LC 4

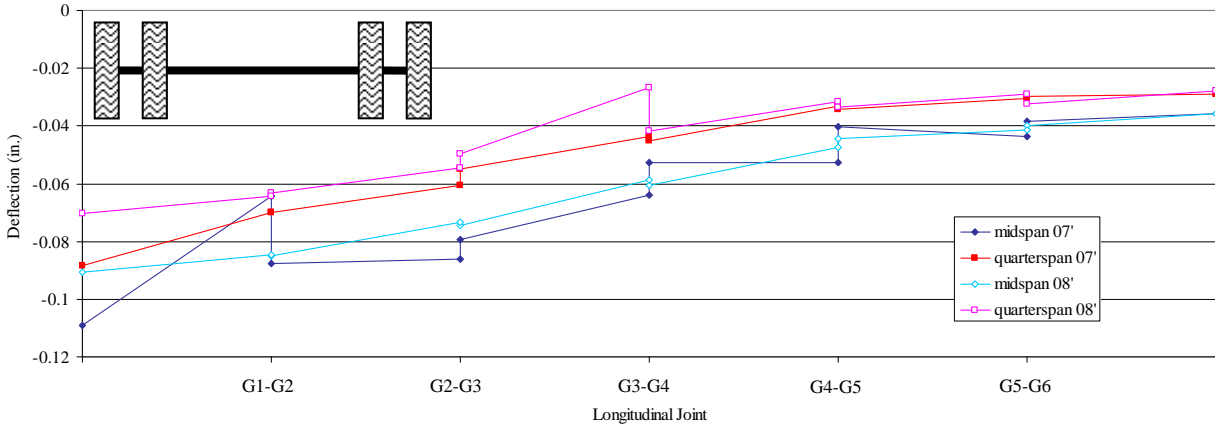


e. LC 5



f. LC 6

Figure 6.2. 2007 and 2008 transverse deflected shape at midspan and quarterspan



g. LC 7

Figure 6.2. 2007 and 2008 transverse deflected shape at midspan and quarterspan

Figure 6.3 shows the absolute maximum differential deflection at midspan and quarterspan for each of the 2007 and 2008 load cases. Again, the 2008 differential deflections were normalized to the 2007 load truck weight. The obtained differential deflections for both testing periods were less than 0.03 in. During the 2007 testing, the differential between girder G1-G2 was the largest for all load cases. The differential deflection at G1-G2 was also nearly constant for all load cases and appears to be independent of the load truck position. The largest difference occurred for LC 3 with a magnitude of 0.028in. The 2008 testing had maximum differential deflection of 0.023 in., which occurred at the quarterspan joint of G3-G4 for LC1. This location showed the same phenomenon as the 2007 G1-G2 joint, in which the differential deflection seems to be independent of load truck position. It is uncertain why the constant differential deflection occurred at these locations and why it was not consistent during both testing periods. In general, when comparing the midspan differential deflections, the 2007 results showed larger values than 2008 values. The quarterspan location had similar differential deflection results for both years, with the exception of G3-G4. Overall the deflections were small leading one to believe the grouted shear key and hand tight post tensioning rod are adequate for load transfer and limiting problems with wearing surfaces deterioration. This limited testing does not allow for conclusions to be drawn as to whether or not this behavior would continue throughout the bridge life.

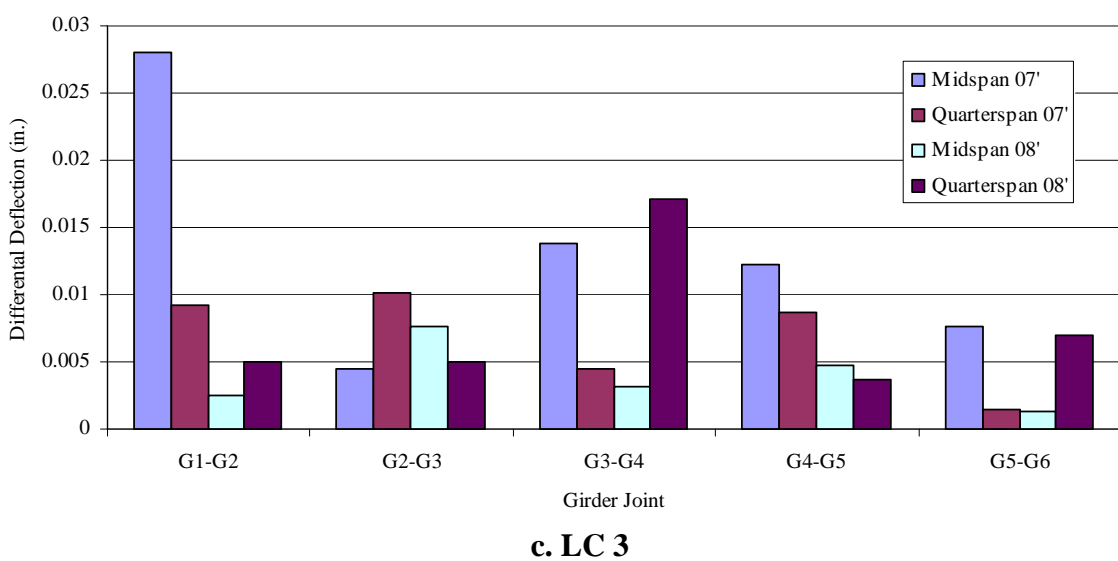
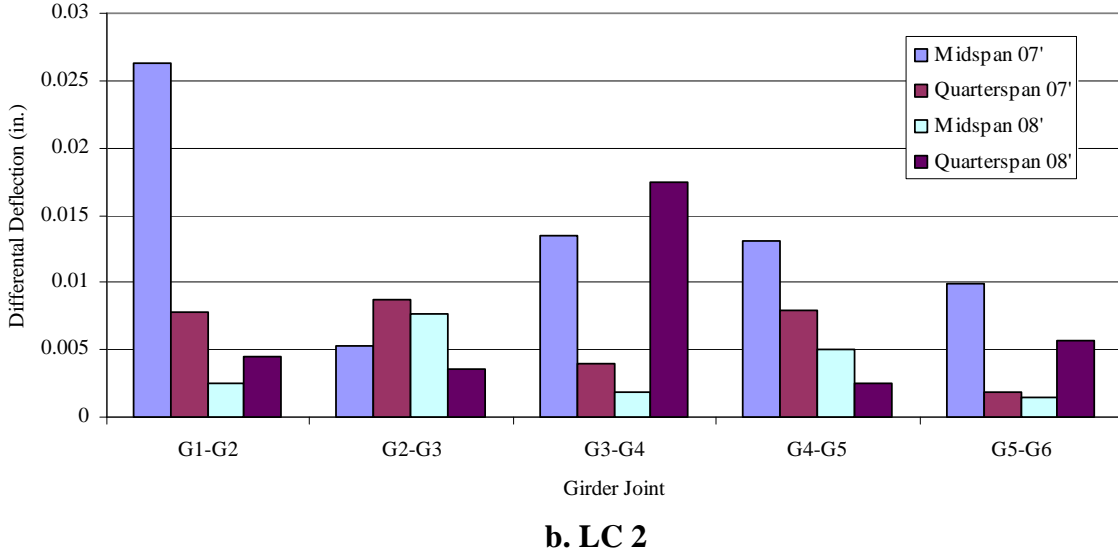
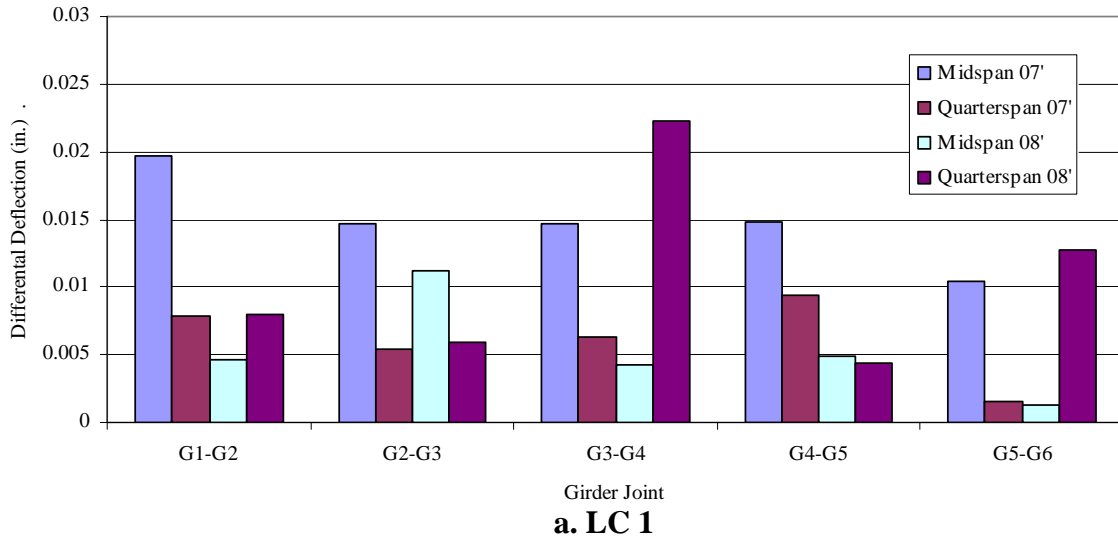


Figure 6.3. 2007 and 2008 differential deflections

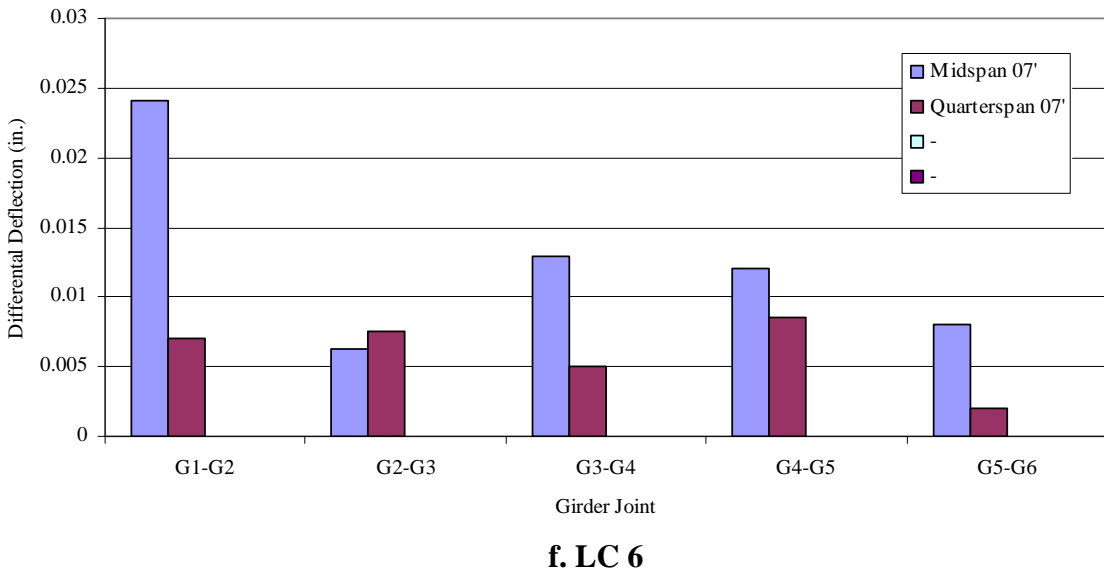
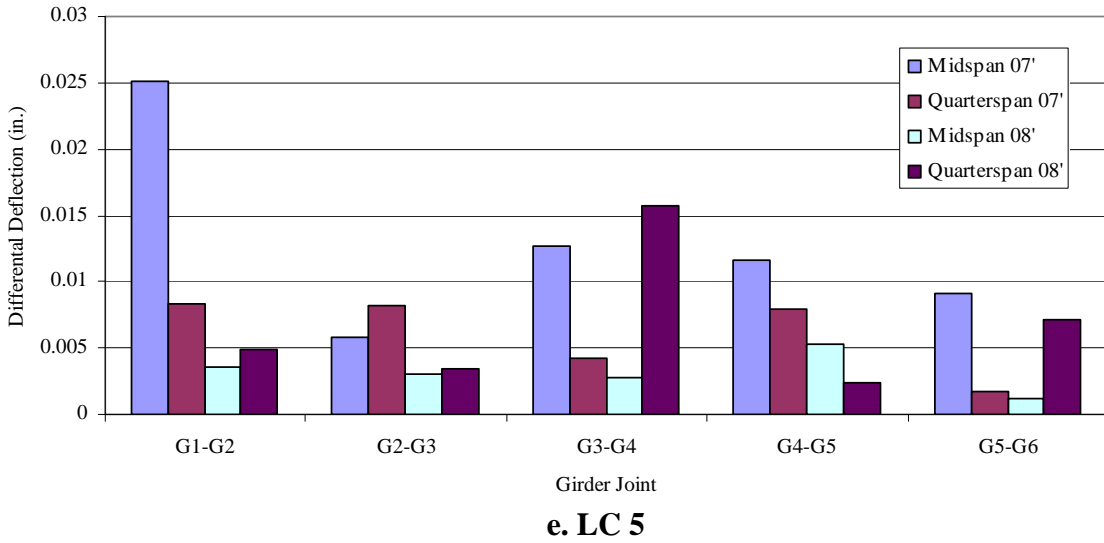
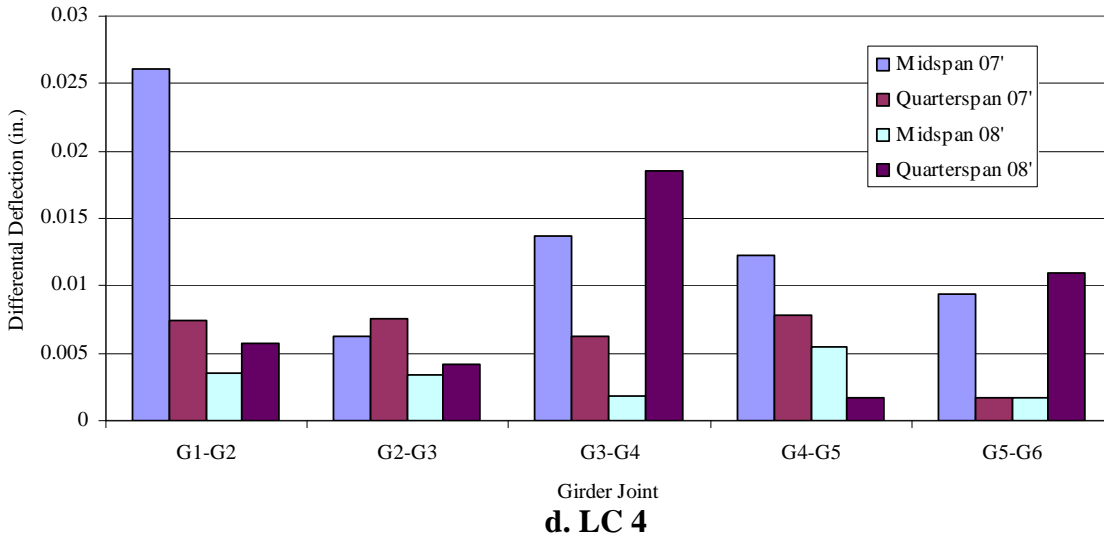


Figure 6.3. 2007 and 2008 differential deflections

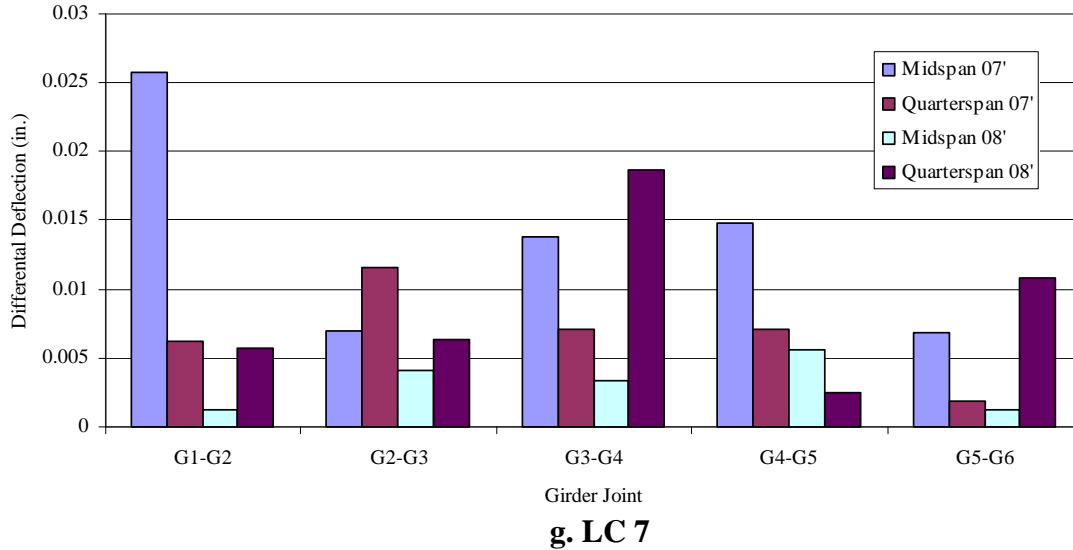


Figure 6.3. 2007 and 2008 differential deflections

6.1.2 Bridge Strains

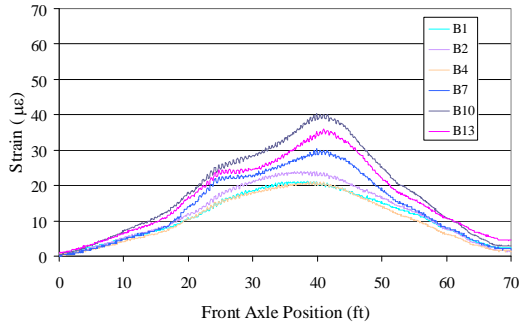
BDI strain transducers were placed on the underside of the girders to obtain strain information for each load case. The maximum strains for each load case during the 2007 and 2008 testing can be seen in Tables 6.3 and 6.4, respectively. The maximum strain obtained during the 2007 load testing occurred during LC 7 at quarterspan transducer B28 with a strain of $118 \mu\epsilon$. In 2008 transducer B27 had the highest strain of $49 \mu\epsilon$ also taking place during LC 7. It is not clear why the strain levels were dramatically smaller in 2008. In general, when the load path was located on the south side of the bridge, i.e., load case LC 4 through LC 7, the quarterspan transducers on girder G1 and G2 had higher strains than the midspan strains. Figure 6.4 and 6.5 show this characteristic for 2007 and 2008 LC 7 midspan, quarterspan, and eighthspan strains respectively. Load case 4, LC 5, and LC 6 have similar strain characteristics as seen with LC 7.

Table 6.3. 2007 Maximum midspan girder strains

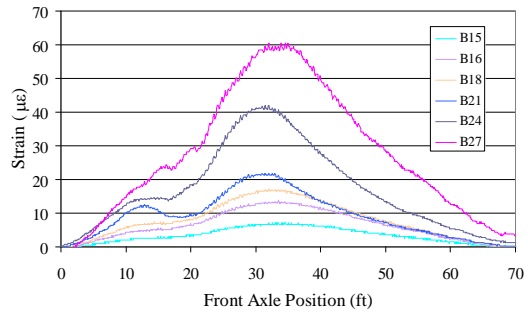
	Load Case						
	LC 1	LC 2	LC 3	LC 4	LC 5	LC 6	LC 7
Strain ($\mu\epsilon$)	43	47	39	90	86	84	118
Gauge Location	G5 (B2)	G1 (B28)	G5 (B2)	G1 (B28)	G1 (B28)	G1 (B28)	G1 (B28)

Table 6.4. 2008 Maximum midspan girder strains

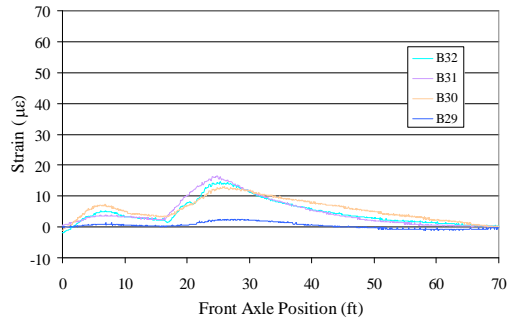
	Load Case						
	LC 1	LC 2	LC 3	LC 4	LC 5	LC 6	LC 7
Strain ($\mu\epsilon$)	37	33	34	41	36	-	49
Gauge Location	G5 (B2)	G3 (B8)	G5 (B2)	G1 (B27)	G2 (B11)	-	G1 (B27)



a. midspan strain

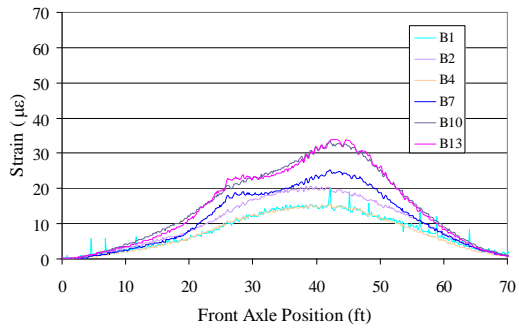


b. quarterspan strain

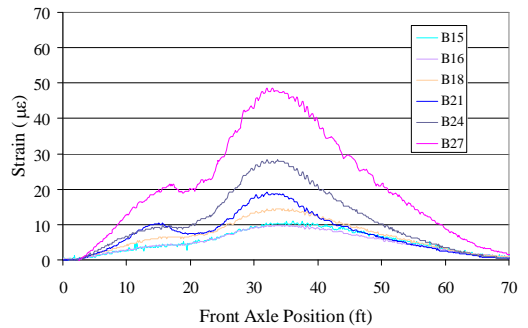


c. eighthspan strain

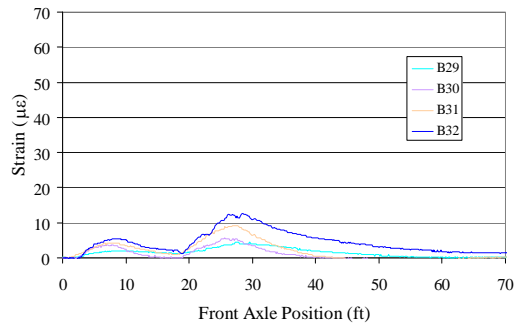
Figure 6.4. 2007 Experimental strains; LC 7



a. midspan strain



b. quarterspan strain



c. eighthspan strain

Figure 6.5. 2008 Experimental strains; LC 7

The experimental strain measurements were compared with analytical strains. The analytical strains were computed using the material properties obtained from the laboratory results and load fraction values discussed herein. The analytical and experimental results were compared using data obtained from girder G4 during LC3. This load case and girder were selected because the load case represents the most likely load path the bridge will encounter while in-service on a low volume road and the girder was directly influenced by the load truck. Figure 6.6 and 6.7 show the 2007 and 2008 respective results for the comparison between analytical and experimental strain. From Figure 6.6 it can be seen that the midspan behavior of girder G4 lies between “pinned-pinned” and “fixed-fixed”, however, when the same comparison is made at the quarterspan and eighthspan the experimental results are nearly identical to the analytical results. Similar results are shown for the load test conducted in 2008 in Figure 6.7. The comparisons indicate the girders exhibit very little rotational restraint at the supports and act as simply supported beams.

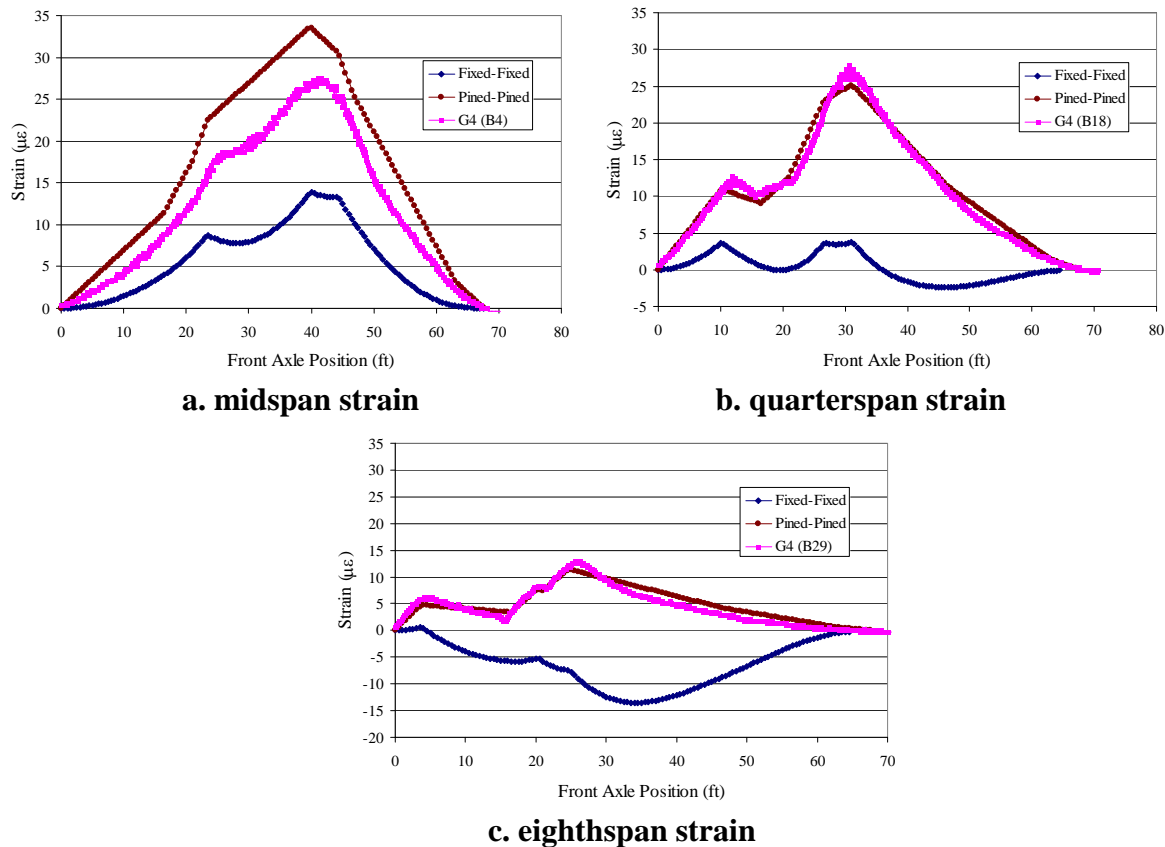


Figure 6.6. 2007 Experimental and analytical strain comparison; LC 3

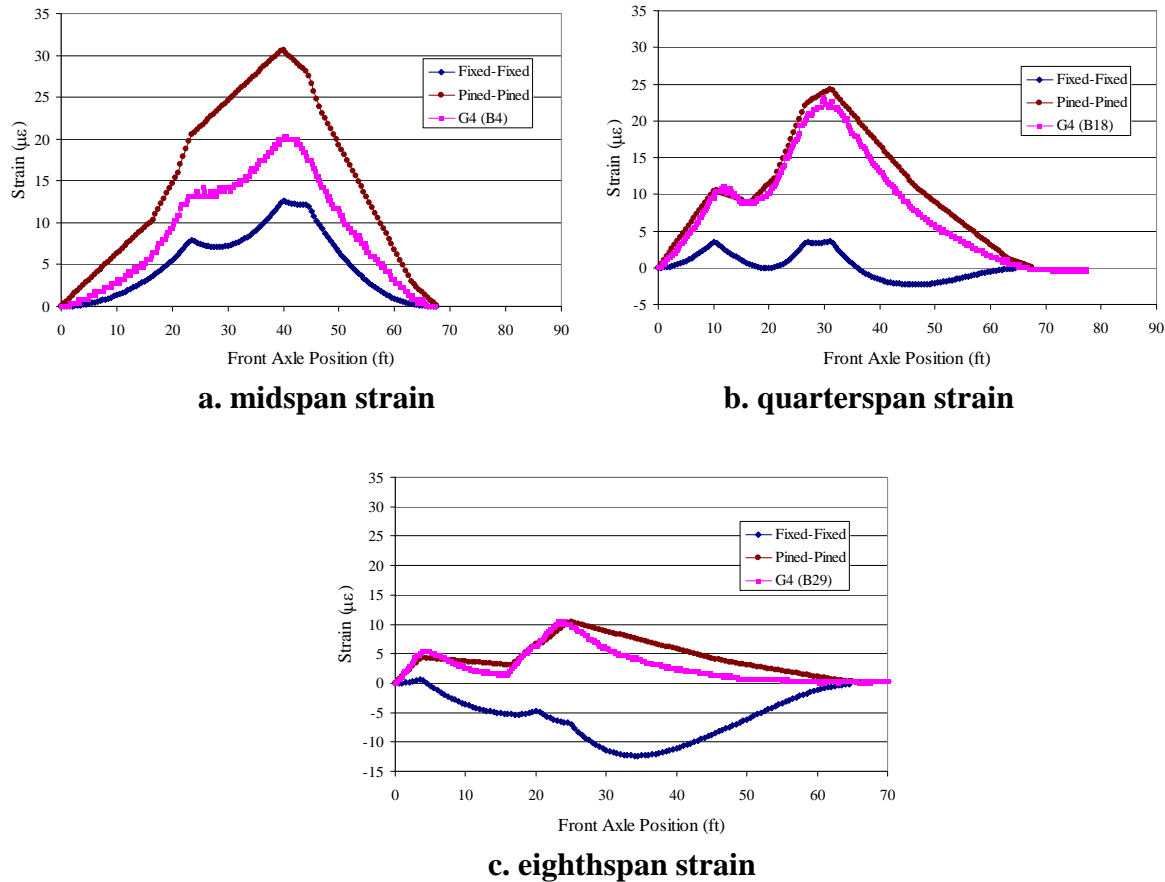


Figure 6.7. 2008 Experimental and analytical strain comparison; LC 3

6.1.3 Bridge Load Fraction and Load Distribution

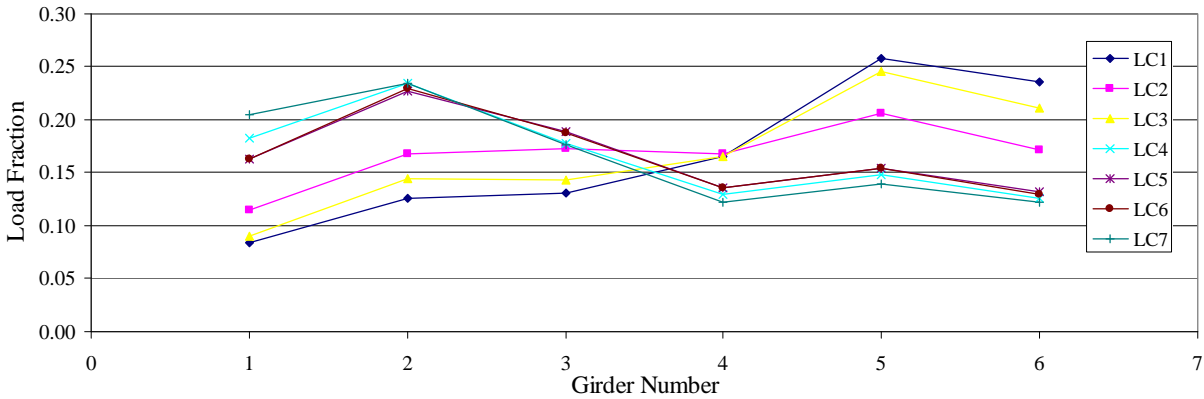
Load fraction was calculated for each load case based on the assumption that the girders are of equal stiffness. The approximate load fraction for each girder can, therefore, be obtained with the following equation:

$$LF_i = \frac{\varepsilon_i}{\sum_{i=1}^n \varepsilon_i} \quad (6.1)$$

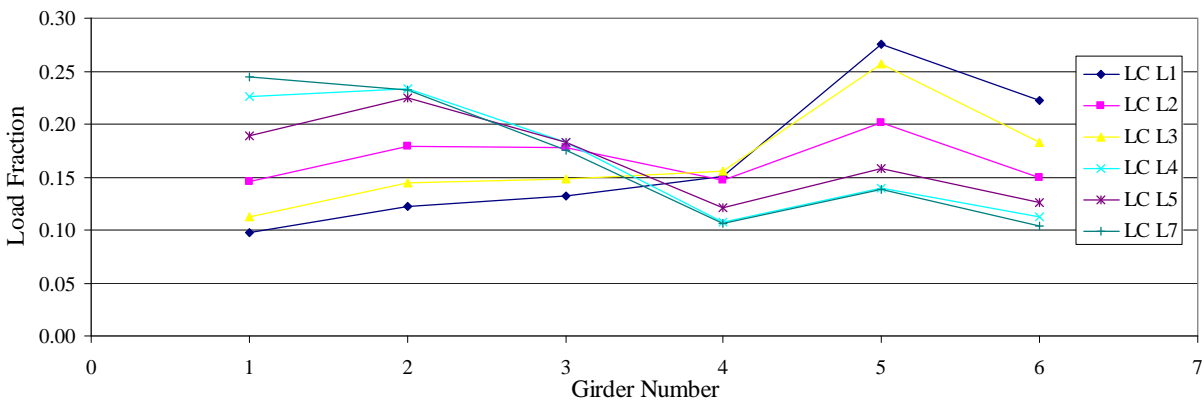
Where LF_i = load fraction of the i th girder, ε_i = strain of the i th girder, $\sum \varepsilon_i$ = sum of all girder strains, and n = number of girders.

Figure 6.8 shows the load fraction for the 2007 and 2008 testing. Girder G5 was seen to have the largest load fraction for both the 2007 and 2008 testing. The largest load fraction occurred during the 2008 LC 1 and was 0.28. LC 1 also had the lowest load fraction which occurred in 2007 with a value of 0.08. The load fraction was generally largest at the girders located directly below the truck. The load fraction decreased as the transverse distance from the girder to the load truck

increased. When the load truck was located in the center of the bridge (i.e. LC2) the load was approximately distributed evenly to all girders.



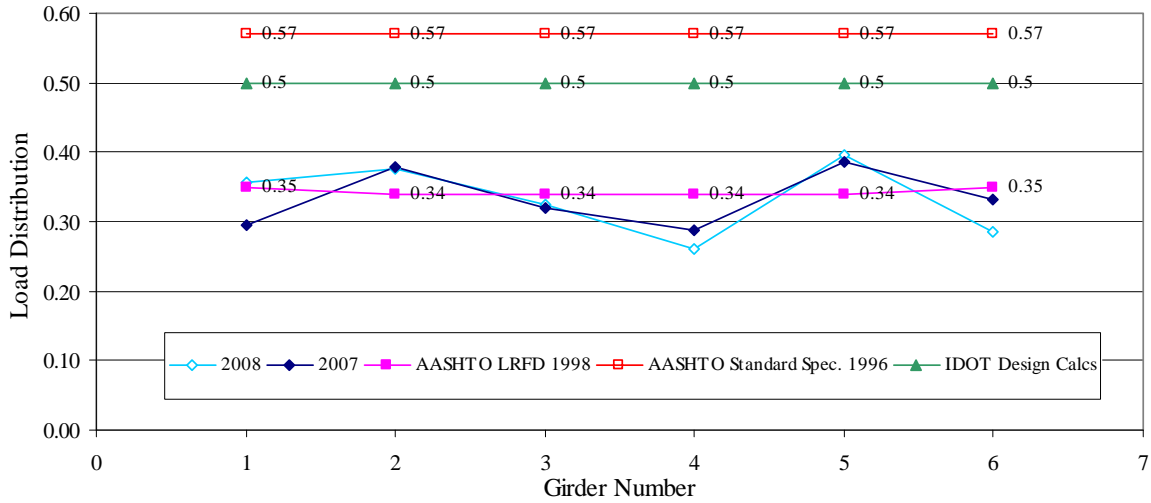
a. 2007 midspan load fraction for seven load cases



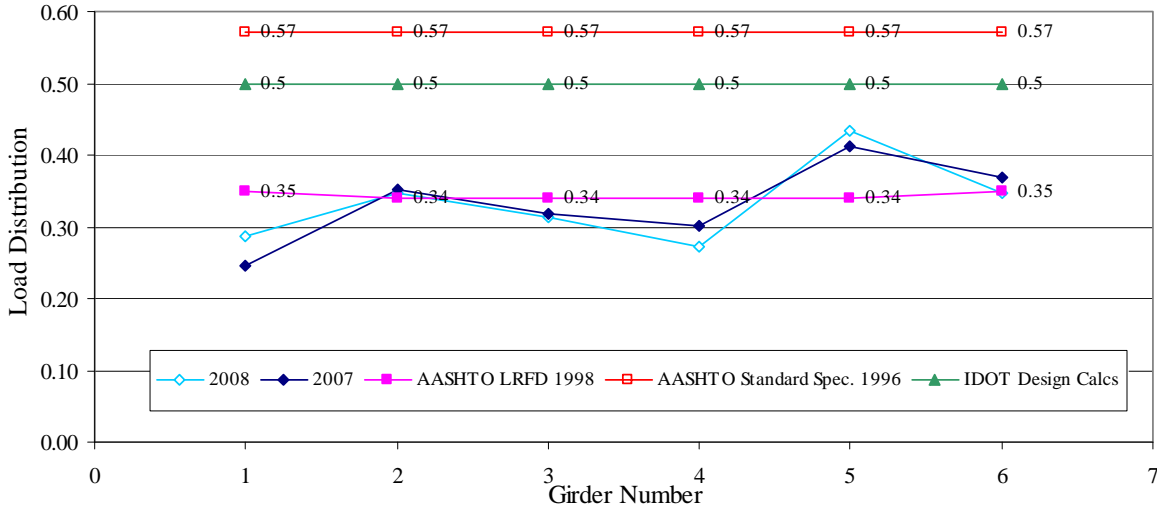
b. 2008 midspan load fraction for six load cases

Figure 6.8. Experimentally obtain load fraction

Load distribution was determined experimentally by adding the load fractions of two complementing load cases. Combining LC 1 plus LC 5 and LC 3 plus LC 7 provided proper lane loads for determining load distribution. Figure 6.9 shows the 2007 and 2008 experimental load distributions along with the design value used by the Iowa DOT, and code distribution factors from AASHTO LRFD 1998, and AASHTO Standard Specification 1996. The largest obtained load distribution factor was obtained during the 2008 combination LC 1 and LC 5 testing with a value of 0.43 at G5, however both 2007 and 2008 testing showed very similar results. The lowest value was 0.25 at girder G1. When comparing the experimental test results with the AASHTO LRFD load distributions, the experimental values exceed the codified distributions at the center of the driving lanes. When the experimental test results are compared with the Iowa DOT design values and the AASHTO Standard Specification recommendations, the experimental results show the bridge performance is conservative.



a. LC3 + LC7



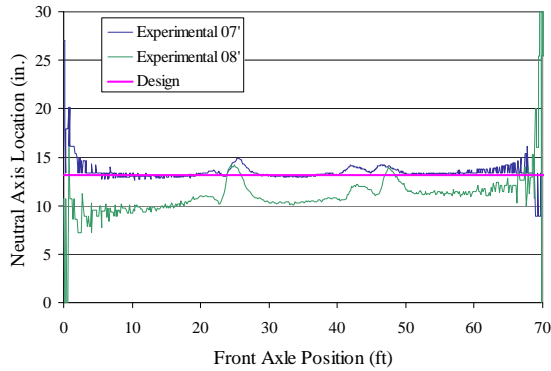
b. LC1 + LC5

Figure 6.9. Experimental and codified load distributions

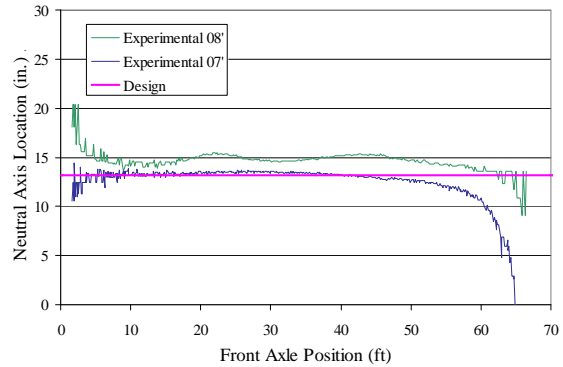
6.1.4 Girder Neutral Axis Location

In addition to strain transducers placed on the bottom of the girders during testing, transducers were placed on top of the girders at B4, B10, and B13 locations for various load cases. The top strains, in combination with the bottom strain data, were used to estimate the neutral axis location of the girders during testing. Figure 6.10 shows the neutral axis location for girders G1, G2 and G4 for LC1, LC2, and LC5 respectively. The location of the neutral axis used for design was 13.15 in. measured from the bottom of the girder, which is also shown in Figure 6.10. The experimentally obtained neutral axis varies between testing periods. The experimental neutral axis location for the 2007 testing was very close to the design value for girder G4 and G2. In 2008 the experimentally obtained neutral axis location was close the design location for girder

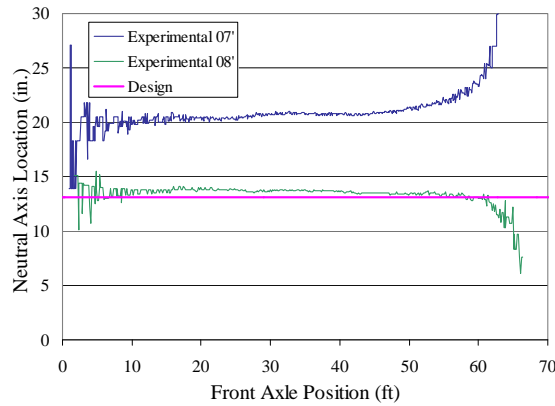
G1. Explanations for the high neutral axis location during the 2007 testing for girder G1 could not be determined..



a. Girder G4, LC1



b. Girder G2, LC2



c. Girder G1, LC5

Figure 6.10. Experimental neutral axis location

6.2 Dynamic Loading

Load case 2 and 7 were used for dynamic load testing. During testing the truck was driven over the bridge at a crawl speed to determine the base line strain and deflection. Then the truck was driven over the bridge at 10mph, 20mph, 25mph, and 35mph to obtain dynamic deflections and strains. Bridge accelerations were also obtained to determine free vibration and damping characteristics.

6.2.1 Dynamic Amplification Factor

To account for the load “increase” induced by vehicle/bridge interaction, the dynamic load allowance was evaluated (Bigelow et.al., 2005). The dynamic load allowance, which is also known as the dynamic amplification factor (DAF), accounts for the irregularity of the deck surface, the bridges static and vibratory deflection and stress, and the interaction between the

vehicle and the bridge. The current AASHTO LRFD DAF design value is 1.33, while the AASHTO Standard Specification is 1.29. The experimentally obtained dynamic amplification (DA) is the ratio defined as:

$$DA = \frac{\epsilon_{dyn} - \epsilon_{stat}}{\epsilon_{stat}} \quad (6.2)$$

Where ϵ_{dyn} = the maximum strain of the vehicle traveling at normal speed (at a given location) and ϵ_{stat} = the maximum strain of the vehicle traveling at crawl speeds (at the same location). The amplification factor is then given by:

$$DAF = 1 + DA \quad (6.3)$$

The dynamic response of B6 for LC2 and B11 for LC7 are the focus herein for determining the DAF because they were found to be one of the most heavily loaded and because they fell in the zone of direct influence. However, it should be pointed out that similar results were obtained at other locations.

Figure 6.11 shows the dynamic B6 strains at the various speeds. The bridge's maximum DAF was obtained during the 2008 testing with a value of 1.30 at a 10mph speed. The B6 DAF for LC 2 testing can be seen in Figure 6.12. The maximum B6 DAF was 1.26 in 2007 at 10mph. In general the 2007 and 2008 B6 DAF plots for the bridge were very similar. The plot shows that at low speeds (<25mph) the DAF is largest starting at 10mph. As the speed increases, the DAF decreases until reaching a low DAF of 1.04 at 25mph. The DAF then increases at 35 mph.

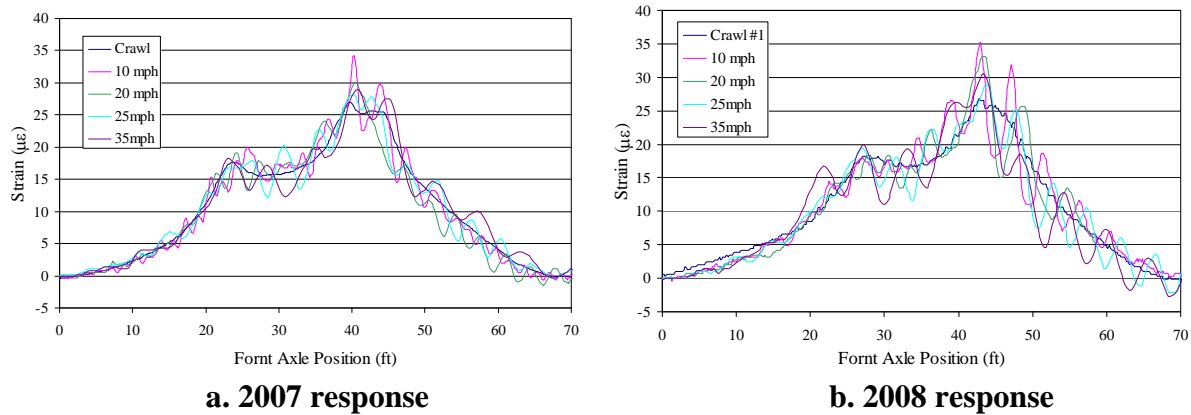


Figure 6.11. Transducer B6 dynamic response LC2

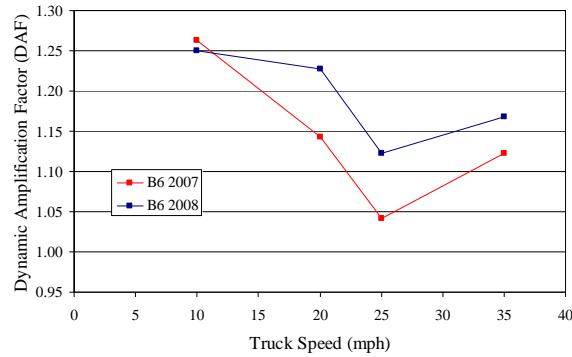
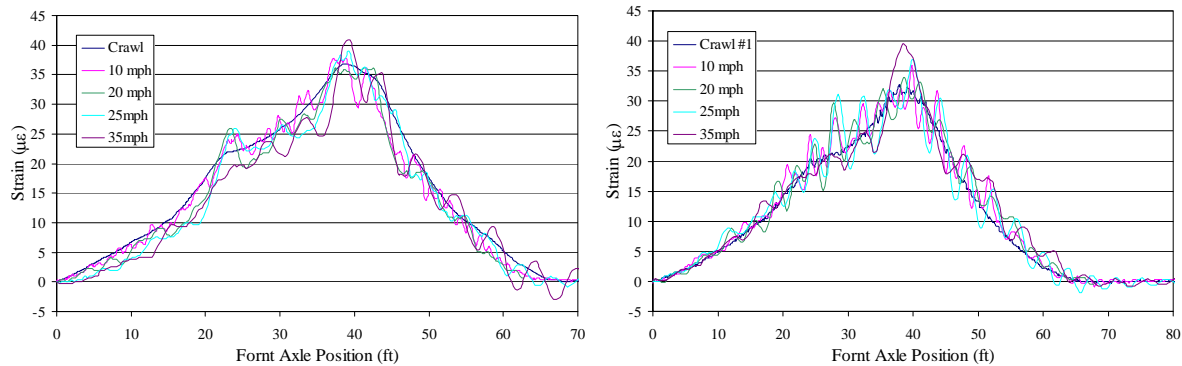


Figure 6.12. 2007 and 2008 DAF LC 2

Figure 6.13 shows the dynamic transducer B11 strains at the various speeds for load case LC7 in 2007 and LC4 in 2008. Due to road conditions during the 2008 testing the higher speed truck passes could not be completed for LC7, therefore, LC4 was used for comparative purposes. The maximum DAF obtained during the 2008 testing was of 1.23 at 25mph speed at transducer B7. The B11 DAF for load case LC7 and LC4 can be seen in Figure 6.14. In general the 2007 and 2008 B11 DAF had very similar patterns, however the 2008 testing had consistently a higher DAF (by approximately 0.10). The plot shows that as the DAF decreases from low speeds to moderate speeds and then increase as the speed increases to higher speeds.



a. 2007 response LC7

b. 2008 response LC4

Figure 6.13. Transducer B11 dynamic response LC7

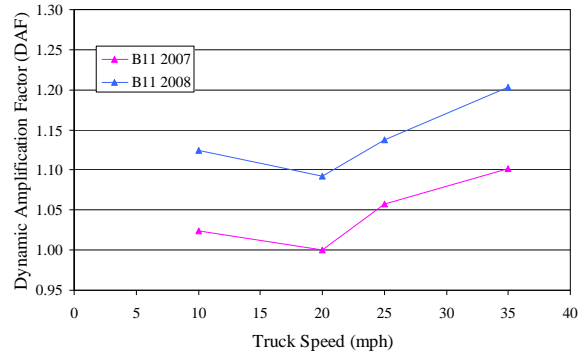
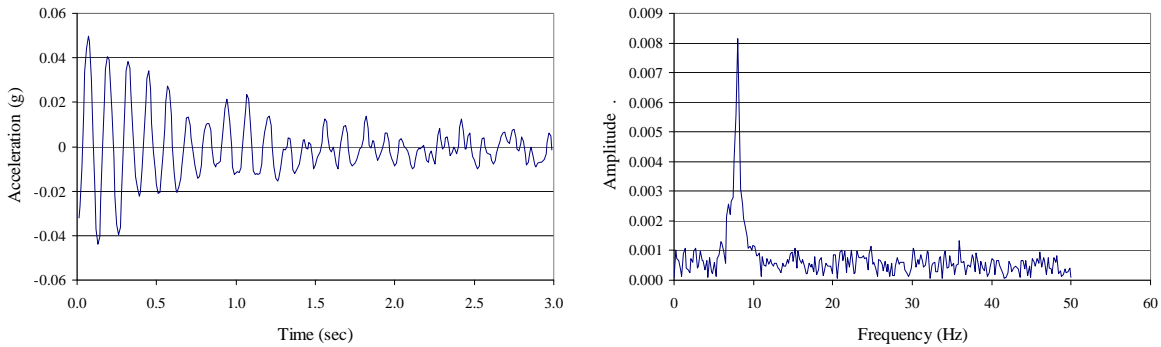


Figure 6.14. 2007 and 2008 DAF LC7

6.2.2 Vibration and Damping

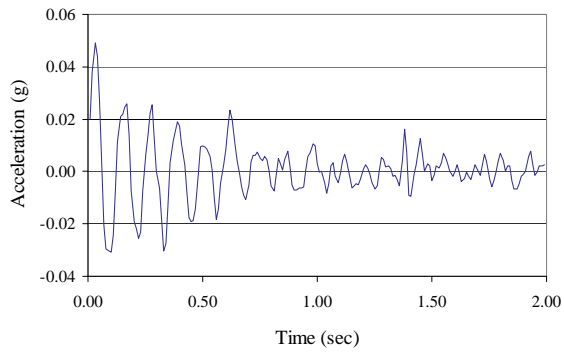
From the free vibration records one vibration mode was identified. The free vibration record and FFT results showing the vibration modes can be seen in Figure 6.15 and 6.16 for the 2007 and 2008 testing respectively. The first flexural longitudinal frequency of approximately 8.0 Hz was found for the Madison County Bridge for both the 2007 and 2008 testing. The structural damping determined from the free vibration was recorded to be approximately 2.5% of critical.



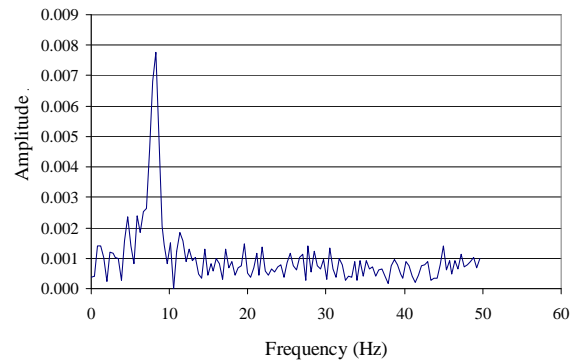
a. Free vibration record; A3; 35mph

b. FFT; A3; 35mph

Figure 6.15. Acceleration and frequency plots for 2007 testing



a. Free vibration record; A3; 35mph



b. FFT; A3; 35mph

Figure 6.16. Acceleration and frequency plots for 2008 testing

6.3 Corrosion Monitoring

Corrosion monitoring of the strands was completed with the use of Vetek V2000 corrosion monitoring system. The V2000 braided silver electrode that is wrapped around the monitored strands can be seen in Figure 6.17. The V2000 monitor works by measuring the electric potential between the strand and the electrode with the pore water of the concrete acting as an electrolyte between the two. An increase in the electric indicates that corrosion activity is taking place. The electric potential is measured with a voltmeter with three different ranges of readings representing three different stages of corrosion. The three different stages are listed below in Table 6.5.



Figure 6.17. Corrosion electrode wrapped around strand

Table 6.5. Vetek V2000 electrode readings

Range	Voltmeter Reading	Range Description
Range 1	Less than 300mV dc	No corrosion activity is taking place
Range 2	From 300mV to 400mV dc	Corrosion is either just starting or just stopping due to lack of oxygen
Range 3	400mV dc and above	Corrosion is fully active on the steel strand

The strands that were selected for monitoring, as described in Section 5.1, were instrumented with approximately 5 ft of electrode plate at the west end, center and east end of the strand. Electrode readings were taken during the construction of the bridge in early 2007 and approximately one year later in 2008. The results of the electrode readings are shown in Table 6.6. The 2007 results show five locations where the voltage reading is in Range 2. These same five locations in 2008, however, were below 300mV dc meaning the corrosion in 2007 was either not occurring or stopping due to lack of oxygen. In 2008 four locations had corrosion readings in Range 3, indicating corrosion of the strand is taking place.

Table 6.6. V2000 millivolt electrode readings

Electrode Location	2007 (mV dc)			2008 (mV dc)		
	West	Center	East	West	Center	East
1 Top	0	0.1	0.1	0	0	36
2 Top	0.5	0	286	186	474**	228
3 Top	333*	0	220	73	409**	148
4 Top	0	37	211	0	71	82
5 Top	301*	203	246	72	286	98
6 Top	245	198	38	28	349*	28
7 Bot	140	205	37	122	200	76
8 Bot	325*	10	17	155	206	72
9 Top	274	36	234	266	5	75
10 Top	330*	318*	243	31	25	103
11 Bot	279	189	1.6	487**	319*	586**
12 Bot	-	128	196	96	11	200

*Readings in Range 2

**Reading in Range 3

7. CONCLUSIONS AND RECOMMENDATIONS

The objective of this project was to evaluate the bridge component and to assess the overall design, construction, and field performance. To complete these objectives both laboratory and field testing took place.

In order to obtain comprehensive conclusions several tasks were completed including observation of the fabrication and construction; laboratory investigation of transverse post-tensioning force, strength properties, and guardrail connection; and in-situ evaluation of performance under live load.

Based on the information obtained from laboratory testing the following conclusions were determined.

- The maximum differential deflection measured between adjacent box girders was 0.011 in.
- The shear key is effective in transferring load to adjacent girders. With the shear key intact, the load fraction for the loaded girder ranged from 0.53 to 0.60. The load fraction for the loaded girder without the shear key and a hand-tight post-tensioning force was 0.95. This indicates that an intact shear key is critical to the performance
- The magnitude of the post-tensioning force exhibited no significant effect on load fractions for adjacent girders.
- Cracking occurred at an applied moment of 781 kip*ft, which is greater than the theoretical moment of 721 kip*ft.
- Cracking did not occur under service loads.
- The flexural strength test was concluded at an applied moment equal to 962 kip*ft, which exceeded the theoretical moment strength of 955 kip*ft.
- Service limit state stresses were not exceeded by service level loads.
- The experimental shear strength equaled 197 kips, which exceeded the theoretical shear strength of 79 kips.
- The guardrail connection exceeded the AASHTO design transverse force for two of the four tests. Tests where the connection did not meet the AASHTO requirements were likely the result of the surrounding posts already having been tested to failure and the resulting poor load transfer capability.

Based on the results of the laboratory testing, the following actions are recommended:

- Apply a minimum post-tensioning force equal to hand-tightening the transverse tie rod.
- If a higher post-tensioning force is desired, the force should be greater than 25 kips. A slight benefit in load distribution was noticed for post-tensioning forces greater than 25 kips.

The following are conclusions and recommendations based on the results from field testing.

- The maximum deflection obtained from testing was 0.109 in., which is less than current code requirements and predicted design values.
- Very little differential movement was seen between longitudinal girder joints. The maximum differential deflection for the girders was less than 0.03.
- The maximum strain was $118\mu\epsilon$ which was obtained at the quarterspan location. The quarterspan strains were generally found to be larger than the midspan strains for all load cases where the truck was on the south side of the bridge.
- The bridge girders exhibit very little rotational restraint and should be designed as simply supported beams.
- An intact shear key and a transverse, hand-tight post-tension tie appear to adequately distribute load to adjacent girders.
- The use of 0.5 load distribution factor is conservative and is recommended for future box girder bridge design.
- The maximum DAF obtained from testing was 1.30. This was slightly greater than the AASHTO Standard Specification but less than AASHTO LRFD design values.
- The natural frequency of the bridge was approximately 8.0Hz falling between the body bounce and axle hop vehicle frequencies.
- Of the 12 strands monitored for corrosion three were indicating that full corrosion activity was taking place. Two of the strands were located in the top of the girder, while one was located in the bottom of the girder.

REFERENCES

- AASHTO. 1996. *Stand Specifications for Highway Bridges*. Washington, DC: American Association of State Highway and Transportation Officials.
- AASHTO. 2002. *Stand Specifications for Highway Bridges*. Washington, DC: American Association of State Highway and Transportation Officials.
- AASHTO LRFD. 1998. *LRFD Bridge Design Specifications*. Washington, DC: American Association of State Highway and Transportation Officials.
- Bigelow, J., Phares, B., Wipf, T., Ritter, M., Wood, D. 2005. Dynamic Field Performance of Glued-Laminated Timber Bridges. Transportation Research Record No. 1928. Washington D.C
- Hawkins, N. M., and J. B. Fuentes. 2002. *Test to Failure of a 54 ft. Deteriorated Pretensioned Precast Concrete Deck Beam*. Illinois Cooperative Highway and Transportation Series No. 281. University of Illinois: Urbana-Champaign.
- Hawkins, N. M., and J. B. Fuentes. 2003. *Structural Condition Assessment and Service Load Performance of Deteriorated Pretensioned Deck Beam Bridges*. Illinois Cooperative Highway and Transportation Series No. 285. University of Illinois: Urbana-Champaign.
- Nawy, Edward G. 2003. *Reinforced Concrete: A Fundamental Approach*. New Jersey: Pearson Education, Inc.

APPENDIX A. MADISON COUNTY BOX GIRDER BRIDGE PLANS

ITEM NO.	ITEM CODE	ITEM DESCRIPTION	UNIT	TOTAL	AS BUILT QUANTITY
1	2102-2710010	EXCAVATION, CL 10, RORRY+BORROW	CY	264	
2	2401-6746025	REMOVAL OF EXISTING BRIDGE	LS	1	
3	2402-2720000	EXCAVATION, CL 20	CY	66.2	
4	2403-0100010	STRUCTURAL CONCRETE (BRIDGE)	CY	6.4	
5	2404-2115000	REINFORCING STEEL	LB	725	
6	2405-1001000	CULV. CUP ENT 18"	LF	34	
7	2501-5450042	PILE, DRIVE STEEL BEAR, HP 1042	LF	350	
8	2501-5550042	PILE, TURN STEEL BEAR, HP1042	LF	350	
9	2505-4058000	INSTALL OF GRAIL	EA	225	
10	2505-4021862	GRAIL, TERMINAL, BEAM, FLARED, RE-76	EA	50	
11	2508-4984000	FLOWABLE MORTAR	CY	5.0	
12	2507-2520005	ENGINEER FABRIC	SF	136	
13	2507-6800042	REVIEW/CLASS D	TON	174	
14	2518-6910000	SAFETY CLOSURE	EACH	4	
15	2518-6910000	TRAFFIC CONTROL	LS	1	
16	2533-4380005	MOBILIZATION	LS	1	
17	2539-9939005	PRECAST ABUTMENT FOOTING	EACH	2	
18	2539-9939005	PRECASTIONED PRECAST 48" X 27" DECK PANEL	EACH	6	

ESTIMATE REFERENCE INFORMATION

- 3 INCLUDES FURNISHING AND PLACING SUBGRAIN (INCLUDING EXCAVATION), GRANULAR SUBGRAIN, CURB, SIDEWALK, AND CURB AND GUTTER. INCLUDES ALL PREFORMED EXPANSION JOINT FILLER REQUIRED.
- 17 THIS ITEM INCLUDES ALL COSTS FOR FURNISHING AND PLACING THE PRECAST ABUTMENT FOOTING INCLUDING ONE ABUTMENT 9.4 C.Y. OF STRUCTURAL CONCRETE (BRIDGE), 1287 LBS. REINFORCING STEEL, MECHANICAL SPLICERS, 18.0 L.F. OF 27" CUP, AND 1.8 C.Y. OF STRUCTURAL CONCRETE (MISC.) TO BACKFILL THE PILE. THE CONTRACTOR SHALL BE RESPONSIBLE FOR OBTAINING ALL NECESSARY PERMITS. THE METHOD OF MEASUREMENT AND BASIS OF PAYMENT WILL BE FOR EACH PRECAST ABUTMENT FOOTING FURNISHED AND PLACED.
- 18 INCLUDES ALL COSTS ASSOCIATED WITH FURNISHING AND PLACING THE PRETENSIONED SUBGRAIN. THIS INCLUDES ALL MATERIALS AND LABOR NECESSARY TO PREPARE AND PLACE THE PRETENSIONED SUBGRAIN. INCLUDES 1.0 C.Y. OF GROUT FOR SHEAR KEYS BETWEEN PANELS. GRADATION OF COARSE AGGREGATES FOR PRESTRESSED CONCRETE BRIDGE UNITS SHALL MEET THE REQUIREMENTS OF SECTION 4115 CLASS 3. SPECIFICATIONS FOR HIGH PERFORMANCE CONCRETE FOR PRECAST ABUTMENT FOOTING OF THE CORSE AGGREGATE SHALL MEET THE REQUIREMENTS OF SECTION 2407.02B.

GENERAL NOTES:

THIS DESIGN IS FOR THE REPLACEMENT OF THE EXISTING 22' X 17'-7" SINGLE SPAN BRIDGE OVER RORRY CREEK AND THE EXISTING BRIDGE SUPERSTRUCTURE CONSISTS OF TIMBER GIRDERS WITH A TIMBER DECK. THE EXISTING BRIDGE SUPERSTRUCTURE CONSISTS OF TIMBER PILING AND TIMBER BACKWALLS. THE INTENT IS TO REPLACE THE EXISTING STRUCTURE WITH AN INDEPENDENT BRIDGE SUPERSTRUCTURE WHICH CONSTRUCTION BRIDGE BEAMS SHALL BE CONSTRUCTED WITH PRECAST ABUTMENT FOOTINGS AND PRECAST PRESTRESSED DECK BOX BEAMS.

THE JUMP SIGN BID FOR REMOVAL OF EXISTING BRIDGES SHALL INCLUDE THE REMOVAL OF THE EXISTING 22' X 17'-7" TIMBER SUPERSTRUCTURE AND SUBSTRUCTURE OF THE EXISTING BRIDGE.

REMOVALS SHALL BE IN ACCORDANCE WITH SECTION 2401 OF THE STANDARD SPECIFICATIONS FOR HIGHWAY CONSTRUCTION. EXISTING BRIDGE SHALL BECOME THE PROPERTY OF THE CONTRACTOR.

FAINT LINES ON PLANS INDICATE THE EXISTING STRUCTURE.

UTILITY COMPANIES WHOSE FACILITIES ARE SHOWN ON THE PLANS OR KNOWN TO BE WITHIN THE CONSTRUCTION LIMITS SHALL BE NOTIFIED BY THE BRIDGE CONTRACTOR OF THE STARTING DATE.

THIS BRIDGE IS DESIGNED FOR HS20-44 LOADING, PLUS 50 LBS. PER SQUARE FOOT OF ROADWAY FOR FUTURE OVERLAY.

THE BRIDGE CONTRACTOR IS ENCOURAGED TO TAKE FULL ADVANTAGE OF ANY AVAILABLE CONTRACTORS' EQUIPMENT AND CONCEPTUAL PROPOSAL FORM WILL BE AVAILABLE AT THE PRECONSTRUCTION CONFERENCE.

IF NECESSARY TO PREVENT DAMAGE TO THE END OF THE BRIDGE DECK OR BACKWALL FROM CONSTRUCTION EQUIPMENT, AN APPROPRIATE METHOD OF PROTECTION APPROVED BY THE ENGINEER SHALL BE PROVIDED BY THE BRIDGE CONTRACTOR AT NO EXTRA COST TO THE STATE OR COUNTY.

THE BRIDGE CONTRACTOR IS TO INSTALL SUBDRAINS BEHIND THE ABUTMENTS AS DETAILLED. THE SUBDRAINS SHALL BE 4" DIA. PERFORATED SUBDRAIN (POLYETHYLENE CORRUGATED TUBING). THE SUBDRAIN OUTLET WILL CONSIST OF A 6" LENGTH OF PIPE WITH A REMOVABLE RODENT GUARD AS DETAILED IN THESE PLANS.

IT SHALL BE THE BRIDGE CONTRACTOR'S RESPONSIBILITY TO PROVIDE SITES FOR EXCESS EXCAVATED MATERIAL. NO PAYMENT FOR OVERHAUL WILL BE ALLOWED FOR MATERIAL HAULED TO THESE SITES.

THESE BRIDGE PLANS LABEL ALL REINFORCING STEEL WITH ENGLISH NOTATION (50) IS A INCH DIAMETER BARL. ENGLISH REINFORCING STEEL RECEIVED IN THE FIELD MAY DISPLAY THE FOLLOWING "BAR DESIGNATION". THE "BAR DESIGNATION" IS EQUIVALENT TO THE BAR DIAMETER IN MILLIMETERS.

THESE BRIDGE PLANS LABEL ALL REINFORCING STEEL WITH ENGLISH NOTATION (50) IS A INCH DIAMETER BARL. ENGLISH REINFORCING STEEL RECEIVED IN THE FIELD MAY DISPLAY THE FOLLOWING "BAR DESIGNATION". THE "BAR DESIGNATION" IS EQUIVALENT TO THE BAR DIAMETER IN MILLIMETERS.

MADISON COUNTY SHALL BE RESPONSIBLE FOR THE CONSTRUCTION OF THE BRIDGE AND SHALL BE RESPONSIBLE FOR THE PRESERVATION OF STAKES AND MARKS IN ACCORDANCE WITH STANDARD SPECIFICATION 1105.06.

SOUNDING AND TEST BORING DATA SHOWN ON PLANS WERE ACCUMULATED FROM DESIGNING AND ESTIMATING PURPOSES. CONTRACTOR SHALL VERIFY ALL CONDITIONS OTHER THAN THOSE INDICATED WILL NOT BE ENCOUNTERED.

TRAFFIC CONTROL PLAN
NOTE: THE ROADWAY WILL BE CLOSED TO THRU TRAFFIC.

ENGLISH SIZE	BAR DESIGNATION
3	10
4	13
5	16
6	19
7	22
8	25
9	29
10	32
11	36

SPECIFICATIONS:

DESIGN AASHTO SERIES OF 1996.
CONSTRUCTION IOWA DEPARTMENT OF TRANSPORTATION STANDARD SPECIFICATIONS FOR HIGHWAY CONSTRUCTION (2002), PLUS APPLICABLE GENERAL SUPPLEMENTAL SPECIFICATIONS AND DEVELOPMENTAL SPECIFICATIONS, SUPPLEMENTAL SPECIFICATIONS AND SPECIAL PROVISIONS, INCLUDING "DEVELOPMENTAL SPECIFICATIONS FOR HIGH PERFORMANCE CONCRETE FOR PRECAST ABUTMENT FOOTING CONSTRUCTION WORK ON THIS PROJECT."

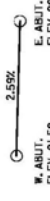
DESIGN STRESSES:

DESIGN STRESSES FOR THE FOLLOWING MATERIALS ARE IN ACCORDANCE WITH THE AASHTO STANDARD SPECIFICATIONS FOR HIGHWAY BRIDGES, SERIES OF 2002. REINFORCING STEEL IN ACCORDANCE WITH SECTION 8, GRADE 60. PRESTRESSED CONCRETE BEAMS, SEE DESIGN SHEET 4. PRECAST ABUTMENT FOOTING CONCRETE IN ACCORDANCE WITH SECTION 8, $f_c = 5,000$ PSI.

DESIGN FOR 0° SKEW
46'-8 X 24' PRECAST PRETENSIONED BOX GIRDER BRIDGE
46'-8 END SPANS
GENERAL NOTES AND QUANTITIES
STA. 99+97
MADISON COUNTY
IOWA DEPARTMENT OF TRANSPORTATION - HIGHWAY DIVISION
DESIGN SHEET NO. 1 OF 12 FILE NO. 250339 DESIGN NO. 106

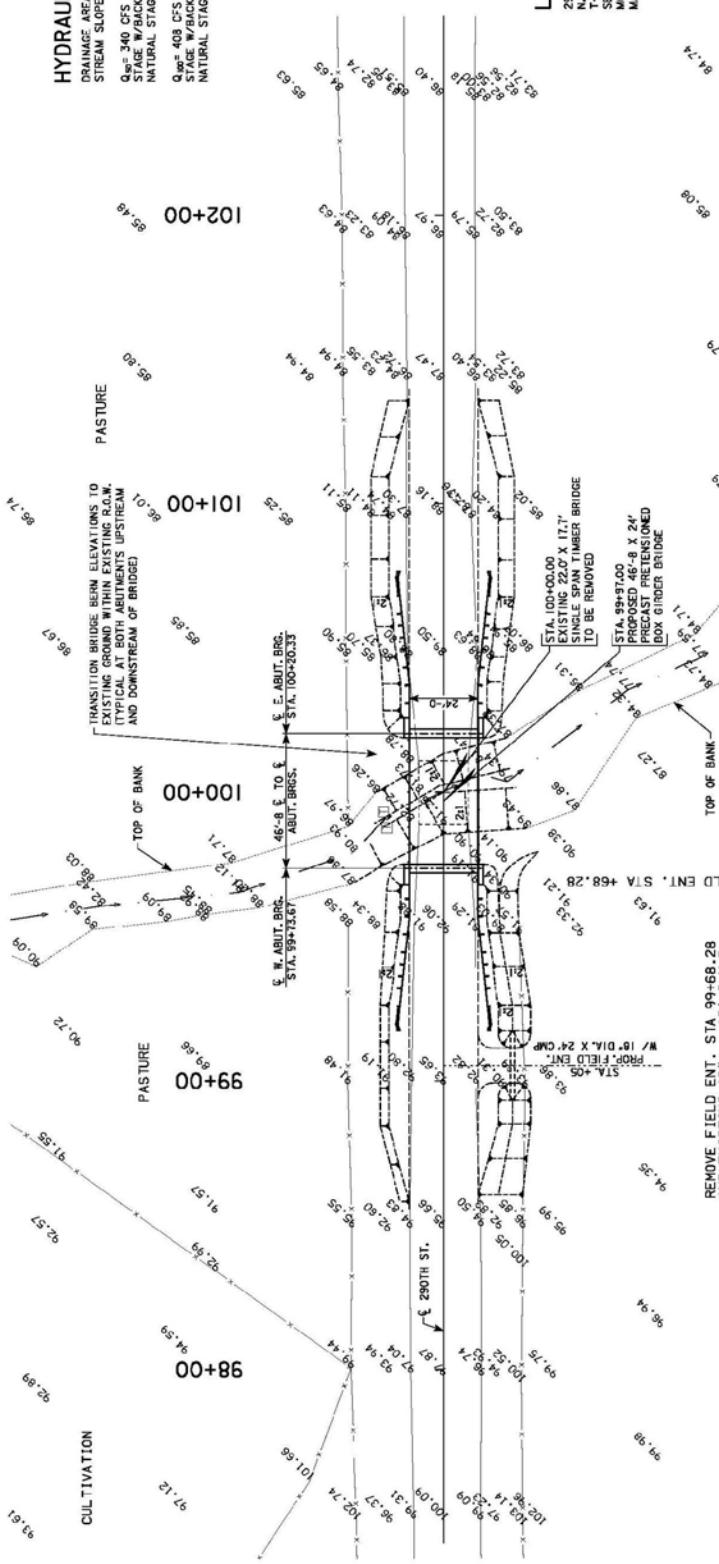
BENCH MARK #1 SET 654 SPIKE IN POWER POLE 73.93 FT. STA. 98+25.18 ELEV. 100.00
 BENCH MARK #2 SET 604 SPIKE IN POWER POLE 25.56 FT. STA. 101+30.04 ELEV. 95.22
 NOTE: ASSUMED DATUM

110
100
90
80
70
60



PROPOSED PROFILE
 290TH STREET

LONGITUDINAL SECTION ALONG \bar{C} ROADWAY



HYDRAULIC DATA
 DRAINAGE AREA= 212 ACRES HILLY
 STREAM SLOPE= 79 FT./MI.
 Q_{50} = 340 CFS
 STAGE W/BACKWATER= 83.80
 NATURAL STAGE AT BRIDGE= 83.68
 Q_{100} = 408 CFS
 STAGE W/BACKWATER= 84.11
 NATURAL STAGE AT BRIDGE= 83.57

LOCATION
 290TH STREET OVER
 ALBANY CLAYTON CREEK
 T-74 N R-28 W
 SECTION 12
 MONROE TOWNSHIP
 MADISON COUNTY

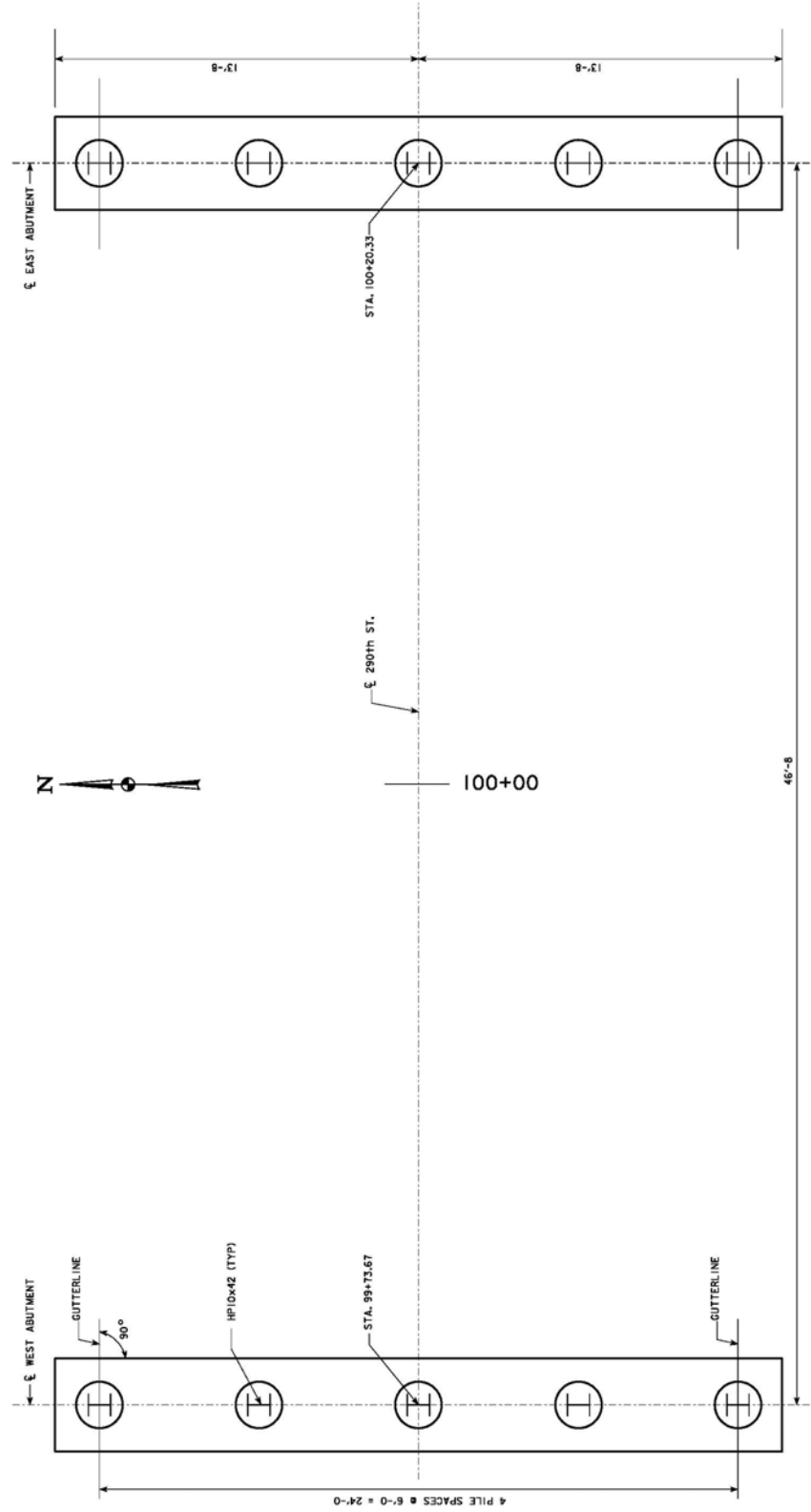
DESIGN FOR C^0 SKEW
**46'-8 X 24' PRECAST PRETENSIONED
 BOX GIRDER BRIDGE**
 46'-8 END SPANS
SITUATION PLAN
 STA. 99+97
 MADISON COUNTY
 IOWA DEPARTMENT OF TRANSPORTATION - HIGHWAY DIVISION
 DESIGN SHEET NO. 2 OF 12. FILE NO. 30139 DESIGN NO. 106
 APRIL 2006



SITUATION PLAN

DESIGN TEAM: 24-MY-2007 13.82
 PROJECT NUMBER: IBRC-C06(116)-BE-61
 SHEET NUMBER: 3

BENCH MARK #1 SET 600 SPIKE IN POWER POLE, 27.93 RT., STA. 98+35.16, ELEV. 100.00
 BENCH MARK #2 SET 600 SPIKE IN POWER POLE, 25.56 RT., STA. 101+36.04, ELEV. 85.22
 NOTES ASSUMED DATUM



DESIGN FOR 0° SKEW
**46'-8 X 24' PRECAST PRETENSIONED
 BOX GIRDER BRIDGE**
 46'-8 END SPANS
 STA. 99+97
STAKING DIAGRAM
 MADISON COUNTY
 IOWA DEPARTMENT OF TRANSPORTATION - HIGHWAY DIVISION
 DESIGN SHEET NO. 3 OF 12 FILE NO. 30335 DESIGN NO. 108
 APRIL 2006

STAKING DIAGRAM

DESIGN TEAM: 24-MAY-2007 13:32
 PROJECT NUMBER: IBRC-C0617D-9E-61
 MADISON COUNTY
 SHEET NUMBER: 4

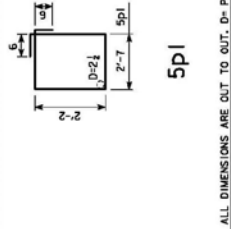
REINFORCING BAR LIST

BAR	LOCATION	SHAPE	NO.	LENGTH WEIGHT
B1	ABUTMENT FOOTING - LONGITUDINAL - FACES	26-11	515	
S12	ABUTMENT FOOTING - LONGITUDINAL - TOP	4-0	34	
S1	ABUTMENT HOOPS	17-6	570	
S3	ABUTMENT WING, HORIZ.	16	3-10	64
S4	ABUTMENT TO WING ANCHOR	16	1-5	24
				REINFORCING STEEL (LBS.) 267

NOTE: THE S4 BARS ARE SLICED WITH MECHANICAL SPLICERS TO THE S3 BARS. MECHANICAL SPLICERS SHALL BE IN ACCORDANCE WITH MATERIALS (M 45), APPENDIX E.

THE SPACING AND MINIMUM SPACER ARE INCLUDED IN THE SUPERSTRUCTURE QUANTITIES.

BENT BAR DETAILS



PRECAST ABUTMENT FOOTING & PILE NOTES:

MINIMUM CLEAR DISTANCE FROM FACE OF CONCRETE TO NEAR REINFORCING BAR IS TO BE 2" UNLESS OTHERWISE NOTED OR SHOWN.

THE DESIGN BEARING FOR THE ABUTMENT PILES IS 33 TONS.

THE COST OF FURNISHING AND PLACING SUBDRAIN (INCLUDING EXCAVATION), GRANULAR BACKFILL AND POROUS BACKFILL IS TO BE INCLUDED IN THE QUANTITY FOR STRUCTURAL CONCRETE.

THE PRECAST ABUTMENT FOOTING PICK POINT OR LIFTING LOOPS SHALL BE DESIGNED BY THE PRECAST MANUFACTURER. FLEXURAL EFFECTS SHALL BE CONSIDERED IN THE DESIGN.

PICK POINTS OR LIFTING LOOP LOCATIONS SHALL BE APPROVED BY THE ENGINEER PRIOR TO FABRICATION.

THE METHOD OF SUPPORTING THE PRECAST ABUTMENT FOOTING DURING ERECTION SHALL BE SUBMITTED TO THE ENGINEER PRIOR TO THE ERECTION. SPECIAL EMPHASIS IS PLACED ON THE CONTRACTORS METHOD OF ELEVATION CONTROL.

THE STRUCTURAL CONCRETE (MISC.) USED TO FILL THE ABUTMENT PILING ENCASEMENTS SHALL BE CLASS C-4 CONCRETE WITH A HIGH RANGE WATER REDUCER. THE MAXIMUM SLUMP ACHIEVED WITH WATER SHALL BE 2 INCHES. THE HRWR SHALL BE ADDED AT THE POUR SITE. THE MAXIMUM SIZE OF AGGREGATE SHALL BE 1 1/2" TOP SIZE.

OTHER MIXES MAY BE CONSIDERED PROVIDING THEY HAVE BEEN REVIEWED AND APPROVED BY THE DISTRICT MATERIALS ENGINEER.

DISTRICT MATERIALS WILL PROVIDE COMPRESSIVE STRENGTH TESTING OF THE CONCRETE USED TO FILL THE ABUTMENT PILING ENCASEMENTS. BLOCKING AND TEMPORARY SHORING SHALL NOT BE REMOVED UNTIL 3500 PSI HAS BEEN ACHIEVED.

FINAL PILE HEAD POSITIONS SHALL NOT DEVIATE FROM THE LOCATION DESIGNATED IN THESE PLANS BY MORE THAN 3/4" IN ANY DIRECTION IN ORDER TO ALLOW THE PRECAST FOOTING TO BE PLACED.

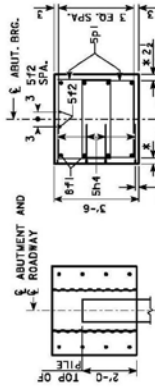
ESTIMATED QUANTITIES ONE PRECAST ABUTMENT FOOTING

ITEM	UNIT	QUANTITY
STRUCTURAL CONCRETE (BRIDGE)	CY	8.4
REINFORCING STEEL	LBS	1267
EXCAVATION CLASS 20	CY	33.1
21" x 4" CMP	LF	18.0

PILE QUANTITIES BOTH ABUTMENTS

E. ABUT. 15 - HP10X42 @ 35'-0"	175'-0"
W. ABUT. 15 - HP10X42 @ 35'-0"	175'-0"
TOTAL	350'-0"

PRECAST ABUTMENT WEIGHT = 19.21 TONS



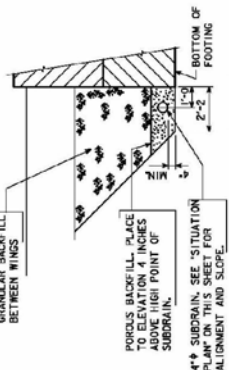
SECTION A-A

SECTION B-B

NOTE: PILE SPIRALS NOT SHOWN.

6 BOX BEAMS @ 4'-0" = 24'-0" ROADWAY

BENCH MARK #1 SET 60G SPIKE IN POWER POLE, 27.93 RT., STA. 98+35.18, ELEV. 100.00
 BENCH MARK #2 SET 60G SPIKE IN POWER POLE, 25.56 RT., STA. 101+36.04, ELEV. 85.22
 NOTE: ASSUMED DATUM



SECTION A-A
 NOTE: SPECIAL SLOPE SHALL BE SUBSTITUTED FOR GRANULAR BACKFILL.

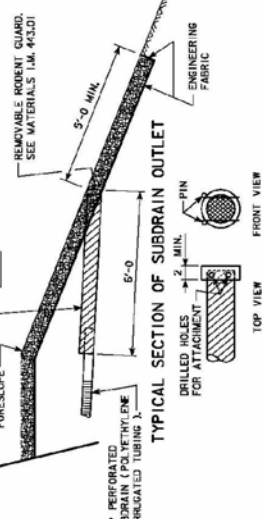
GRANULAR BACKFILL DETAILS

SUBDRAIN NOTES :

THIS PLAN SHEET SHOWS DETAILS FOR PLACING ALL SUBDRAINS AND SUBDRAIN OUTLETS. THE SUBDRAINS SHALL BE 4" IN DIAMETER AND MEET THE REQUIREMENTS OF SECTION 4143.01B OF THE CURRENT I.D.O.T. STANDARD SPECIFICATION. THE SUBDRAIN OUTLET SHALL CONSIST OF A 6'-0" LENGTH OF PIPE WITH A REMOVABLE RODENT GUARD AS DETAILED ON THIS SHEET. THE COST OF FURNISHING AND PLACING SUBDRAIN (INCLUDING EXCAVATION, GRANULAR BACKFILL, POROLS BACKFILL, AND SUBDRAIN OUTLET IS TO BE INCLUDED IN THE PRICE BID. NO EXTRA PAYMENT WILL BE MADE. THE DIMENSIONS SHOWN FOR THE PROPOSED SUBDRAINS ARE BASED ON THE PROPOSED GRADING LAYOUT. THE DIMENSIONS SHOWN FOR THE PROPOSED SUBDRAINS ARE SUBJECT TO CHANGE DUE TO FIELD ADJUSTMENTS OF THE GRADING LAYOUT.

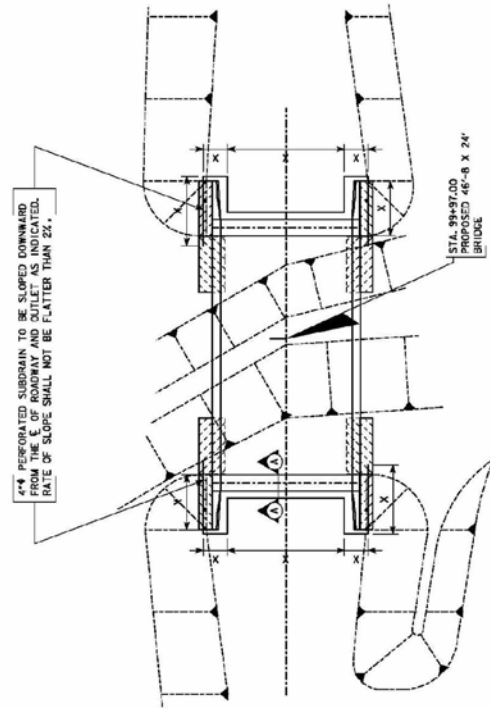
SUBDRAIN OUTLET ELEVATIONS	
LOCATION	ELEVATION
WEST ABUTMENT	AS DIRECTED BY
EAST ABUTMENT	ENGINEER IN FIELD

- 4" CORRUGATED METAL PIPE OUTLET, OR 4" PERFORATED SUBDRAIN (POLYETHYLENE CORRUGATED TUBING), SHALL BE USED. IF METAL PIPE IS USED, THE PIPES SHALL BE COUPLED IN ONE OF THE TWO FOLLOWING WAYS:
- USE AN INSULATED REDUCED COUPLER (C.P. 100) WITH A MINIMUM OF 1'-0" INTO CMP.
 - INSERT 1'-0" OF THE 4" SUBDRAIN INTO THE 6" METAL OUTLET PIPE, THEN FULLY SEAL THE ENTIRE OPENING WITH GROUT.
- REMOVABLE RODENT GUARD. SEE MATERIALS I.M. 443.01



**REMOVABLE RODENT GUARD DETAILS
 OUTLET DETAILS**

DESIGN FOR 0° SKEW
**46'-8 X 24' PRECAST PRETENSIONED
 BOX GIRDER BRIDGE**
 SUBDRAIN DETAILS
 APRIL 2006
 46'-8 END SPAN
 STA. 99+97
 MADISON COUNTY
 IOWA DEPARTMENT OF TRANSPORTATION - HIGHWAY DIVISION
 DESIGN SHEET NO. 3 OF 12 FILE NO. 30139 DESIGN NO. 106

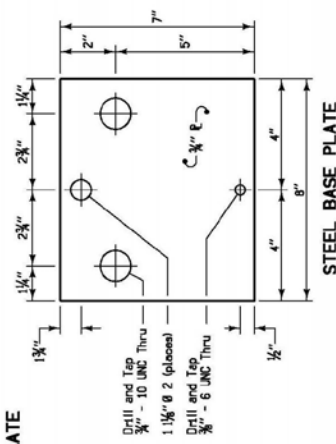
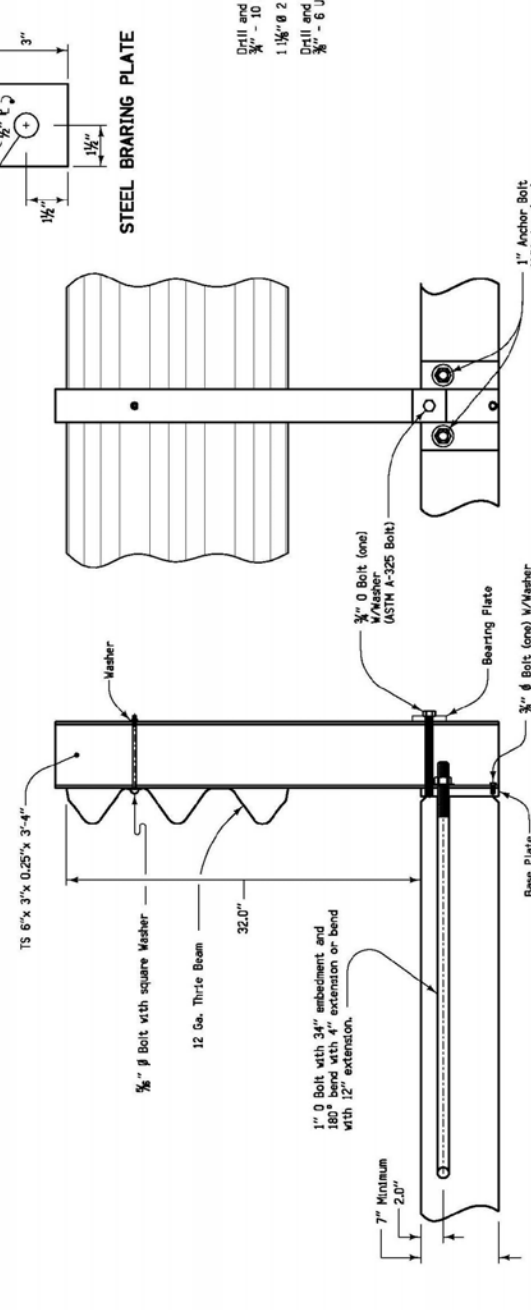
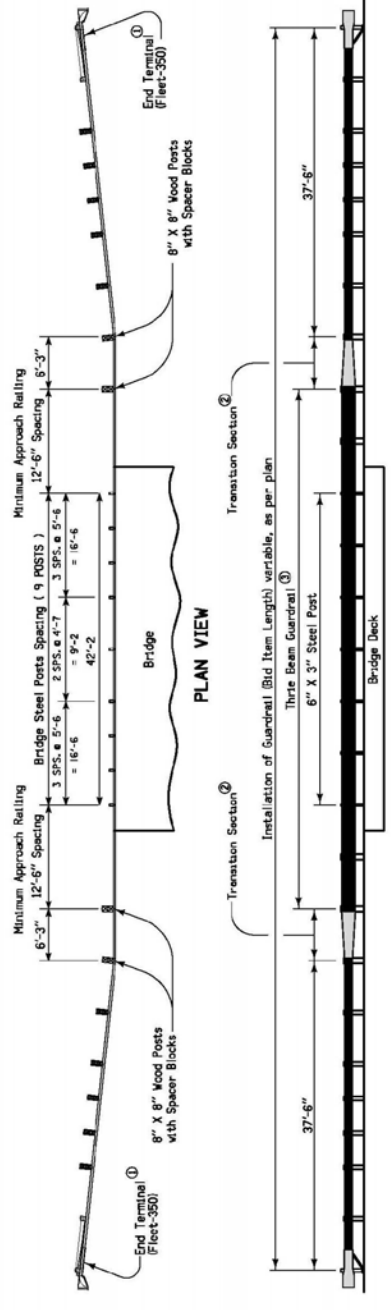


SITUATION PLAN
 SHOWING SUBDRAIN LOCATIONS

General Notes:
 This detail sheet shows the construction details for Service Level I Bridge Rail and the connecting Steel Beam Guardrail for use on the secondary road system.
 Unless otherwise noted bolts shall conform to the requirements of ASTM A307 and nuts to the requirements of ASTM A563 grade A or better. Other bolts shall conform to the requirements of ASTM A325 and nuts to the requirements of ASTM A563 grade C or better all nuts and washers shall be galvanized in accordance with ASTM A153.
 Deck anchorage of the post assembly shall be provided by applying a 10 kip (45-kN) force to the post at 22 inches above the deck and designed according to the latest AASHTO bridge specifications.
 Steel shall conform to the requirements of ASTM 36, or equivalent, and be galvanized according to ASTM A123. Post elements shall conform to the requirements of ASTM grade B, ASTM 501, and shall be galvanized in accordance with the requirements of ASTM A123.
 Guardrail shall be lapped towards the obstacle.
 Price bid for contract items shall be considered full compensation for furnishing all materials and constructing guardrail essentially as indicated hereon.
 Contract items for guardrail construction are:
 Installation of Guardrail in linear Feet
 Beam Guardrail Terminal (RE-76)

- ① See Standard Road Plan RE-76
- ② See Standard Road Plan RE-28
- ③ See Standard Road Plan RE-128

See Standard Road Plan RE-76
 See Standard Road Plan RE-28
 See Standard Road Plan RE-128



DESIGN FOR 0° SKEW
46'-8 X 24' PRECAST PRETENSIONED BOX GIRDER BRIDGE
 46'-8 END SPANS
SERVICE LEVEL I BRIDGE RAIL DETAILS
 APRIL 2006
 STA. 99+37
 MADISON COUNTY
 IOWA DEPARTMENT OF TRANSPORTATION - HIGHWAY DIVISION
 DESIGN SHEET NO. 10 OF 12 FILE NO. 30135 DESIGN NO. 106

CLIENT		PROJECT		TESTS	
MADISON COUNTY ENGINEER		REPLACEMENT BRIDGE - IBRC (61)		UNCONFIRMED	
MADISON COUNTY, IOWA		MADISON COUNTY, IOWA		DRY UNIT WT	
Approx. Boring Location: 20' East of existing east abutment, 7' South of centerline.		Approx. Boring Location: 23' West of existing west abutment, 7' North of centerline.		WATER CONTENT, %	
DESCRIPTION		DESCRIPTION		SFT - N + 1 BLOWS / ft	
Approx. Surface Elev.: 90 ft		Approx. Surface Elev.: 91.5 ft		RECOVERY, in.	
1-6 Inches Gravel at Surface		1-12 Inches Gravel at Surface		TYPE	
FILL: LEAN CLAY With Sand, Trace		FILL: LEAN CLAY With Sand and Dark Brown		USCS SYMBOL	
Dark Gray and Brown Gray		Brown and Dark Brown		DEPTH, ft	
8		4		4	
LEAN TO FAT CLAY, Trace Sand (DOT CLASSIFICATION: FIRM SILTY CLAY)		LEAN TO FAT CLAY, Trace Sand (DOT CLASSIFICATION: STIFF SILTY CLAY)		5	
Very Silty		Brown Gray, Stiff		1	
14		8		10	
SANDY LEAN CLAY With Sand Seams (DOT CLASSIFICATION: STIFF SANDY CLAY)		SANDY LEAN CLAY With Sand Seams (DOT CLASSIFICATION: FIRM SANDY CLAY)		2	
Very Silty		Gray Brown		3	
15		10		4	
SANDY LEAN CLAY With Sand Seams (DOT CLASSIFICATION: STIFF SANDY CLAY)		LEAN TO FAT CLAY With Sand, Trace Gravel (DOT CLASSIFICATION: FIRM GLACIAL CLAY)		5	
Very Silty		Dark Gray, Stiff		6	
16		11		7	
FAT CLAY, Trace Sand and Organics (DOT CLASSIFICATION: STIFF SILTY CLAY)		LEAN TO FAT CLAY With Sand, Trace Gravel (DOT CLASSIFICATION: FIRM GLACIAL CLAY)		8	
Very Dark Gray		Dark Gray, Stiff		9	
17		12		10	
FINE TO MEDIUM SAND, Trace Gravel (DOT CLASSIFICATION: STIFF SANDY CLAY)		FAT CLAY, Trace Sand and Organics (DOT CLASSIFICATION: FIRM TO VERY FIRM GLACIAL CLAY)		11	
Very Dark Gray		Dark Brown, Very Silty		12	
18		13		13	
LEAN TO MEDIUM SAND, Trace Gravel (DOT CLASSIFICATION: VERY FIRM SANDY GLACIAL CLAY)		FAT CLAY With Sand, Trace Gravel (DOT CLASSIFICATION: VERY FIRM SANDY GLACIAL CLAY)		14	
Gray, Hard		Dark Brown, Very Silty		15	
19		14		16	
SHALE *** With Limestone Stringers		FAT CLAY With Sand, Trace Gravel (DOT CLASSIFICATION: VERY FIRM SANDY GLACIAL CLAY)		17	
Gray		Dark Brown, Very Silty		18	
20		15		19	
LIMESTONE ***		LEAN TO MEDIUM SAND, Trace Gravel (DOT CLASSIFICATION: STIFF SANDY CLAY)		20	
Light Gray		Very Dark Gray		21	
21		16		22	
LIMESTONE ***		FINE TO MEDIUM SAND, Trace Gravel (DOT CLASSIFICATION: STIFF SANDY CLAY)		23	
Light Gray		Very Dark Gray		24	
22		17		25	
LIMESTONE ***		LEAN TO MEDIUM SAND, Trace Gravel (DOT CLASSIFICATION: STIFF SANDY CLAY)		26	
Light Gray		Very Dark Gray		27	
23		18		28	
LIMESTONE ***		FINE TO MEDIUM SAND, Trace Gravel (DOT CLASSIFICATION: STIFF SANDY CLAY)		29	
Light Gray		Very Dark Gray		30	
24		19		31	
LIMESTONE ***		LEAN TO MEDIUM SAND, Trace Gravel (DOT CLASSIFICATION: STIFF SANDY CLAY)		32	
Light Gray		Very Dark Gray		33	
25		20		34	
LIMESTONE ***		FINE TO MEDIUM SAND, Trace Gravel (DOT CLASSIFICATION: STIFF SANDY CLAY)		35	
Light Gray		Very Dark Gray		36	
26		21		37	
LIMESTONE ***		LEAN TO MEDIUM SAND, Trace Gravel (DOT CLASSIFICATION: STIFF SANDY CLAY)		38	
Light Gray		Very Dark Gray		39	
27		22		40	
LIMESTONE ***		FINE TO MEDIUM SAND, Trace Gravel (DOT CLASSIFICATION: STIFF SANDY CLAY)		41	
Light Gray		Very Dark Gray		42	
28		23		43	
LIMESTONE ***		LEAN TO MEDIUM SAND, Trace Gravel (DOT CLASSIFICATION: STIFF SANDY CLAY)		44	
Light Gray		Very Dark Gray		45	
29		24		46	
LIMESTONE ***		FINE TO MEDIUM SAND, Trace Gravel (DOT CLASSIFICATION: STIFF SANDY CLAY)		47	
Light Gray		Very Dark Gray		48	
30		25		49	
LIMESTONE ***		LEAN TO MEDIUM SAND, Trace Gravel (DOT CLASSIFICATION: STIFF SANDY CLAY)		50	
Light Gray		Very Dark Gray		51	
31		26		52	
LIMESTONE ***		FINE TO MEDIUM SAND, Trace Gravel (DOT CLASSIFICATION: STIFF SANDY CLAY)		53	
Light Gray		Very Dark Gray		54	
32		27		55	
LIMESTONE ***		LEAN TO MEDIUM SAND, Trace Gravel (DOT CLASSIFICATION: STIFF SANDY CLAY)		56	
Light Gray		Very Dark Gray		57	
33		28		58	
LIMESTONE ***		FINE TO MEDIUM SAND, Trace Gravel (DOT CLASSIFICATION: STIFF SANDY CLAY)		59	
Light Gray		Very Dark Gray		60	
34		29		61	
LIMESTONE ***		LEAN TO MEDIUM SAND, Trace Gravel (DOT CLASSIFICATION: STIFF SANDY CLAY)		62	
Light Gray		Very Dark Gray		63	
35		30		64	
LIMESTONE ***		FINE TO MEDIUM SAND, Trace Gravel (DOT CLASSIFICATION: STIFF SANDY CLAY)		65	
Light Gray		Very Dark Gray		66	
36		31		67	
LIMESTONE ***		LEAN TO MEDIUM SAND, Trace Gravel (DOT CLASSIFICATION: STIFF SANDY CLAY)		68	
Light Gray		Very Dark Gray		69	
37		32		69	

DESIGN FOR 0° SKEW
46'-8 X 24' PRECAST PRETENSIONED BOX GIRDER BRIDGE
 46'-8 END SPANS
 STA. 99+97
 MADISON COUNTY
 IOWA DEPARTMENT OF TRANSPORTATION - HIGHWAY DIVISION
 DESIGN SHEET NO. 12 OF 12 FILE NO. 30139 DESIGN NO. 106
 PROJECT NUMBER: IBRC-006(10)-6E-61
 MADISON COUNTY
 SHEET NUMBER: 13

SOIL BORINGS DETAILS
 APRIL 2006

DESIGN TEAM
 21-MAY-2007 13:05
 W:\Projects\Bridges\Structures\LocalSystem\Truss\Routes\Medisoncounty\BIR1\Brd1_1.BRIDGE.GR6 6101060102 \\\NPR15V2\Brd1